

SUPPORTING INFORMATION

Table of Contents

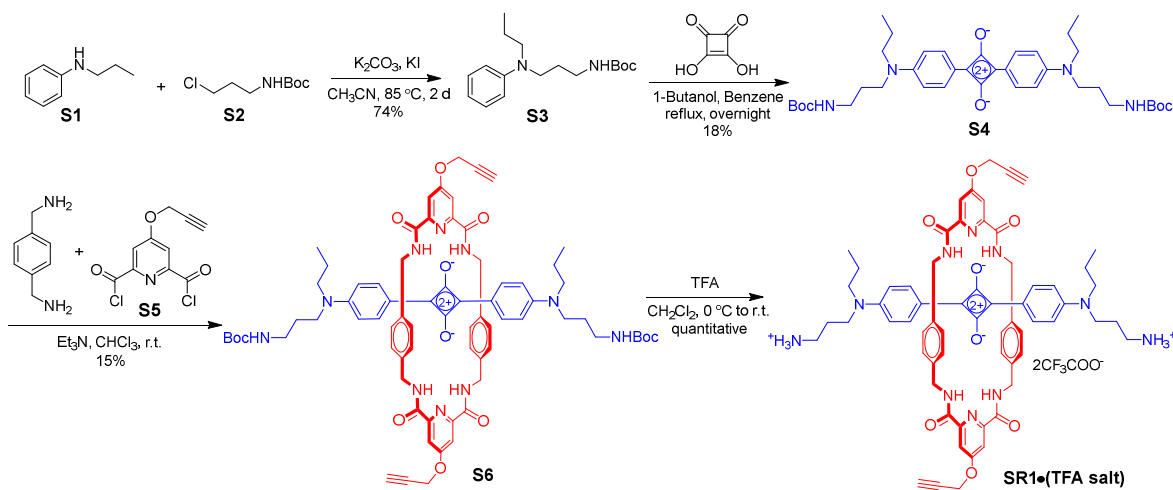
1. General Materials.....	3
2. Synthesis and Compound Characterization.....	3-29
3. X-ray Crystal Structure of SF8(C6) ₂	30-38
4. Variable Temperature ¹ H NMR Studies of SF8(C6) ₂	39-40
5. Photophysical Properties and Stability Studies.....	41-47
6. Liposome Studies.....	48-49
7. Cell and Bone Studies.....	50-52
8. Mouse Imaging Studies.....	53
References.....	54
Author Contributions.....	54

SUPPORTING INFORMATION

1. General Materials

All chemicals and solvents were purchased as reagent grade and used without further purification unless otherwise noted. Reactions were monitored by analytical thin-layer chromatography (TLC) on silica gel 60-F254 plates, visualized by ultraviolet (254, 365 nm). NMR spectra (^1H , ^{13}C , $^1\text{H}-^1\text{H}$ COSY) were recorded on Bruker AVANCE III HD 400 or 500 MHz spectrometer at 25 °C. Chemical shift was presented in ppm and referenced by residual solvent peak. High-resolution mass spectrometry (HRMS) was performed using a Bruker micro TOP II spectrometer. Absorption and fluorescence spectra were collected on Evolution 201 UV/Vis Spectrometer with Thermo Insight software, and Horiba Fluoromax4 Fluorometer with FluoroEssence software, respectively. Measurements were conducted at room temperature with quartz cuvette (1 mL, 10 mm path length). Flash column chromatography was performed using silica gel (silicaFlash P60 from SILICYCLE). 1-Palmitoyl-2-oleoyl-sn-glycero-3-phosphocholine (POPC, 10 mg/mL) and 1-Palmitoyl-2-oleoyl-sn-glycero-3-phospho-L-serine (POPS, 10 mg/mL) were purchased from Avanti Polar Lipids (USA) and stored in a freezer at -20 °C.

2. Synthesis and Compound Characterization



Scheme S1. Synthesis of SR1•(TFA salt).

Note: Compound **S1**^[1], **S2**^[2] and **S5**^[3] were synthesized by reported procedures.

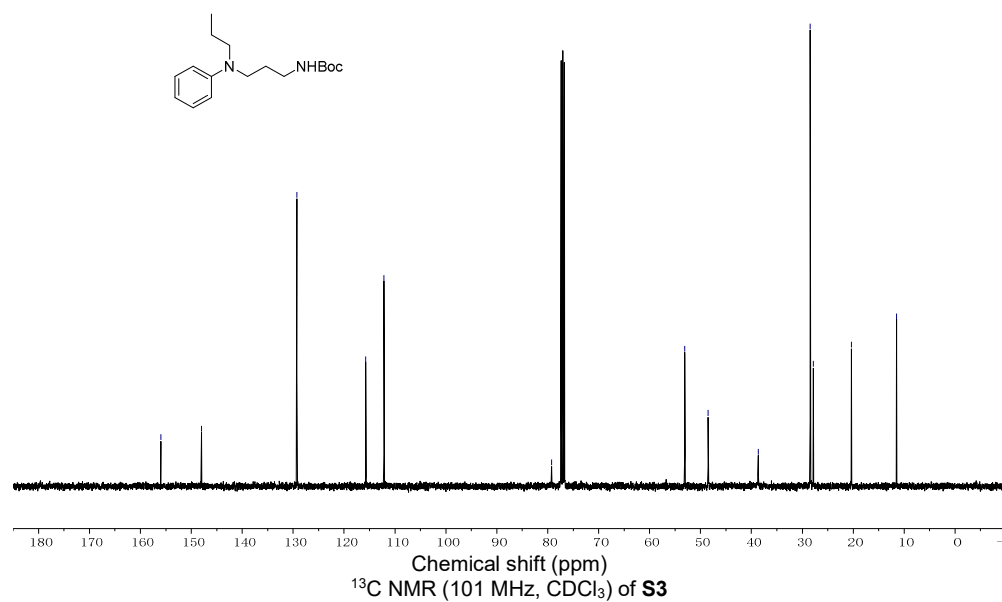
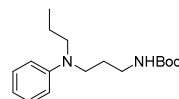
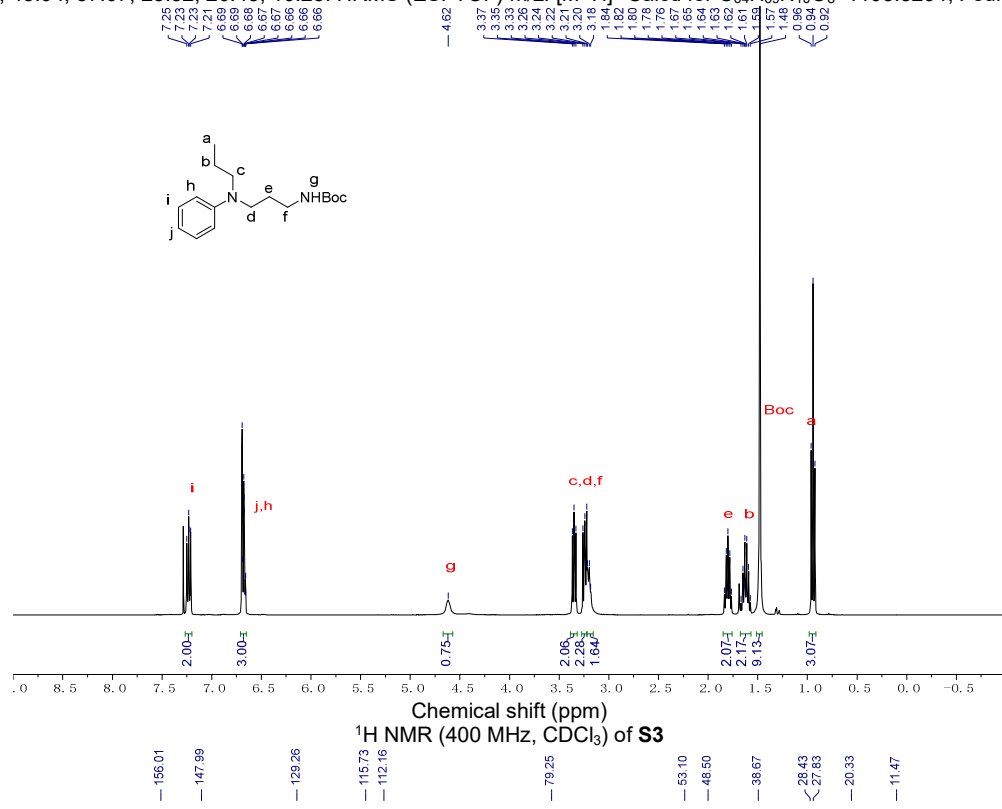
S3. Compound **S2** (8.27 g, 42.7 mmol) was added to a mixture of **S1** (3.85 g, 28.5 mmol), K_2CO_3 (4.72 g, 34.2 mmol) and KI (4.72 g, 34.2 mmol) in CH_3CN (10 mL) (10 mL) in a round-bottom flask. The reaction mixture was put into oil bath and stirred at 85 °C for 3 days. Solvent was removed by rotary evaporation. The resulting residue was extracted with $\text{H}_2\text{O}/\text{CH}_2\text{Cl}_2$ ($\times 3$). The organic layer was combined and dried over anhydrous Na_2SO_4 . The solution was filtered, and solvent was removed by rotary evaporation. The resulting residue was purified by silica gel column chromatography (0-15% Ethyl acetate in Hexane) to yield product **S3** as a yellow liquid (6.16 g, 74%). ^1H NMR (400 MHz, Chloroform- δ) δ 7.23 (dd, $J = 8.7, 7.2$ Hz, 2H), 6.71-6.65 (m, 3H), 4.62 (s, 1H), 3.39-3.32 (m, 2H), 3.27-3.22 (m, 2H), 3.22-3.16 (m, 2H), 1.80 (m, 2H), 1.62 (m, 2H), 1.48 (s, 9H), 0.94 (t, $J = 7.4$ Hz, 3H). ^{13}C NMR (101 MHz, Chloroform- δ) δ 156.01, 147.99, 129.26, 115.73, 112.16, 79.25, 53.10, 48.50, 38.67, 28.43, 27.83, 20.33, 11.47. HRMS (ESI-TOF) m/z: [M+H]⁺ Calcd for $\text{C}_{17}\text{H}_{29}\text{N}_2\text{O}_2^+$ 293.2224; Found 293.2222.

S4. A mixture of **S3** (4.00 g, 13.7 mmol) and squaric acid (0.78 g, 6.84 mmol) in 1-butanol/benzene (V/V, 1/2, 60 mL) was refluxed overnight. The solvent was removed by rotary evaporation and the resulting residue was purified by silica gel column chromatography (0-10% MeOH in CH_2Cl_2) to yield crude product, which was then washed with hexane to obtain compound **S4** as a green blue solid (0.84 g, 18%). ^1H NMR (500 MHz, Chloroform- δ) δ 8.36 (d, $J = 9.0$ Hz, 4H), 6.71 (d, $J = 9.3$ Hz, 4H), 4.68 (s, 2H), 3.50 (t, $J = 7.7$ Hz, 4H), 3.43-3.36 (m, 4H), 3.21 (m, 4H), 1.85 (m, 4H), 1.70-1.65 (m, 4H), 0.97 (t, $J = 7.4$ Hz, 6H). ^{13}C NMR (126 MHz, Chloroform- δ) δ 188.38, 183.60, 156.29, 153.52, 133.53, 119.95, 112.48, 53.28, 49.05, 38.40, 28.62, 28.45, 20.96, 11.54. HRMS (ESI-TOF) m/z: [M+H]⁺ Calcd for $\text{C}_{38}\text{H}_{55}\text{N}_4\text{O}_6^+$ 663.4116; Found 663.4144.

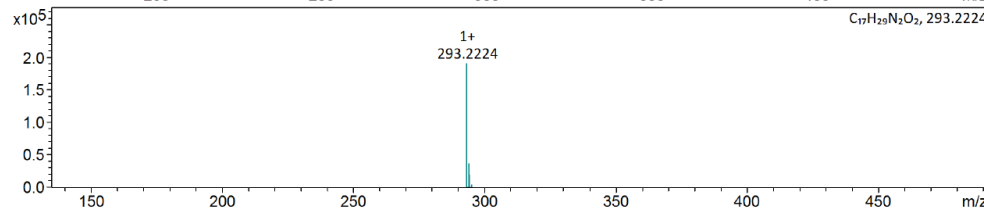
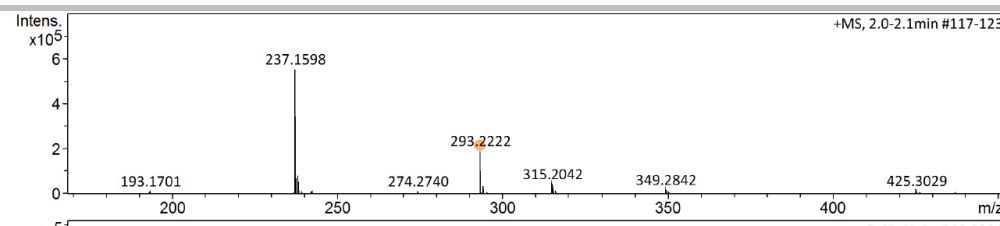
S6. In a 25 mL syringe 1,4-xylylenediamine (272 mg, 1.996 mmol) and Et_3N (554 μL , 3.99 mmol) were dissolved in anhydrous CHCl_3 (9.45 mL). In a second 25 mL syringe, **S5** (515 mg, 1.996 mmol) was dissolved in anhydrous CHCl_3 (10 mL). Both syringes were added dropwise through a syringe pump to a solution of dye **S4** (331 mg, 0.499 mmol) and in anhydrous CHCl_3 (40 mL). The reaction was stirred at room temperature for 2 days and then filtered through celite. Solvent was removed and the residue was purified by silica gel chromatography (0-2% MeOH in CH_2Cl_2). The crude product was washed with hexane ($\times 3$) to afford the blue powder product **S6** (95 mg, 15%). ^1H NMR (500 MHz, Chloroform- δ) δ 9.97 (t, $J = 5.9$ Hz, 4H), 8.13-8.07 (m, 8H), 6.59 (s, 8H), 6.15 (d, $J = 8.9$ Hz, 4H), 4.94 (d, $J = 2.4$ Hz, 4H), 4.83 (s, 2H), 4.51 (d, $J = 5.8$ Hz, 8H), 3.38 (t, $J = 7.7$ Hz, 4H), 3.29 (t, $J = 7.8$ Hz, 4H), 3.16 (q, $J = 6.7$ Hz, 4H), 2.66 (t, $J = 2.4$ Hz, 1H), 1.78 (q, $J = 7.4$ Hz, 4H), 1.60 (q, $J = 7.5$ Hz, 4H), 1.47 (s, 18H), 0.93 (t, $J = 7.4$ Hz, 6H). ^{13}C NMR (126 MHz, Chloroform- δ) δ 185.32, 184.38, 166.58, 163.58, 156.32, 153.45, 151.88, 136.74, 133.81, 129.12, 119.03, 111.86, 111.72, 79.89, 56.56, 53.26, 48.99, 43.62, 38.40, 29.92, 28.63, 28.39, 20.97, 11.49. HRMS (ESI-TOF) m/z: [M+H]⁺ Calcd for $\text{C}_{74}\text{H}_{85}\text{N}_{10}\text{O}_{12}^+$ 1305.6343; Found 1305.6350.

SUPPORTING INFORMATION

SR1•(TFA salt). Trifluoroacetic acid (TFA) (0.15 mL) was added dropwise to a solution of **S6** (25 mg) in CH_2Cl_2 (2 mL) in an ice bath. The reaction was stirred overnight. Solvent was removed and the residue was washed with Et_2O ($\times 3$) to give blue powder product **SR1•(TFA salt)** (21.5 mg, quantitative). ^1H NMR (500 MHz, Methanol- d_4) δ 10.10 (t, J = 6.0 Hz, 4H), 8.11 (d, J = 8.9 Hz, 4H), 8.08 (s, 4H), 6.56 (s, 8H), 6.33 (d, J = 8.9 Hz, 4H), 5.10 (d, J = 2.4 Hz, 4H), 4.49 (d, J = 6.0 Hz, 8H), 3.55 (t, J = 7.7 Hz, 4H), 3.39 (t, J = 7.8 Hz, 4H), 3.22 (t, J = 2.4 Hz, 1H), 3.00–2.94 (m, 4H), 1.95 (dd, J = 15.3, 7.7 Hz, 4H), 1.63 (m, 4H), 0.95 (t, J = 7.3 Hz, 6H). ^{13}C NMR (126 MHz, Methanol- d_4) δ 185.58, 183.17, 167.15, 163.79, 153.91, 151.37, 136.70, 133.69, 128.72, 118.87, 111.79, 111.76, 77.71, 76.92, 56.36, 52.70, 43.04, 37.07, 25.52, 20.45, 10.25. HRMS (ESI-TOF) m/z: [M+H]⁺ Calcd for $\text{C}_{64}\text{H}_{69}\text{N}_{10}\text{O}_8^+$ 1105.5294; Found 1105.5271.



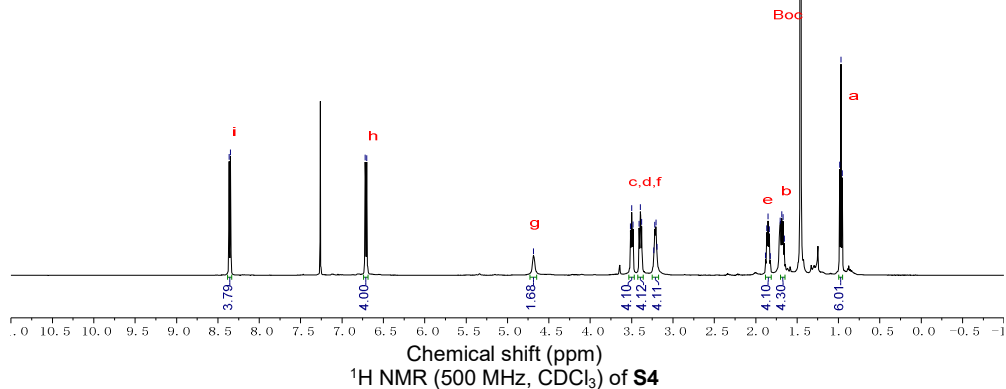
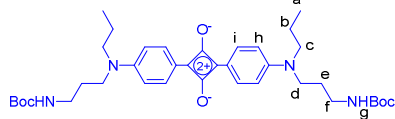
SUPPORTING INFORMATION



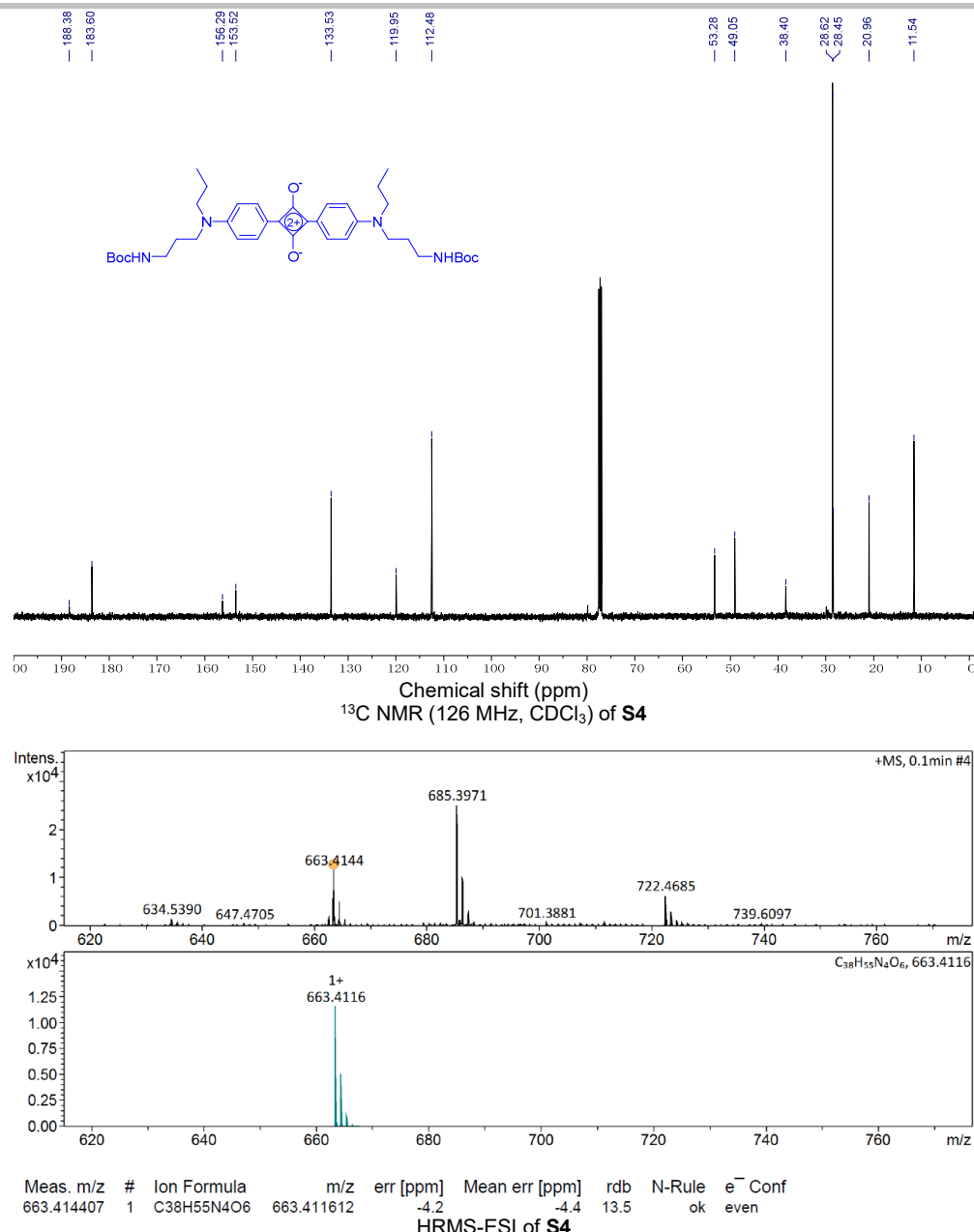
Meas. m/z	#	Ion Formula	m/z	err [ppm]	Mean err [ppm]	rdb	N-Rule	e ⁻ Conf
293.222179	1	$C_{17}H_{29}N_2O_2$	293.222355	0.6	1.1	4.5	ok	even

HRMS-ESI of **S3**

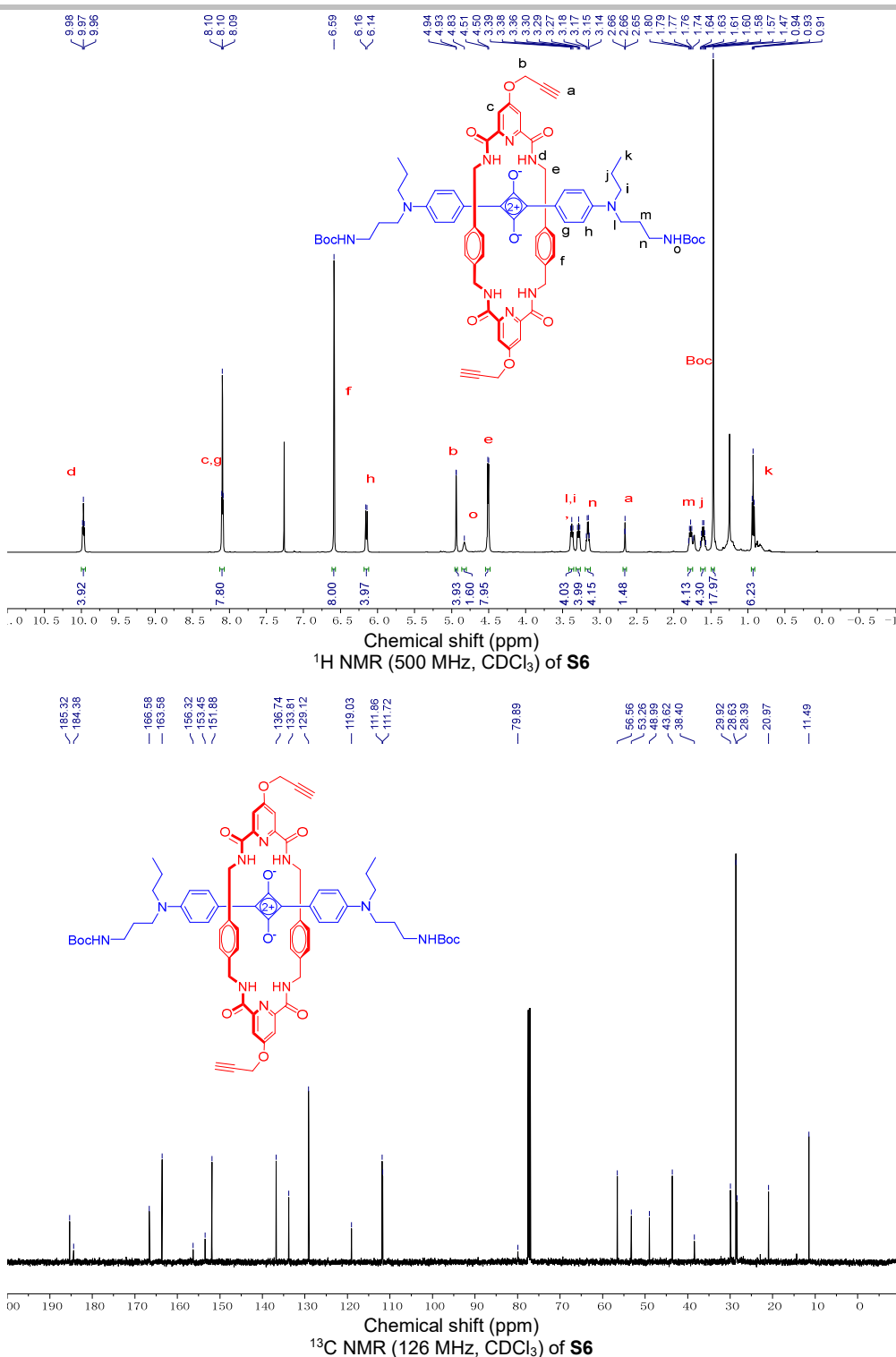
< 8.35 < 6.70 4.68



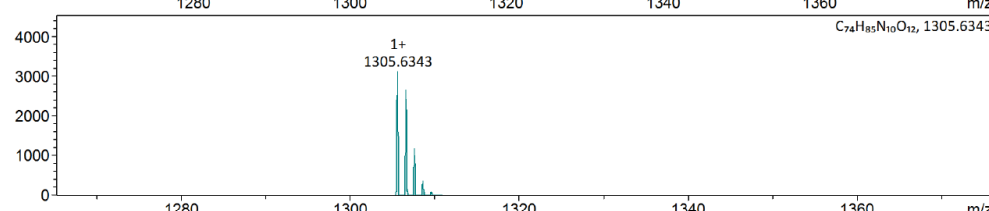
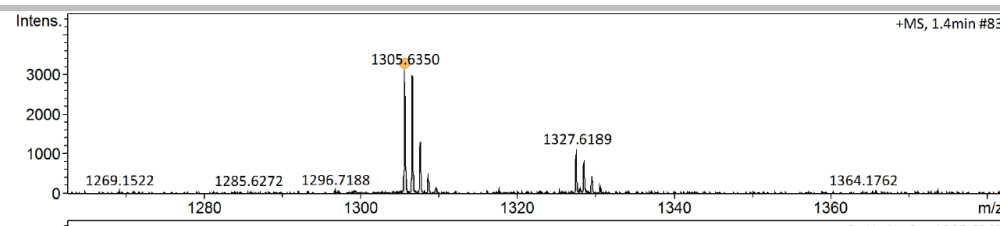
SUPPORTING INFORMATION



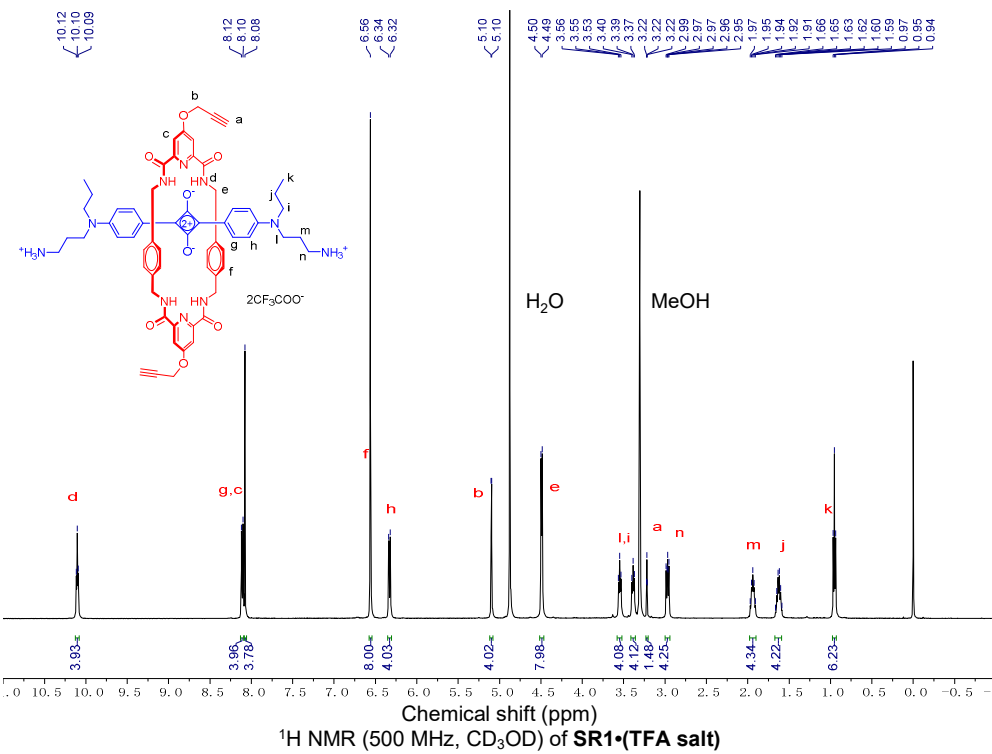
SUPPORTING INFORMATION



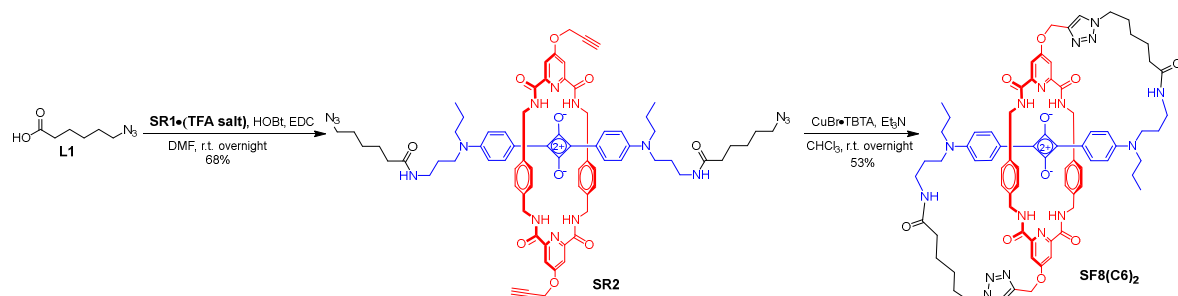
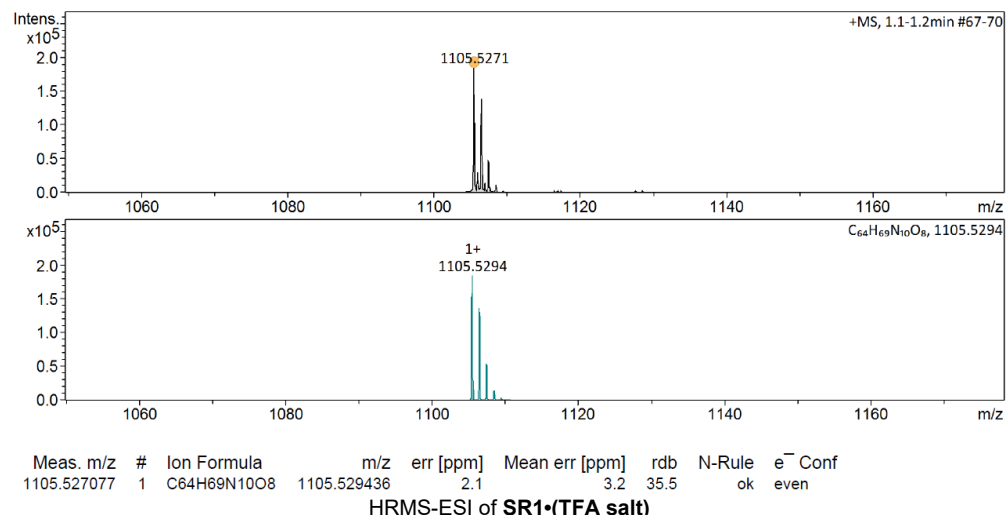
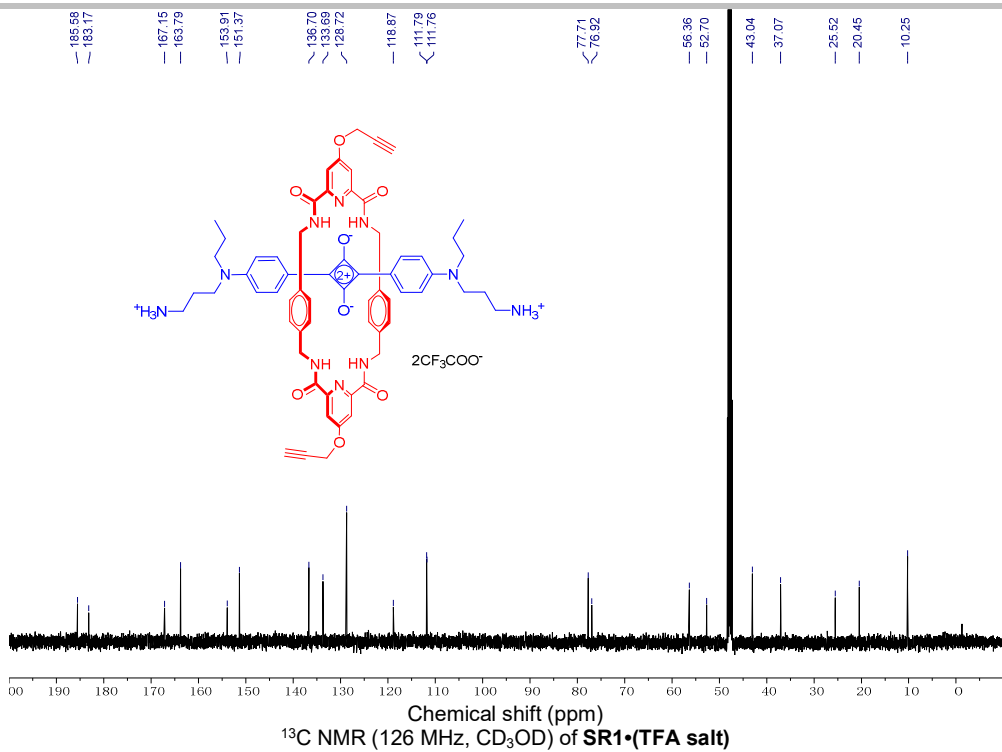
SUPPORTING INFORMATION



Meas. m/z	#	Ion Formula	m/z	err [ppm]	Mean err [ppm]	rdb	N-Rule	e ⁻ Conf
1305.635037	1	$C_{74}H_{85}N_{10}O_{12}$	1305.634295	-0.6	298.3	37.5	ok	even

HRMS-ESI of **S6**

SUPPORTING INFORMATION



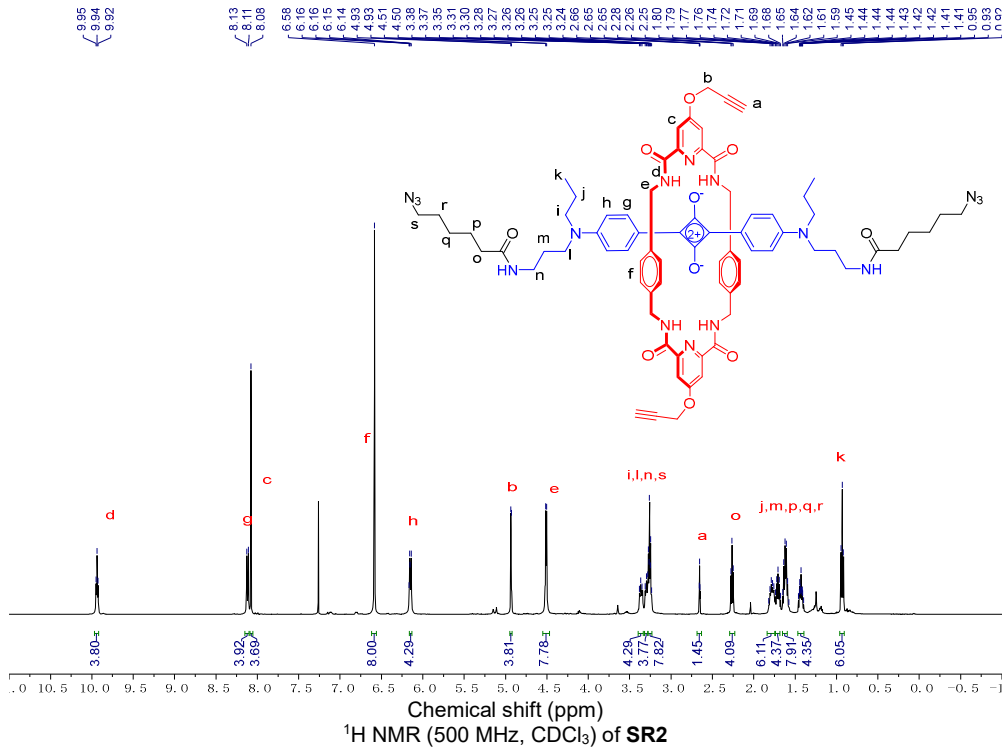
Scheme S2. Synthesis of SF8(C6)₂.

Note: Compound **L1**^[4] was synthesized by reported procedures.

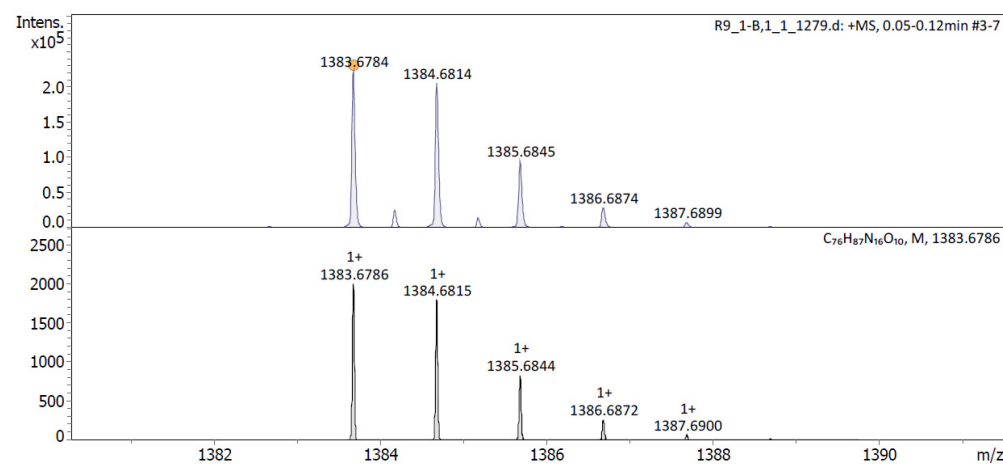
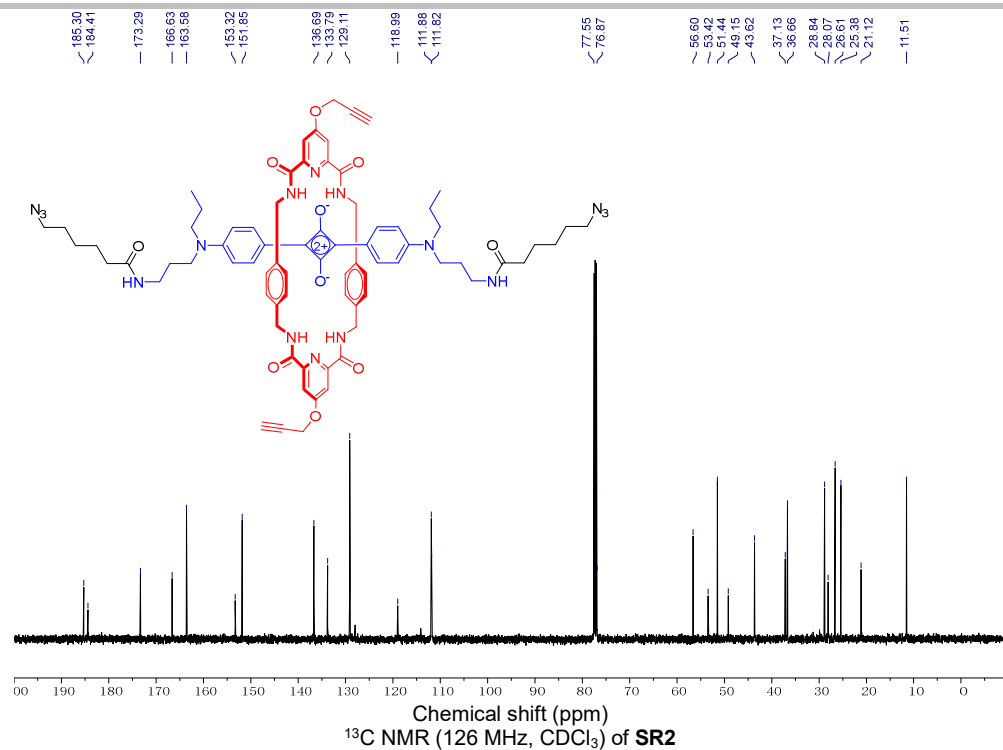
SUPPORTING INFORMATION

SR2. A mixture of **SR1-TFA salt** (11 mg, 0.00995 mmol), **L1** (19 mg, 0.119 mmol), 1-hydroxybenzotriazole hydrate (HOEt) (23 mg, 0.149 mmol) and 1-ethyl-3-(3-dimethylaminopropyl)carbodiimide (EDC) (29 mg, 0.149 mmol) in *N,N*-dimethylformamide (DMF) (0.5 mL) was stirred at room temperature overnight. The solvent was removed by rotary evaporation and the resulting residue was purified by silica gel column chromatography (0-2% MeOH in CH_2Cl_2) to give afford product **SR2** as green blue solid (9.4 mg, 68%). ^1H NMR (500 MHz, Chloroform- d) δ 9.94 (t, J = 5.9 Hz, 4H), 8.12 (d, J = 8.9 Hz, 4H), 8.08 (s, 4H), 6.58 (s, 8H), 6.16-6.13 (m, 4H), 4.93 (d, J = 2.4 Hz, 4H), 4.51 (d, J = 5.9 Hz, 8H), 3.36 (t, J = 7.8 Hz, 4H), 3.30 (d, J = 7.6 Hz, 4H), 3.26 (m, 8H), 2.65 (t, J = 2.4 Hz, 1H), 2.26 (t, J = 7.5 Hz, 4H), 1.79 (m, 6H), 1.71 (q, J = 7.7 Hz, 4H), 1.65-1.59 (m, 8H), 1.47-1.39 (m, 4H), 0.93 (t, J = 7.4 Hz, 6H). ^{13}C NMR (126 MHz, Chloroform- d) δ 185.30, 184.41, 173.29, 166.63, 163.58, 153.32, 151.85, 136.69, 133.79, 129.11, 118.99, 111.88, 111.82, 77.55, 76.87, 56.60, 53.42, 51.44, 49.15, 43.62, 37.13, 36.66, 28.84, 28.07, 26.61, 25.38, 21.12, 11.51. HRMS (ESI-TOF) m/z: [M+H]⁺ Calcd for $\text{C}_{76}\text{H}_{87}\text{N}_{16}\text{O}_{10}^+$ 1383.6786; Found 1383.6784.

SF8(C6)2. Compound **SR2** (11 mg, 0.00759 mmol) was dissolved in CHCl₃ (15 mL). CuBr-TBTA (TBTA: tris(benzyltriazolylmethyl)amine) (5 mg) and Et₃N (21 μ L, 0.152 mmol) were added to the solution. The reaction mixture was stirred at room temperature overnight. The solvent was removed by rotary evaporation and the resulting residue was purified by silica gel column chromatography (0-6% MeOH in CH₂Cl₂) to give product **SF8(C6)2** as a green blue solid (5.6 mg, 53%). ¹H NMR (500 MHz, Chloroform- δ) δ 10.09 (dd, J = 8.0, 2.8 Hz, 4H), 8.12 (s, 4H), 8.01 (br. s, 4H), 7.84 (s, 2H), 6.60 (br. s, 12H), 5.77 (s, 2H), 5.50 (s, 4H), 4.92 (dd, J = 14.5, 7.9 Hz, 4H), 4.45 (d, J = 6.3 Hz, 4H), 4.01 (dd, J = 14.5, 2.7 Hz, 4H), 3.41-3.29 (m, 8H), 3.26 (s, 4H), 2.22 (s, 4H), 1.96 (s, 4H), 1.70 (s, 16H), 0.99 (t, J = 7.3 Hz, 6H). ¹³C NMR (101 MHz, Chloroform- δ) δ 185.06, 183.74, 173.64, 167.01, 164.14, 153.22, 151.90, 136.08, 126.72, 126.41, 118.26, 111.86, 62.36, 53.02, 49.75, 49.53, 43.98, 36.96, 35.83, 29.72, 28.97, 27.62, 24.55, 23.74, 20.95, 11.30. HRMS (ESI-TOF) m/z: [M+H]⁺ Calcd for C₇₆H₈₇N₁₆O₁₀⁺ 1383.6786; Found 1383.6791.



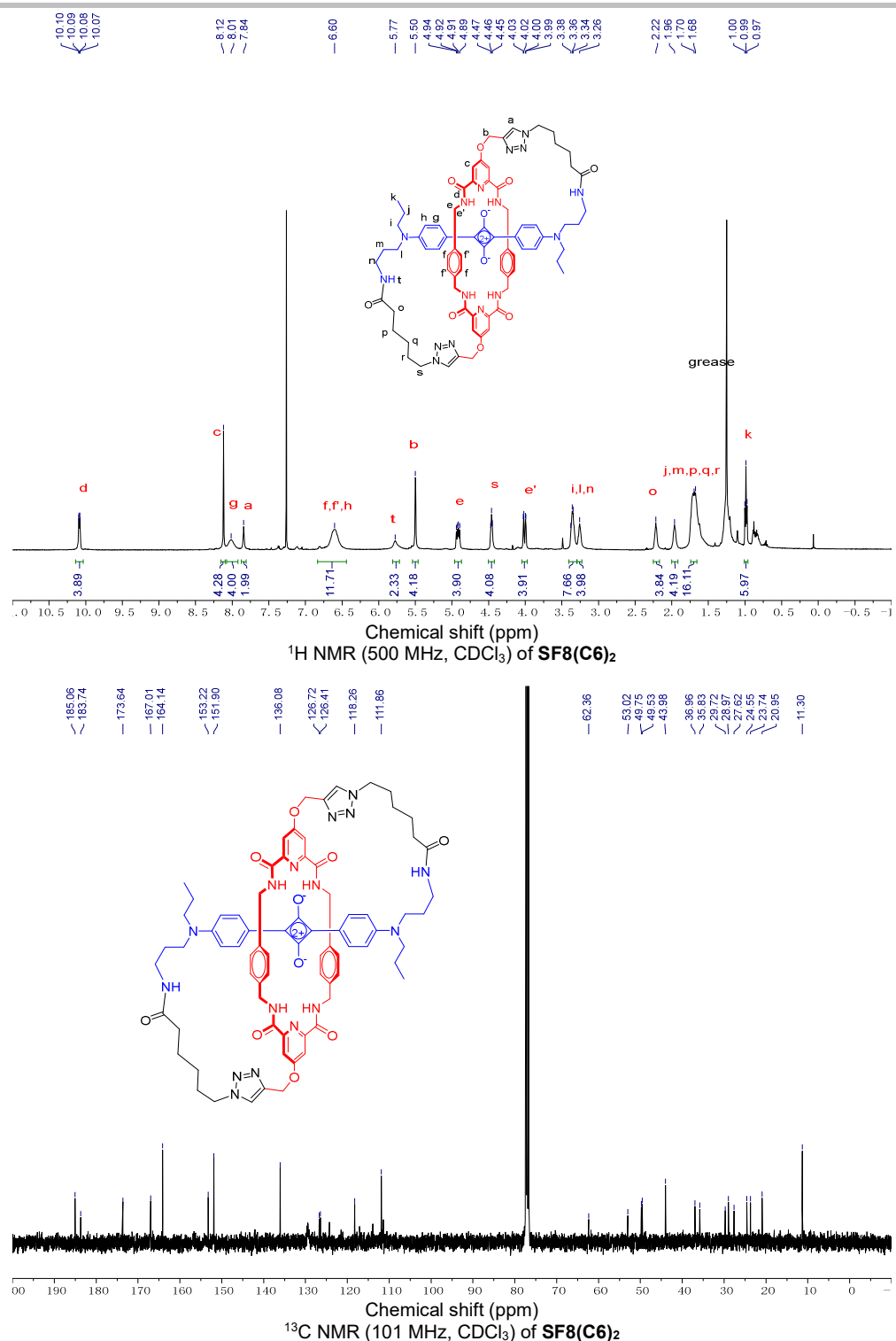
SUPPORTING INFORMATION



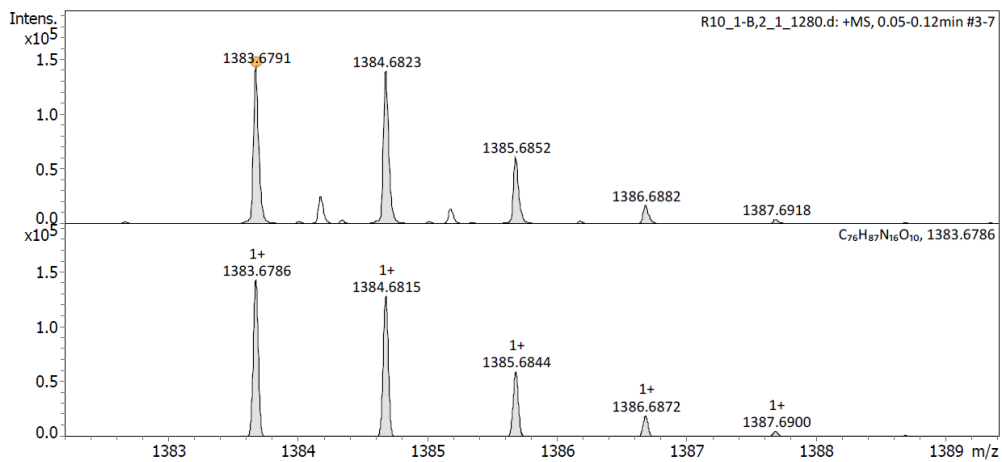
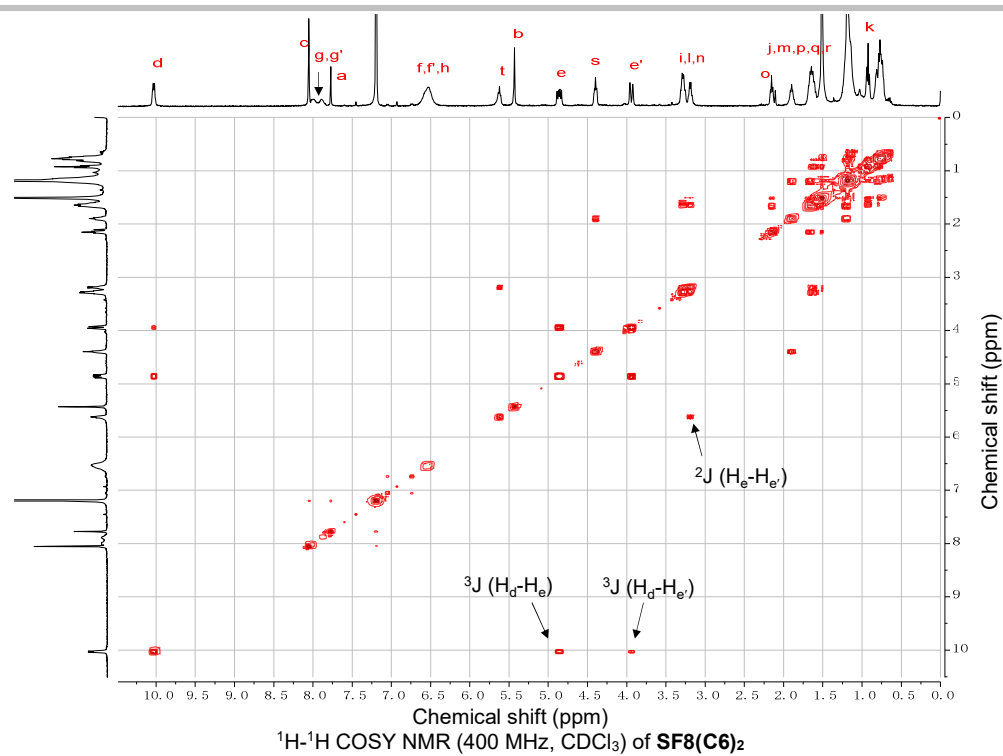
Meas. m/z	#	Ion Formula	m/z	err [ppm]	mSigma	# mSigma	Score	rdb	e ⁻ Conf	N-Rule
1383.6784	1	C ₇₆ H ₈₇ N ₁₆ O ₁₀	1383.6786	0.1	14.3	1	100.00	42.0	even	ok

HRMS-ESI of **SR2**

SUPPORTING INFORMATION



SUPPORTING INFORMATION



Meas. m/z	#	Ion Formula	m/z	err [ppm]	mSigma	# mSigma	Score	rdb	e ⁻ Conf	N-Rule
1383.6791	1	$\text{C}_{76}\text{H}_{87}\text{N}_{16}\text{O}_{10}$	1383.6786	-0.4	36.0	1	100.00	42.0	even	ok

General procedure for the synthesis of side chain protected linear peptide^[5]: Linear peptides were synthesized through solid phase peptide synthesis (SPPS) procedure. H-Gly-2-Cl-Trt Resin (1.0 equiv.) with a loading rate of 0.714 mmol/g or 0.692 mmol/g was used for the solid phase peptide synthesis. Fmoc protecting group was removed using 20% piperidine in DMF for 40 mins. For the coupling reactions of amino acids, Fmoc-aa(PG)-OH (3.0 equiv.), 6-chloro-1-hydroxybenzotriazole (HOEt-Cl) (5.0 equiv.) and *N,N'*-diisopropylcarbodiimide (DIC) (10.0 equiv.) were dissolved in 1-methyl-2-pyrrolidinone (NMP) and the reaction was shaken at room temperature for 6 h or overnight. The Kaiser test was used to determine if the coupling reaction or Fmoc group deprotection was complete. After all the coupling reactions were done, the linear peptide was cleaved from the resin using a mixture of $\text{CH}_2\text{Cl}_2/\text{CF}_3\text{CH}_2\text{OH}/\text{CH}_3\text{COOH}$ (3/1/1, v/v/v) at room temperature for at least 3 h. The solution was transferred into a flask and the solvent was removed through rotary evaporation. The side chain protected linear peptide was obtained as light yellow solid and the compound confirmed by HRMS-ESI.

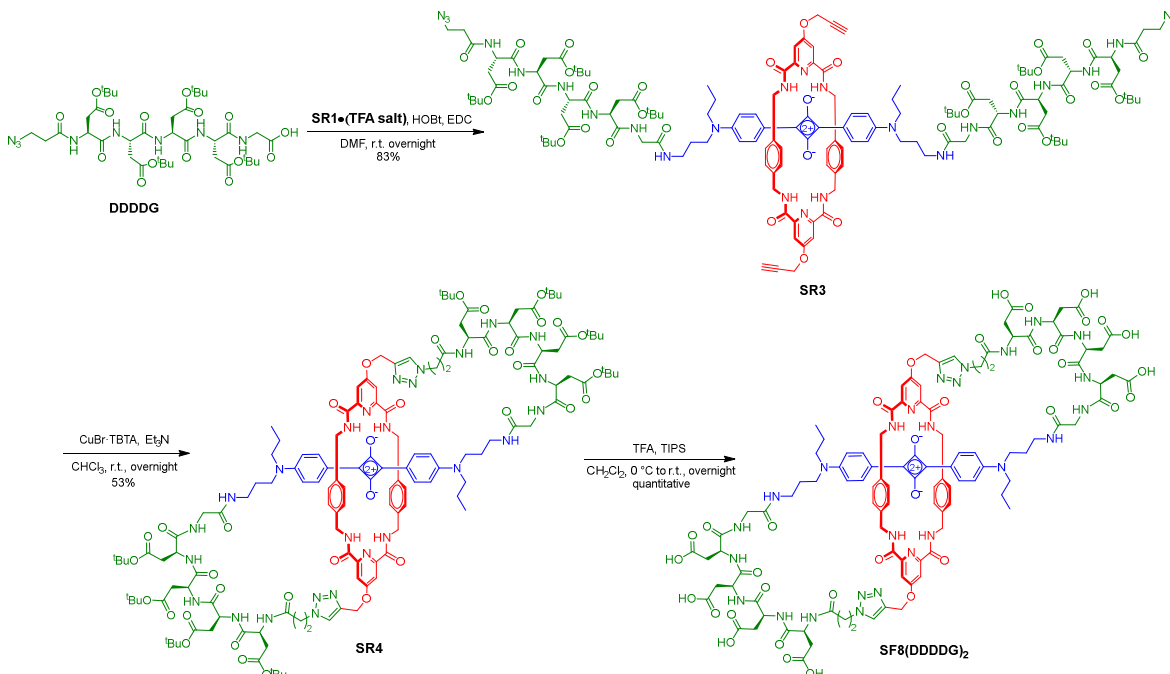
General procedure for amide coupling of side chain protected linear peptide and squaraine rotaxane SR1: A mixture of **SR1•(TFA salt)** (15 mg, 1 equiv.), side chain protected linear peptide (8 equiv.), 1-hydroxybenzotriazole hydrate (HOEt) (12 equiv.) and EDC (12 equiv.) in DMF (1 mL) was stirred at room temperature overnight. The solvent was removed by rotary evaporation and

SUPPORTING INFORMATION

the resulting residue was purified by silica gel column chromatography (0–10% MeOH in CH₂Cl₂) to give the side chain protected linear peptide squaraine rotaxane conjugate as green blue solid (~80% yield).

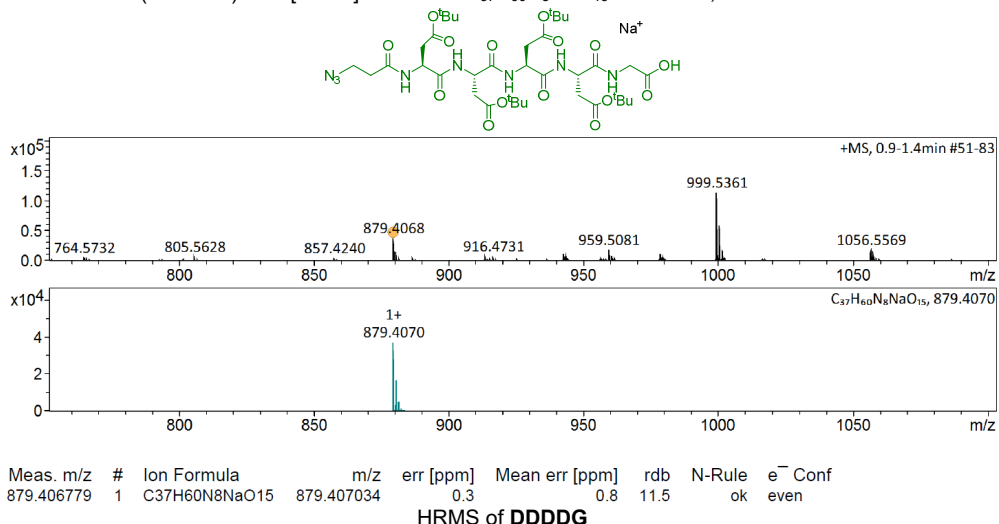
General procedure for double macrocyclization using Cu catalyzed azide-alkyne cycloaddition (CuAAC) to make side-chain protected SF8 molecule: Linear bis(azido)squaraine rotaxane (~20 mg, 1 equiv.) was dissolved in CHCl₃ (0.5 mM reaction solution); CuBr-TBTA (6 mg) and Et₃N (20 equiv.) were added to the solution which was stirred at room temperature overnight. The solvent was removed by rotary evaporation and the resulting residue was purified by silica gel column chromatography (0–15% MeOH in CH₂Cl₂) to produce side-chain protected SF8 product as green blue solid (27%–53% yield).

General procedure for side-chain deprotection: Trifluoroacetic acid (TFA) (2 mL) was added dropwise to a solution of side chain protected SF8 compound (<40 mg) in CH₂Cl₂ (2 mL) and trisopropyl silane (TIPS) (0.2 mL) in an ice bath. The reaction was stirred overnight at room temperature. Solvent was removed and the residue was washed with Et₂O (×3) to yield the blue powder product.



Scheme S3. Synthesis of SF8(DDDDG)₂.

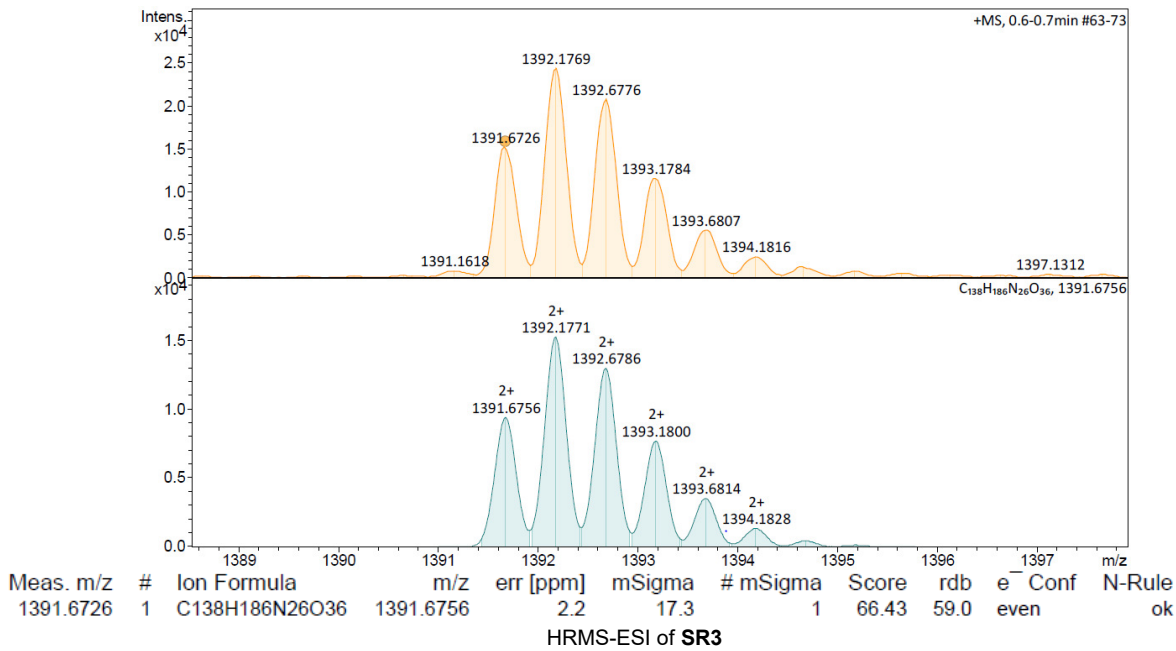
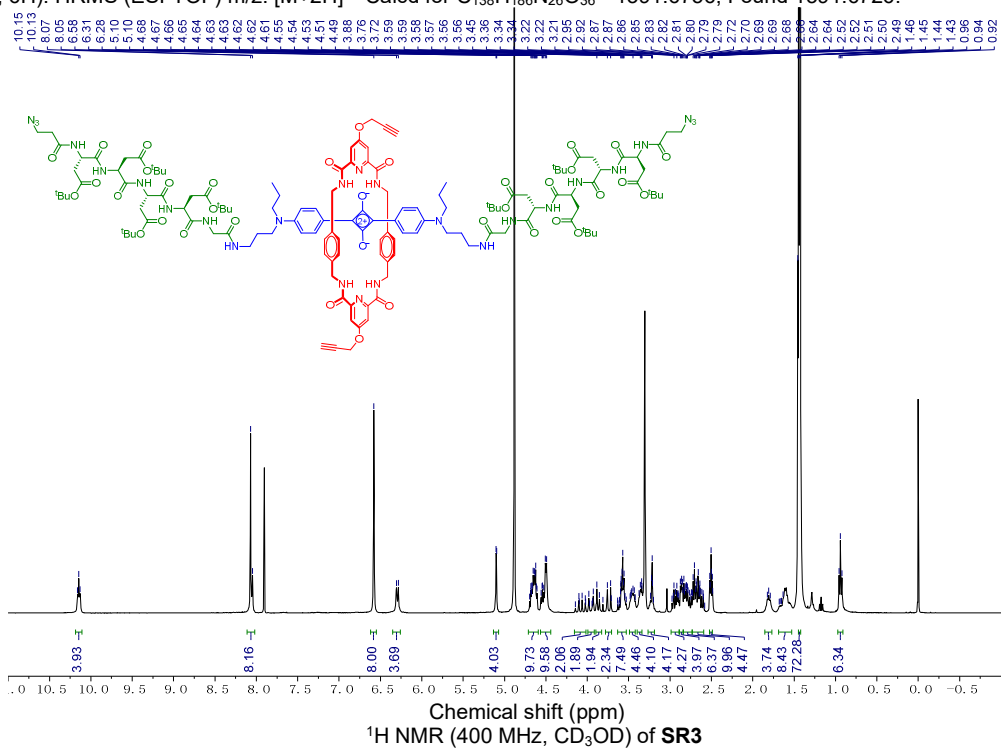
DDDDG. Yield 71%. HRMS (ESI-TOF) m/z: [M+Na]⁺ Calcd for C₃₇H₆₀N₈NaO₁₅⁺ 879.4070; Found 879.4068.



SR3. Yield 83%. ¹H NMR (400 MHz, Methanol-d₄) δ 10.15 (t, J = 5.9 Hz, 4H), 8.06 (d, J = 9.5 Hz, 8H), 6.58 (s, 8H), 6.30 (d, J = 9.0 Hz, 4H), 5.10 (d, J = 2.5 Hz, 4H), 4.71–4.59 (m, 10H), 4.57–4.44 (m, 10H), 4.15–4.02 (m, 2H), 3.99–3.92 (m, 2H), 3.87 (d, J = 12.5 Hz, 2H), 3.74 (d, J = 16.9 Hz, 2H), 3.63–3.53 (m, 7H), 3.46 (m, 4H), 3.40–3.34 (m, 4H), 3.27–3.19 (m, 4H), 2.99–2.89 (m, 4H), 2.86 (dd, J = 6.5,

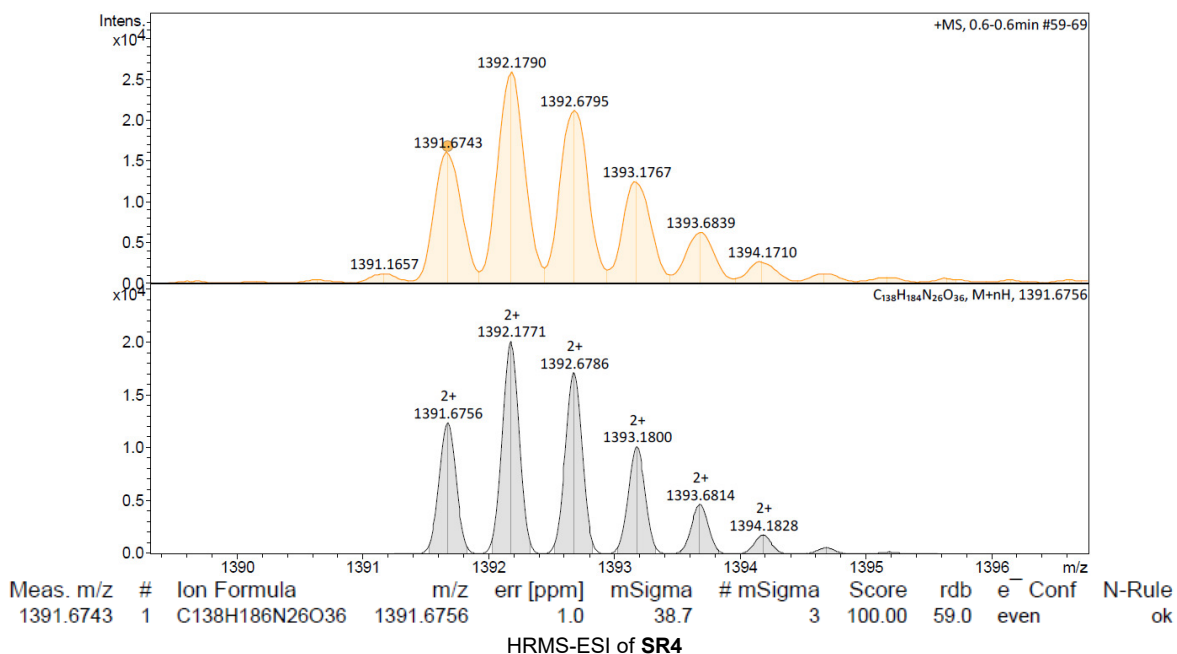
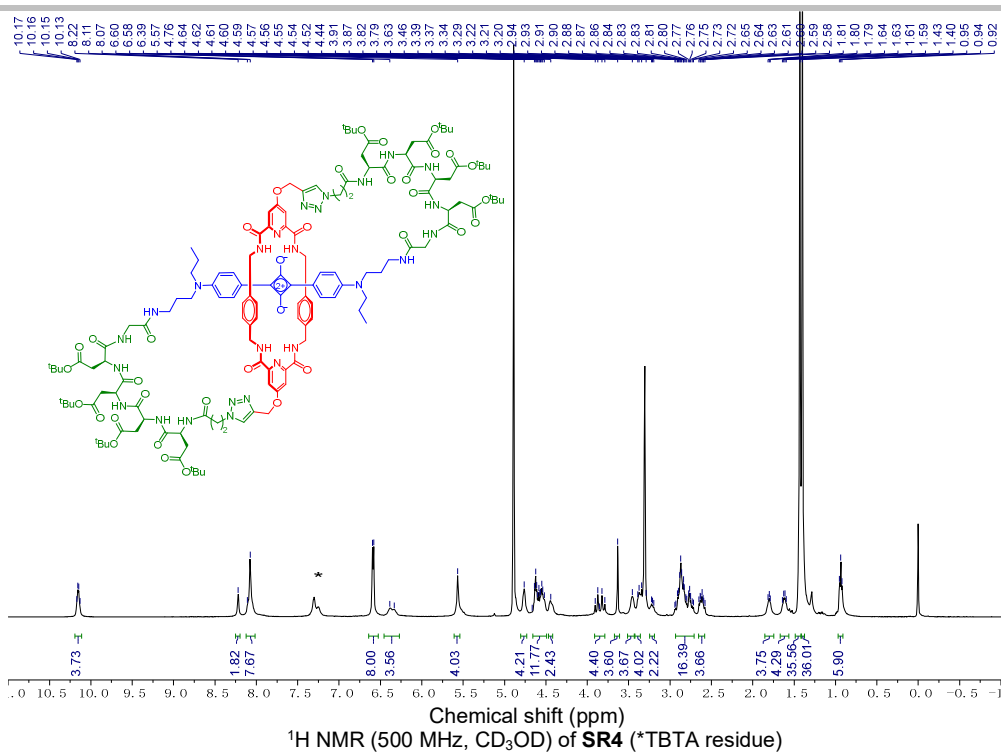
SUPPORTING INFORMATION

3.4 Hz, 4H), 2.84-2.73 (m, 6H), 2.73-2.59 (m, 10H), 2.52-2.49 (m, 4H), 1.85-1.77 (m, 4H), 1.69-1.53 (m, 8H), 1.45-1.42 (m, 72H), 0.94 (t, J = 7.3 Hz, 6H). HRMS (ESI-TOF) m/z: [M+2H]²⁺ Calcd for C₁₃₈H₁₈₆N₂₆O₃₆²⁺ 1391.6756; Found 1391.6726.



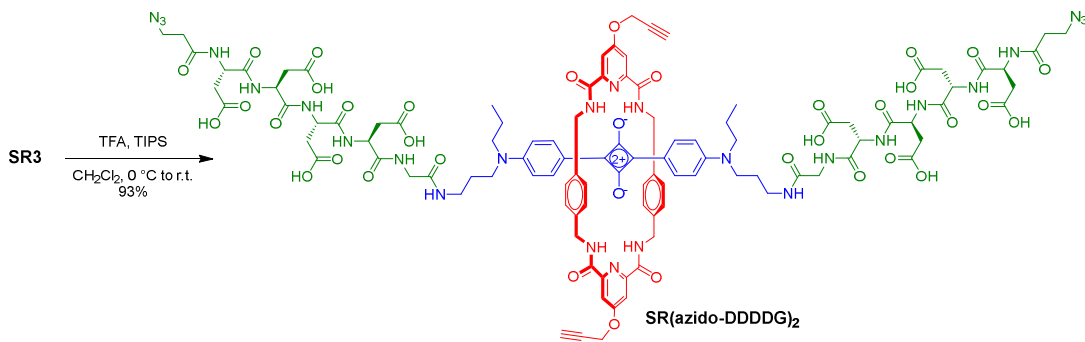
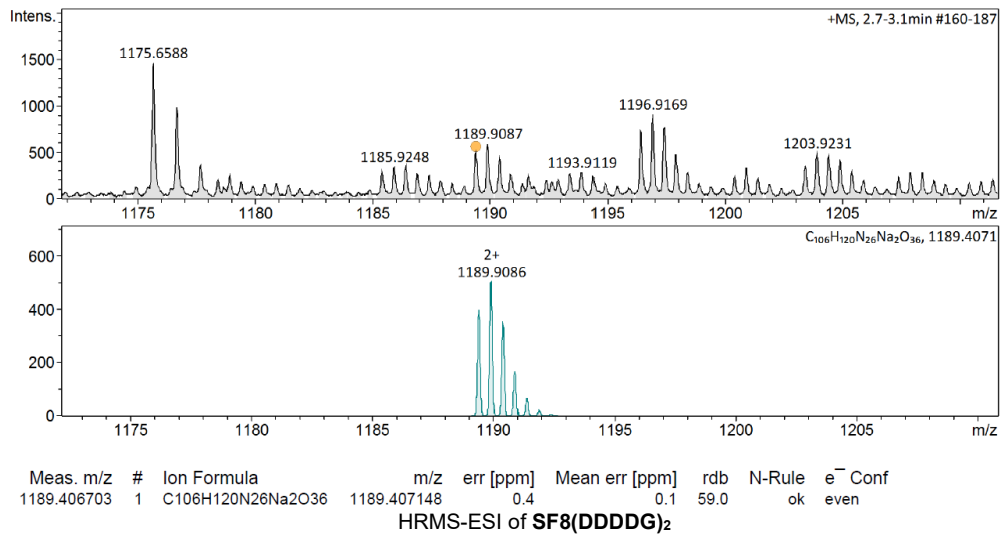
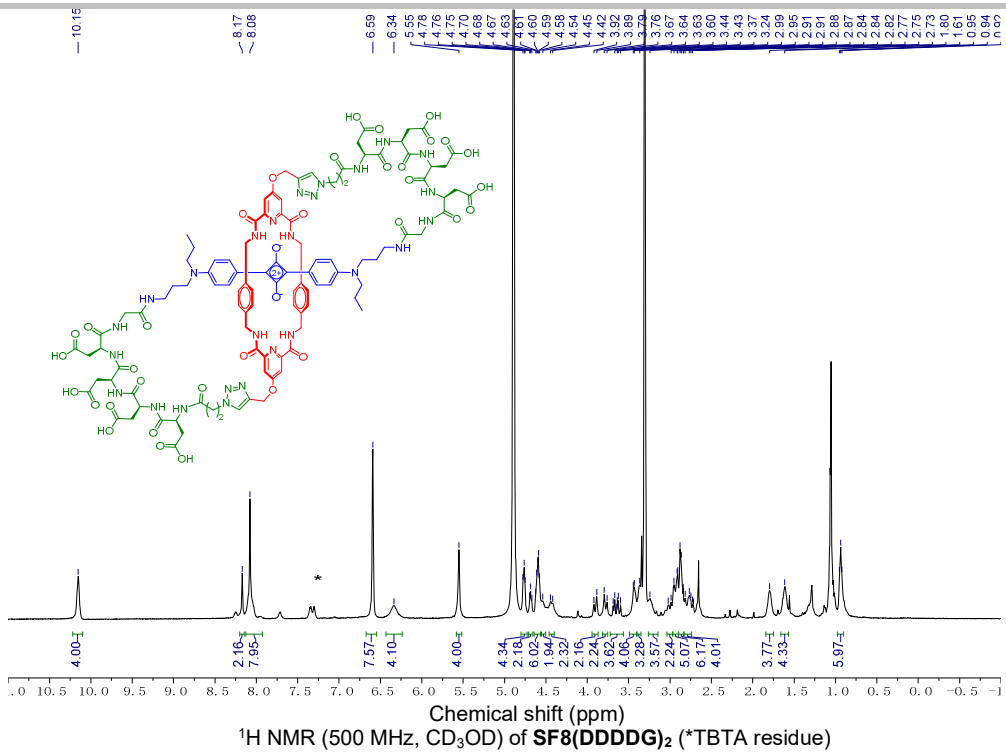
SR4. Yield 53%. ¹H NMR (500 MHz, Methanol-d₄) δ 10.15 (q, J = 6.4 Hz, 4H), 8.22 (s, 2H), 8.07 (s, 8H), 6.59 (d, J = 7.4 Hz, 8H), 6.36 (br, 4H), 5.57 (s, 4H), 4.76 (s, 4H), 4.58 (m, 12H), 4.44 (s, 2H), 3.91-3.79 (m, 4H), 3.63 (s, 4H), 3.46 (s, 4H), 3.38 (d, J = 8.0 Hz, 4H), 3.25-3.19 (m, 2H), 2.93-2.71 (m, 16H), 2.62 (m, 4H), 1.85-1.75 (m, 4H), 1.62 (q, J = 7.6 Hz, 4H), 1.43 (s, 36H), 1.40 (s, 36H), 0.94 (t, J = 7.8 Hz, 6H). HRMS (ESI-TOF) m/z: [M+2H]²⁺ Calcd for C₁₃₈H₁₈₆N₂₆O₃₆²⁺ 1391.6756; Found 1391.6743.

SUPPORTING INFORMATION



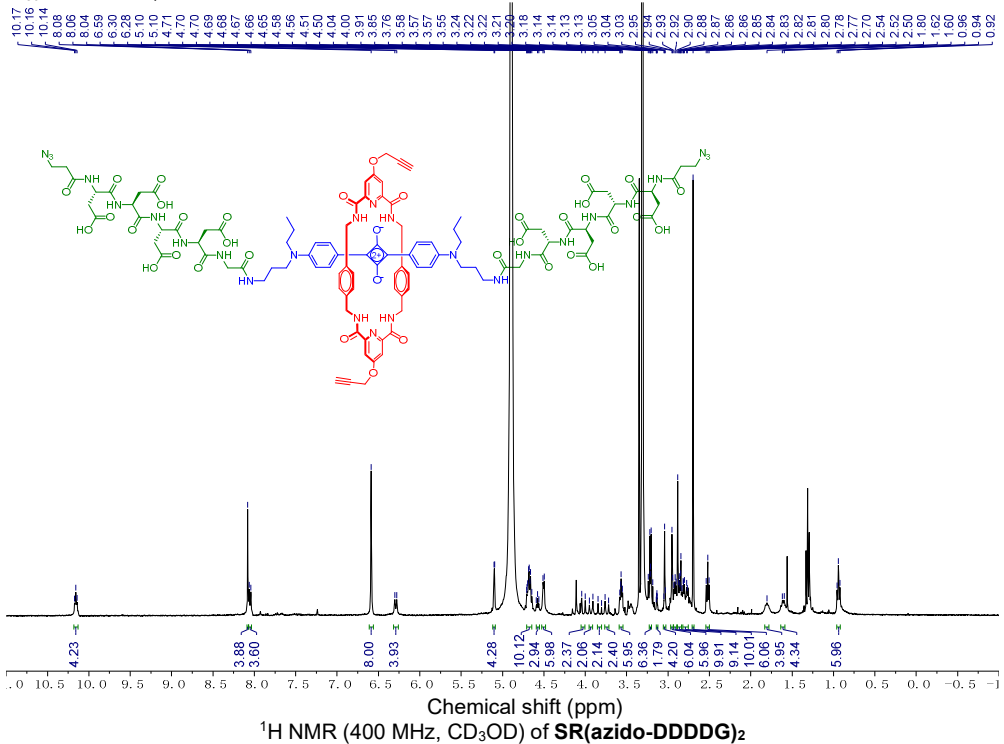
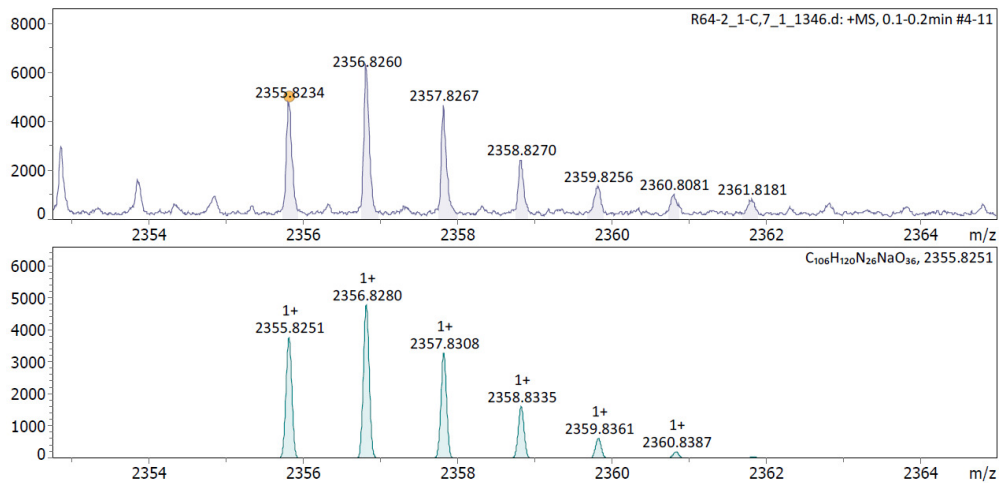
SF8(DDDG)₂. Yield quantitative. ¹H NMR (500 MHz, Methanol-d₄) δ 10.15 (s, 4H), 8.17 (s, 2H), 8.08 (s, 8H), 6.59 (s, 8H), 6.34 (br s, 4H), 5.55 (s, 4H), 4.76 (t, J = 6.1 Hz, 4H), 4.69 (d, J = 6.5 Hz, 2H), 4.60 (m, 6H), 4.54 (s, 2H), 4.43 (d, J = 14.2 Hz, 2H), 3.90 (d, J = 17.1 Hz, 2H), 3.78 (d, J = 16.8 Hz, 2H), 3.72-3.56 (m, 4H), 3.49-3.40 (m, 4H), 3.37 (s, 3H), 3.24 (s, 4H), 3.00 (d, J = 17.5 Hz, 2H), 2.97-2.90 (m, 5H), 2.87 (m, 6H), 2.79 (m, 4H), 1.80 (s, 4H), 1.61 (s, 4H), 0.93 (d, J = 7.6 Hz, 6H). HRMS (ESI-TOF) m/z: [M+2Na]²⁺ Calcd for C₁₀₆H₁₂₀N₂₆O₃₆²⁺ 1189.9086; Found 1189.9087.

SUPPORTING INFORMATION

Scheme S4. Synthesis of SR(azido-DDDDG)₂

SUPPORTING INFORMATION

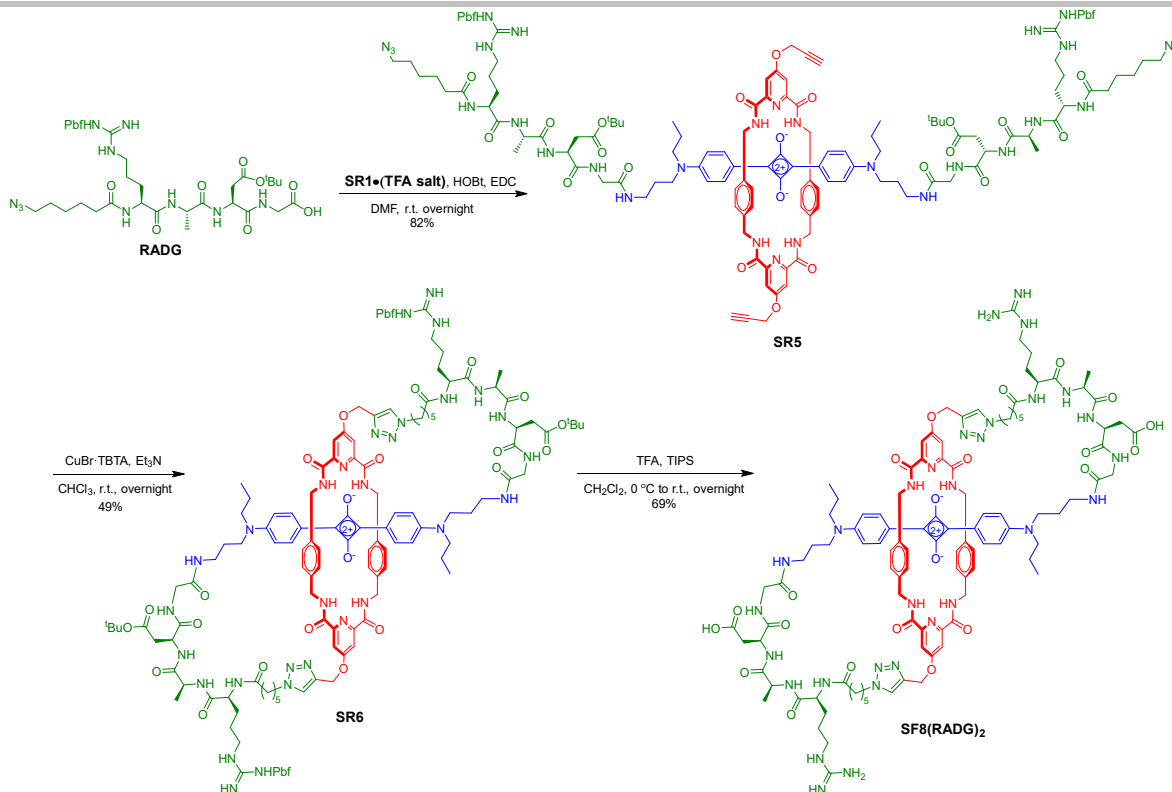
SR(azido-DDDDG)₂. Yield 93%. ¹H NMR (400 MHz, Methanol-d₄) δ 10.16 (t, J = 5.9 Hz, 4H), 8.08 (s, 4H), 8.05 (d, J = 8.9 Hz, 4H), 6.59 (s, 8H), 6.29 (d, J = 9.0 Hz, 4H), 5.10 (d, J = 2.4 Hz, 4H), 4.68 (m, 10H), 4.58 (t, J = 6.1 Hz, 3H), 4.50 (d, J = 5.8 Hz, 6H), 4.02 (d, J = 17.2 Hz, 2H), 3.93 (d, J = 16.8 Hz, 2H), 3.83 (d, J = 17.2 Hz, 2H), 3.74 (d, J = 16.8 Hz, 2H), 3.57 (t, J = 6.8 Hz, 6H), 3.23-3.20 (m, 6H), 3.14-3.12 (m, 2H), 3.04 (d, J = 3.7 Hz, 4H), 2.95 (d, J = 2.8 Hz, 6H), 2.93-2.89 (m, 6H), 2.89-2.84 (m, 10H), 2.82-2.76 (m, 9H), 2.70 (s, 10H), 2.52 (t, J = 6.5 Hz, 6H), 1.80 (m, 4H), 0.94 (t, J = 7.3 Hz, 6H). HRMS (ESI-TOF) m/z: [M+Na]⁺ Calcd for C₁₀₆H₁₂₀N₂₆NaO₃₆⁺ 2355.8251; Found 2355.8234.

¹H NMR (400 MHz, CD₃OD) of SR(azido-DDDDG)₂

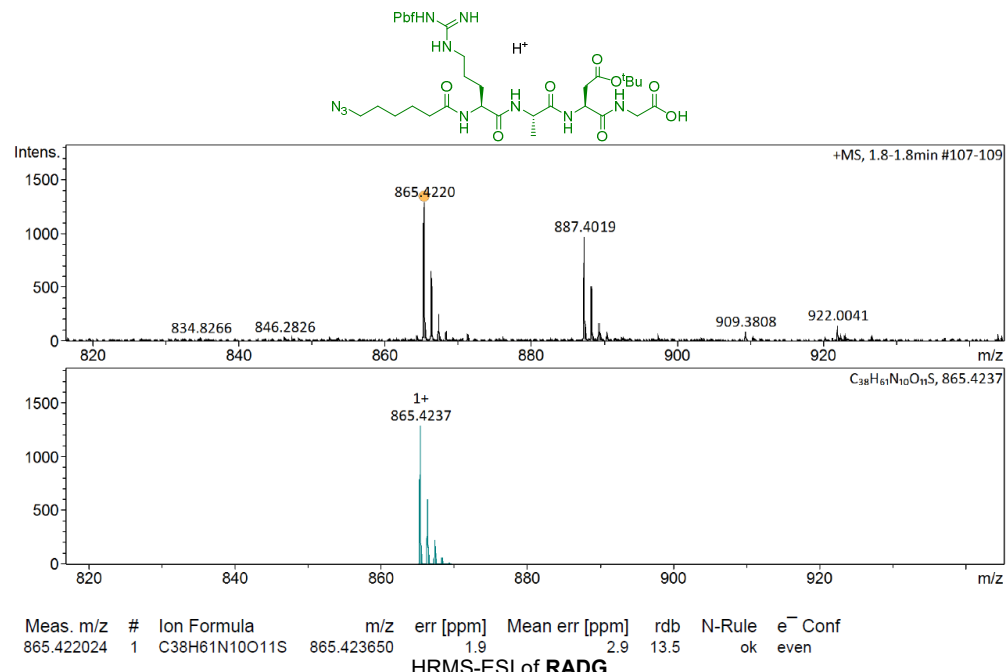
Meas. m/z	#	Ion Formula	m/z	err [ppm]	mSigma	# mSigma	Score	rdb	e ⁻ Conf	N-Rule
2355.8234	1	C ₁₀₆ H ₁₂₀ N ₂₆ NaO ₃₆	2355.8251	0.7	56.1	1	100.00	60.0	even	ok

HRMS-ESI of SR(azido-DDDDG)₂

SUPPORTING INFORMATION

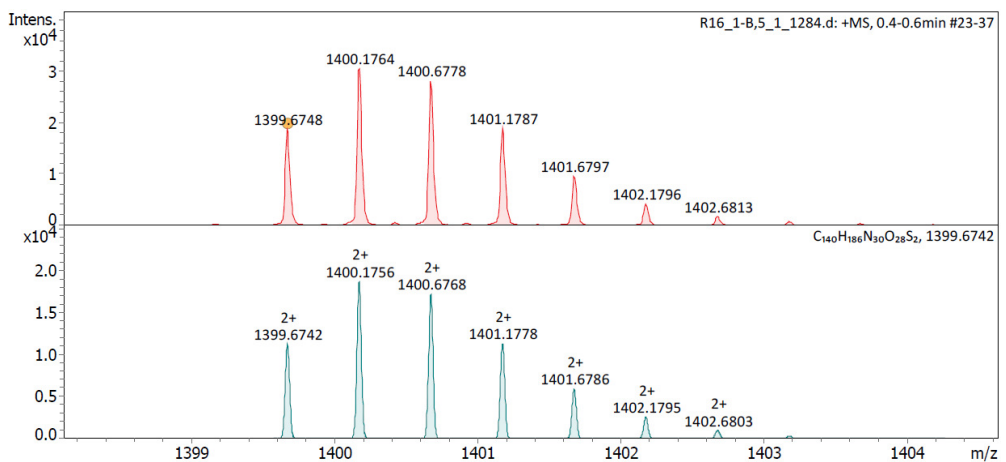
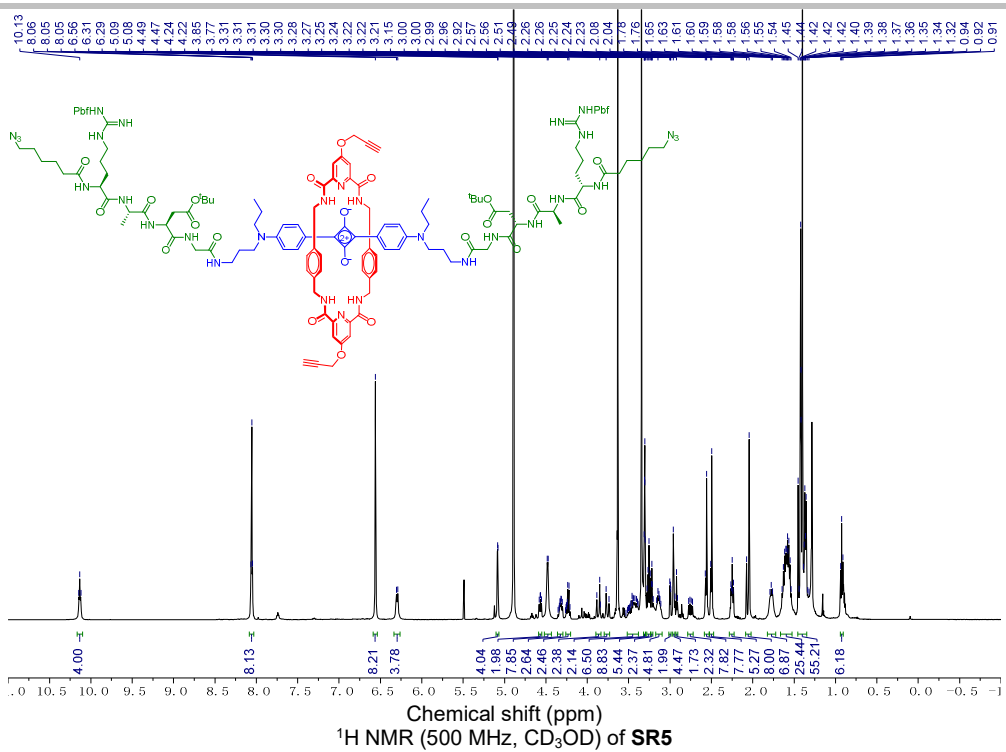
**Scheme S5.** Synthesis of SF8(RADG)₂.

RADG. Yield 69%. HRMS (ESI-TOF) m/z: [M+H]⁺ Calcd for C₃₈H₆₁N₁₀O₁₁S⁺ 865.4237; Found 865.4220.



SR5. Yield 82%. ¹H NMR (500 MHz, Methanol-d₄) δ 10.13 (t, J = 6.0 Hz, 4H), 8.09-8.03 (m, 8H), 6.56 (s, 8H), 6.30 (d, J = 8.9 Hz, 4H), 5.08 (d, J = 2.5 Hz, 4H), 4.57 (dd, J = 7.9, 5.5 Hz, 2H), 4.48 (d, J = 5.9 Hz, 8H), 4.33 (m, 3H), 4.26-4.20 (m, 2H), 3.87 (d, J = 17.0 Hz, 2H), 3.75 (d, J = 16.9 Hz, 2H), 3.52-3.38 (m, 7H), 3.31 (m, 9H), 3.26 (q, J = 6.5 Hz, 5H), 3.22 (t, J = 2.4 Hz, 2H), 3.14 (m, 5H), 3.01-2.99 (m, 2H), 2.95 (d, J = 8.8 Hz, 4H), 2.91 (d, J = 5.8 Hz, 2H), 2.75 (dd, J = 16.4, 8.0 Hz, 2H), 2.56 (d, J = 7.7 Hz, 8H), 2.50 (d, J = 6.7 Hz, 8H), 2.28-2.22 (m, 5H), 2.06 (d, J = 15.7 Hz, 8H), 1.82-1.72 (m, 7H), 1.66-1.53 (m, 25H), 1.46-1.35 (m, 55H), 0.92 (t, J = 7.3 Hz, 6H). HRMS (ESI-TOF) m/z: [M+2H]²⁺ Calcd for C₁₄₀H₁₈₆N₃₀O₂₈S₂²⁺ 1399.6742; Found 1399.6748.

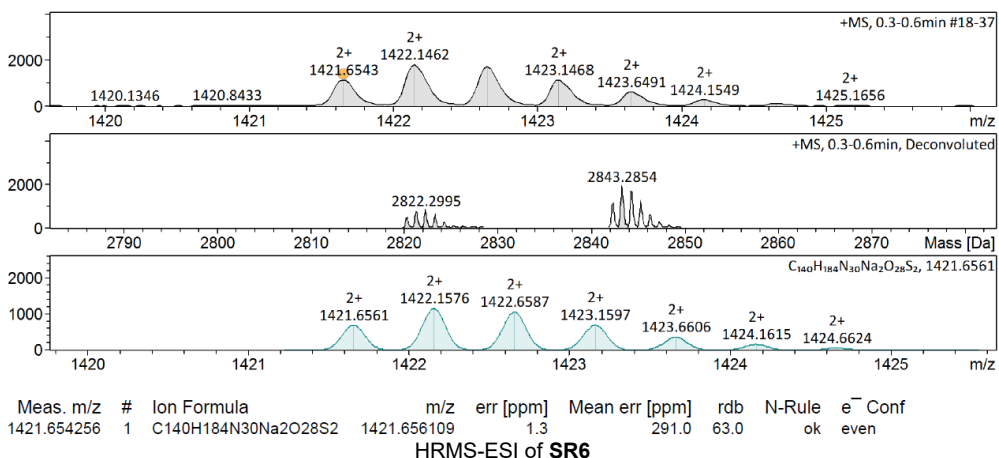
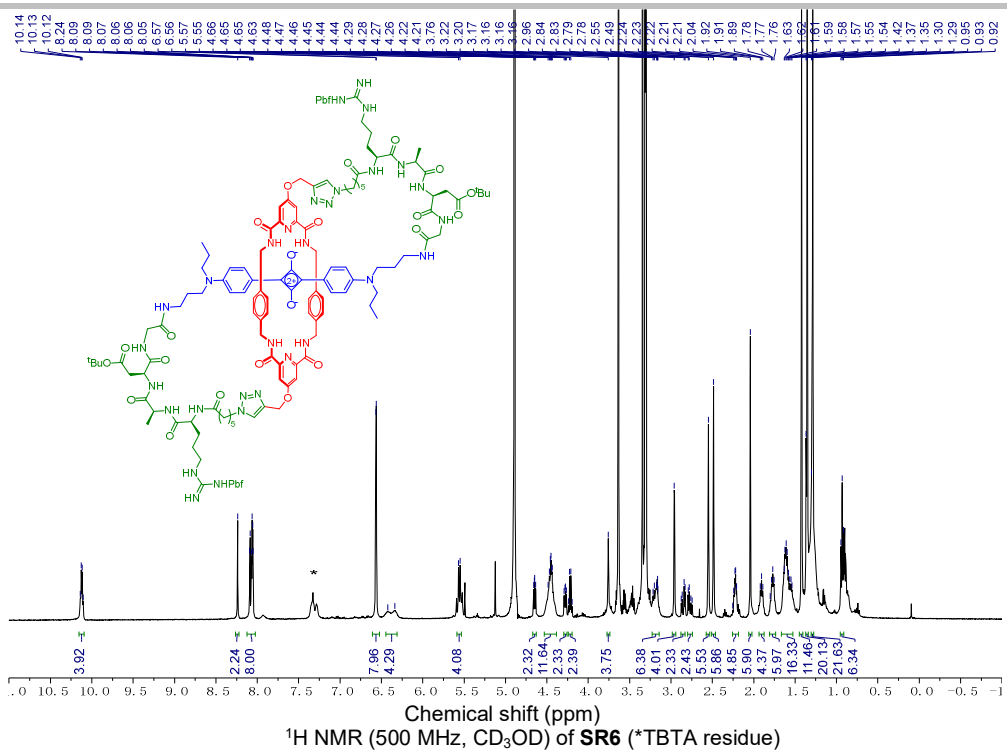
SUPPORTING INFORMATION



Meas. m/z	#	Ion Formula	m/z	err [ppm]	mSigma	# mSigma	Score	rdb	e ⁻ Conf	N-Rule
1399.6748	1	C ₁₄₀ H ₁₈₆ N ₃₀ O ₂₈ S ₂	1399.6742	-0.5	8.3	1	100.00	68.0	even	ok

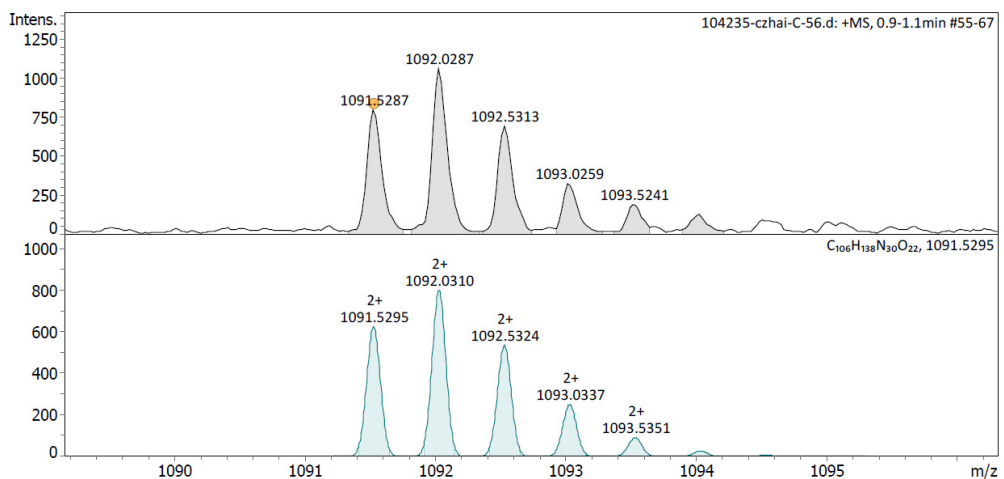
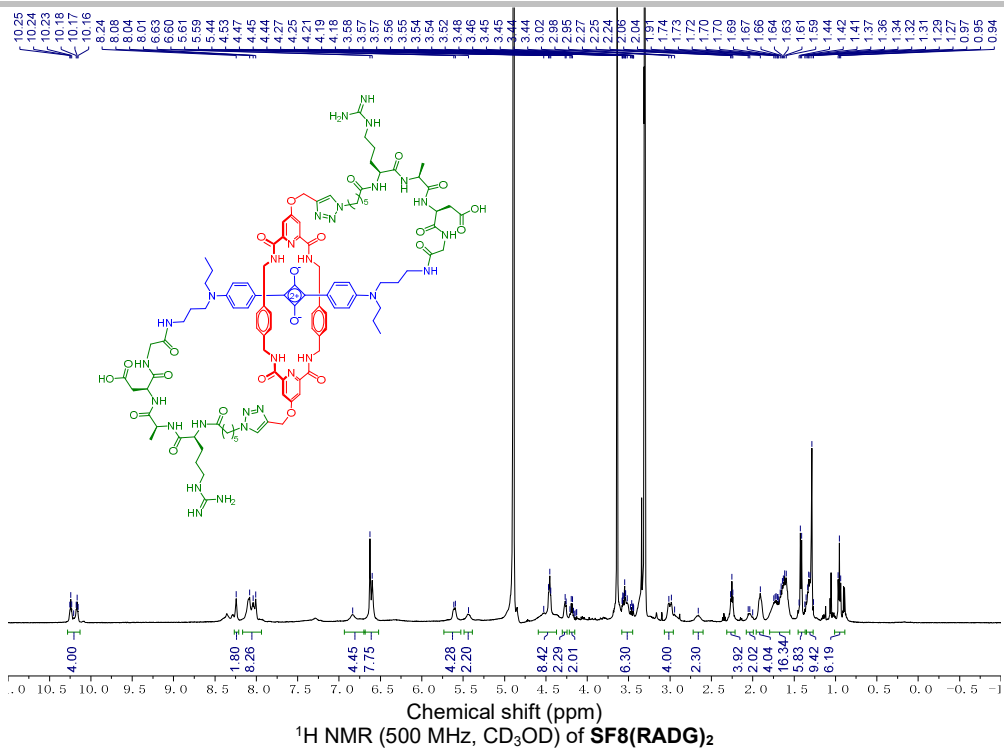
SR6. Yield 49%. ¹H NMR (500 MHz, Methanol-d₄) δ 10.12 (q, *J* = 5.7 Hz, 4H), 8.24 (s, 2H), 8.12-8.02 (m, 8H), 6.56 (d, *J* = 2.3 Hz, 8H), 6.38 (br, 4H), 5.56 (d, *J* = 9.4 Hz, 4H), 4.65 (dd, *J* = 7.4, 5.5 Hz, 2H), 4.53-4.39 (m, 12H), 4.28 (dd, *J* = 8.6, 5.5 Hz, 2H), 4.22 (q, *J* = 7.2 Hz, 2H), 3.76 (s, 4H), 3.23-3.14 (m, 6H), 2.96 (s, 4H), 2.85 (dd, *J* = 16.6, 5.5 Hz, 2H), 2.77 (dd, *J* = 16.6, 7.5 Hz, 2H), 2.55 (s, 6H), 2.49 (s, 6H), 2.26-2.18 (m, 5H), 2.04 (s, 6H), 1.94-1.87 (m, 4H), 1.81-1.74 (m, 6H), 1.59 (m, 16H), 1.42 (s, 11H), 1.35 (s, 20H), 1.29 (s, 22H), 0.93 (t, *J* = 7.6 Hz, 6H). HRMS (ESI-TOF) m/z: [M+2Na]²⁺ Calcd for C₁₄₀H₁₈₄N₃₀Na₂O₂₈S₂²⁺ 1421.6561; Found 1421.6543.

SUPPORTING INFORMATION



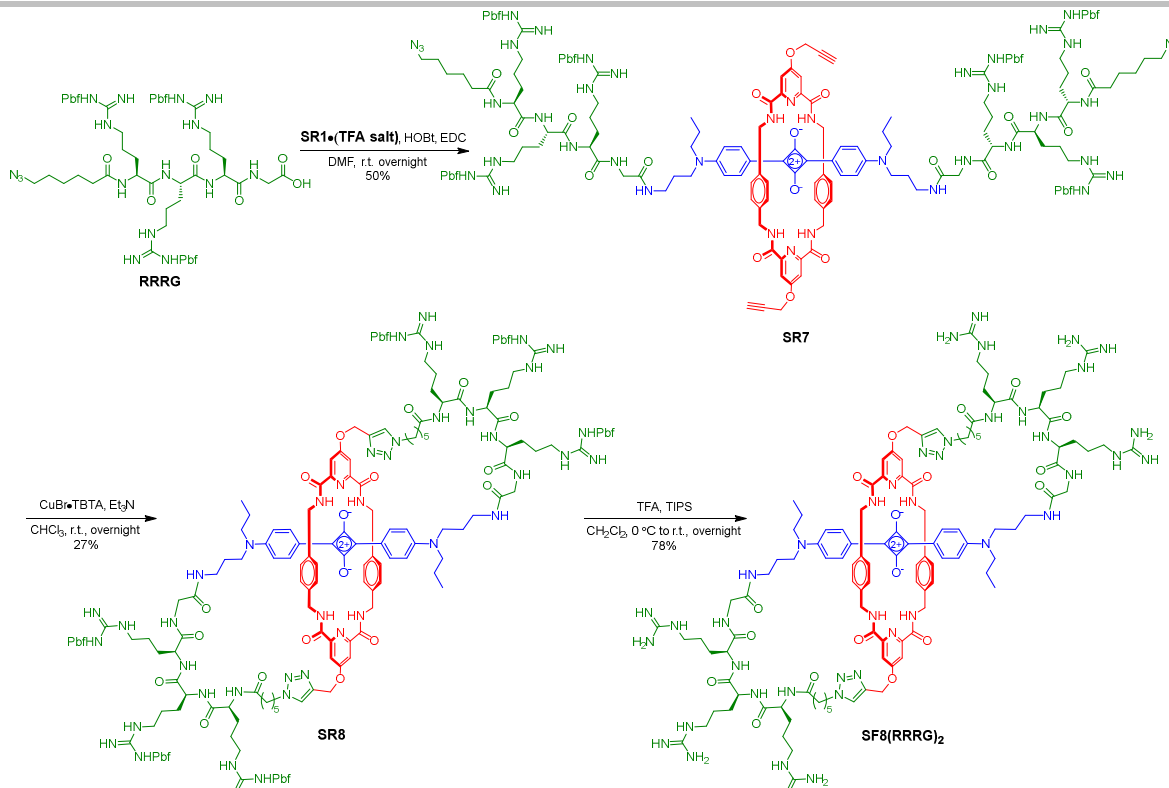
SF8(RADG)₂. Yield 69%. ¹H NMR (500 MHz, Methanol-d₄) δ 10.20 (dt, J = 38.2, 5.6 Hz, 4H), 8.24 (s, 2H), 8.17-7.94 (m, 8H), 6.84 (br s, 4H), 6.61 (d, J = 13.6 Hz, 8H), 5.60 (d, J = 9.1 Hz, 4H), 5.44 (br s, 2H), 4.45 (t, J = 6.7 Hz, 8H), 4.26 (d, J = 7.2 Hz, 2H), 4.19 (q, J = 7.3 Hz, 2H), 3.58-3.45 (m, 6H), 3.00 (d, J = 16.0 Hz, 4H), 2.66 (br s, 2H), 2.25 (t, J = 6.8 Hz, 4H), 2.05 (d, J = 9.7 Hz, 2H), 1.91 (s, 4H), 1.80-1.55 (m, 16H), 1.42 (d, J = 7.1 Hz, 6H), 1.29 (s, 9H), 0.95 (t, J = 7.4 Hz, 6H). HRMS (ESI-TOF) m/z: [M+2H]²⁺ Calcd for C₁₀₆H₁₃₇N₃₀O₂₂²⁺ 1091.5295; Found 1091.5287.

SUPPORTING INFORMATION

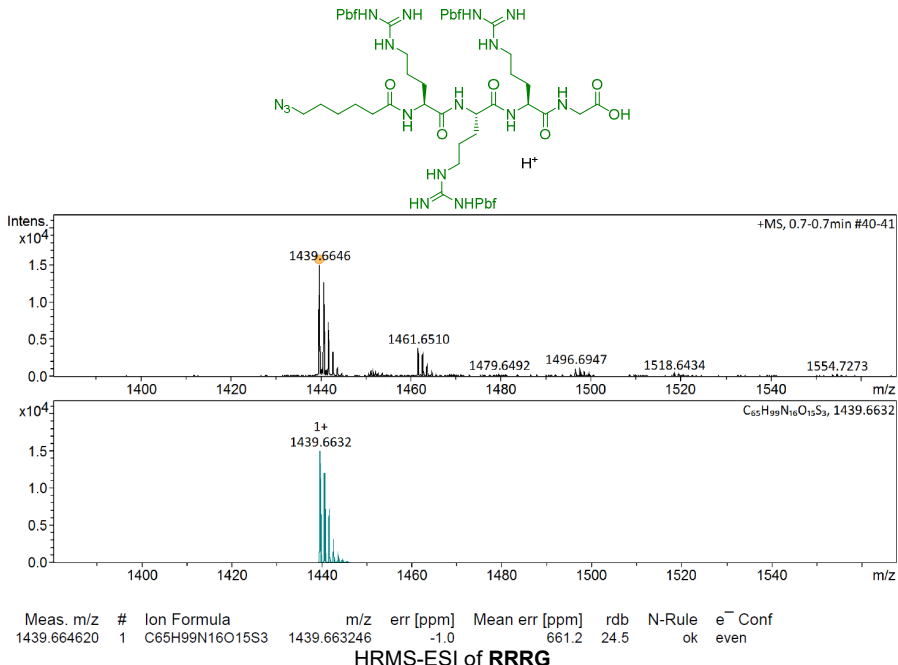


Meas. m/z	#	Ion Formula	m/z	err [ppm]	Mean err [ppm]	rdb	N-Rule	e ⁻ Conf
1091.528680	1	C ₁₀₆ H ₁₃₈ N ₃₀ O ₂₂	1091.529550	0.8	1.9	54.0	ok	even

SUPPORTING INFORMATION

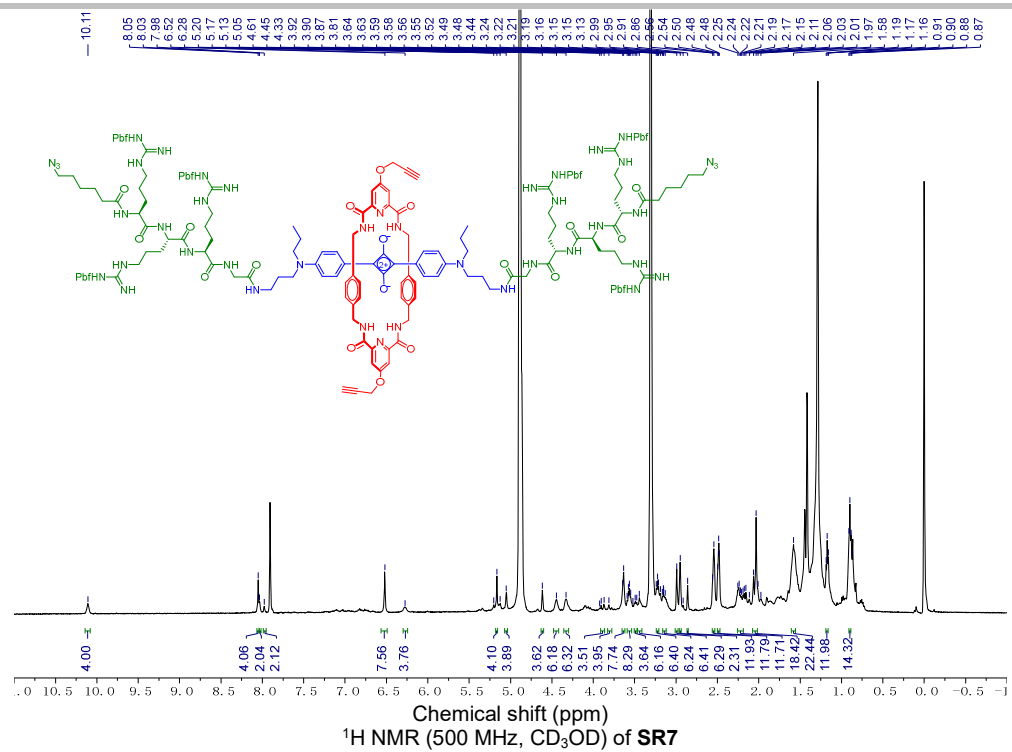
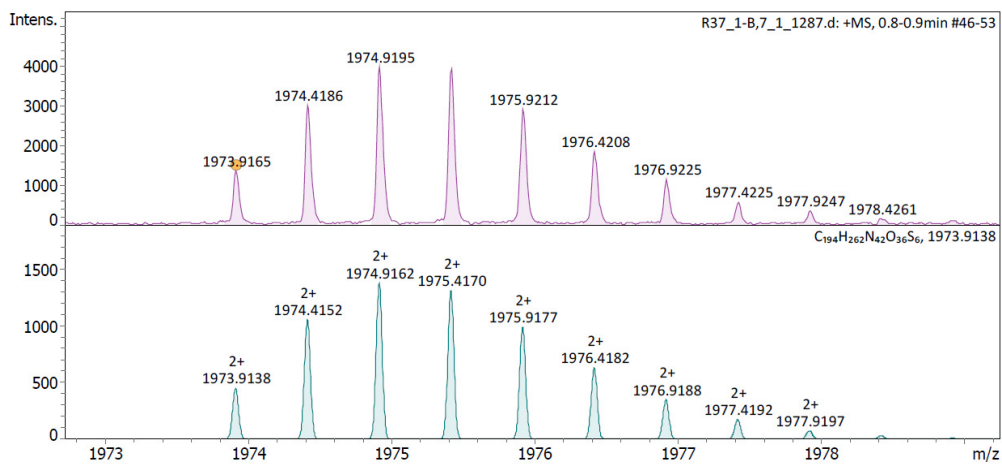
Scheme S6. Synthesis of SF8(RRRG)₂.

RRRG. Yield 54%. HRMS (ESI-TOF) m/z : [M+H]⁺ Calcd for C₆₅H₉₉N₁₆O₁₅S₃⁺ 1439.6632; Found 1439.6646.



SR7. Yield 50%. ¹H NMR (500 MHz, Methanol-d₄) δ 10.11 (s, 4H), 8.05 (s, 4H), 8.03 (s, 2H), 7.98 (s, 2H), 6.52 (s, 8H), 6.28 (br s, 4H), 5.17 (s, 4H), 5.05 (s, 4H), 4.61 (s, 4H), 4.45 (s, 6H), 4.33 (s, 6H), 3.89 (d, $J = 17.0$ Hz, 4H), 3.81 (s, 4H), 3.63 (s, 8H), 3.56 (t, $J = 7.0$ Hz, 8H), 3.48 (d, $J = 8.7$ Hz, 4H), 3.44 (s, 6H), 3.22 (t, $J = 6.5$ Hz, 6H), 3.16-3.12 (m, 6H), 2.99 (s, 6H), 2.95 (s, 6H), 2.86 (s, 2H), 2.55 (d, $J = 8.8$ Hz, 12H), 2.49 (d, $J = 6.8$ Hz, 12H), 2.26-2.19 (m, 12H), 2.05 (m, 18H), 1.58 (s, 22H), 1.18 (m, 12H), 0.90 (s, 14H). HRMS (ESI-TOF) m/z : [M+2H]²⁺ Calcd for C₁₉₄H₂₆₂N₄₂O₃₆S₆²⁺ 1973.9138; Found 1973.9165.

SUPPORTING INFORMATION

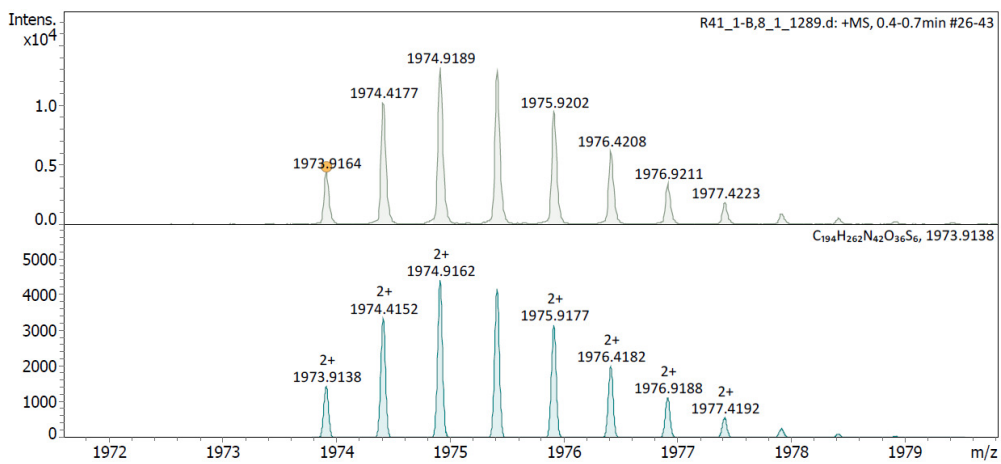
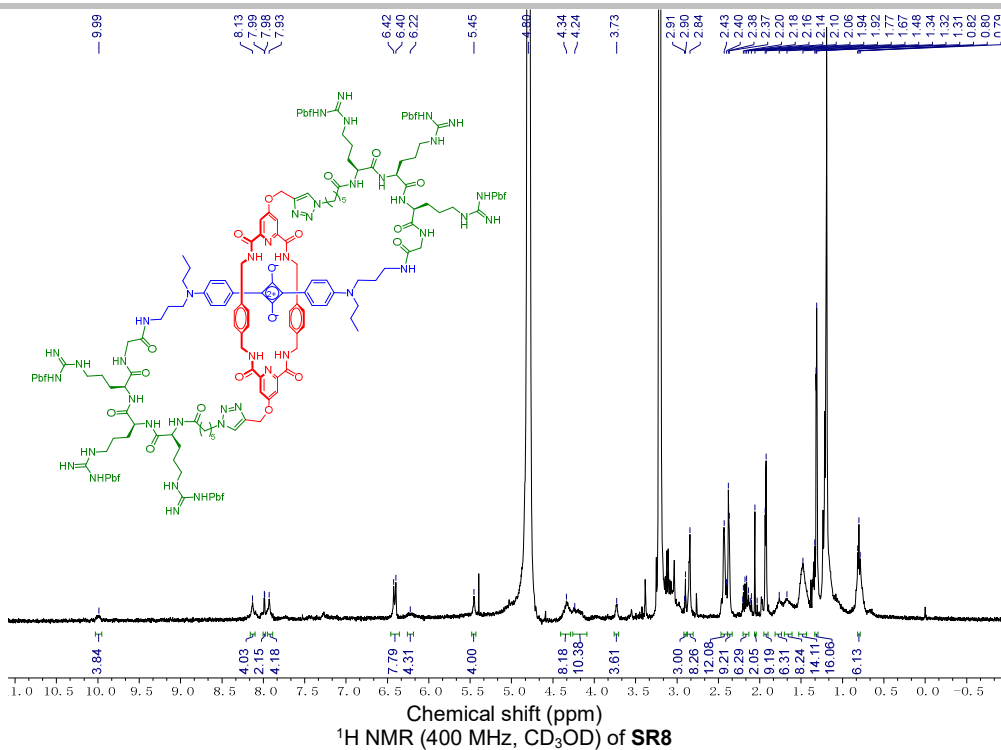
¹H NMR (500 MHz, CD_3OD) of SR7

Meas. m/z	#	Ion Formula	m/z	err [ppm]	mSigma	# mSigma	Score	rdb	e ⁻ Conf	N-Rule
1973.9165	1	$\text{C}_{194}\text{H}_{262}\text{N}_{42}\text{O}_{36}\text{S}_6$	1973.9138	-1.4	27.1	1	100.00	98.0	even	ok

HRMS-ESI of SR7

SR8. Yield 27%. ¹H NMR (400 MHz, Methanol-*d*₄) δ 9.99 (br s, 4H), 8.13 (s, 4H), 7.99 (d, *J* = 2.4 Hz, 2H), 7.93 (s, 4H), 6.41 (d, *J* = 9.5 Hz, 8H), 6.22 (br s, 4H), 5.45 (s, 4H), 4.34 (m, 8H), 4.24 (m, 10H), 3.73 (s, 4H), 2.90 (d, *J* = 4.2 Hz, 3H), 2.84 (s, 8H), 2.42 (d, *J* = 11.2 Hz, 12H), 2.37 (d, *J* = 4.2 Hz, 9H), 2.20-2.13 (m, 6H), 2.06 (s, 2H), 1.93 (d, *J* = 4.6 Hz, 9H), 1.77 (m, 6H), 1.67 (m, 8H), 1.48 (s, 14H), 1.31 (m, 16H), 0.80 (s, 6H). HRMS (ESI-TOF) m/z : [M+2H]²⁺ Calcd for $\text{C}_{194}\text{H}_{262}\text{N}_{42}\text{O}_{36}\text{S}_6^{2+}$ 1973.9138; Found 1973.9164.

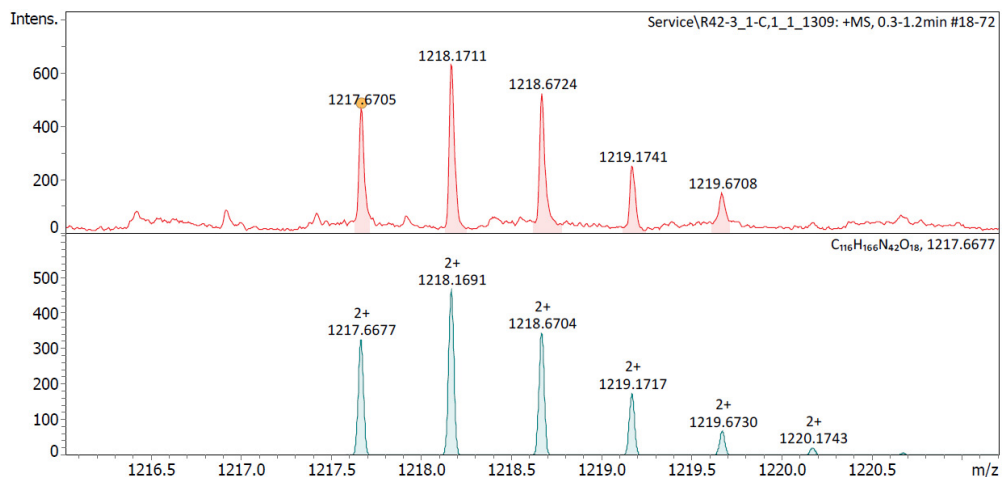
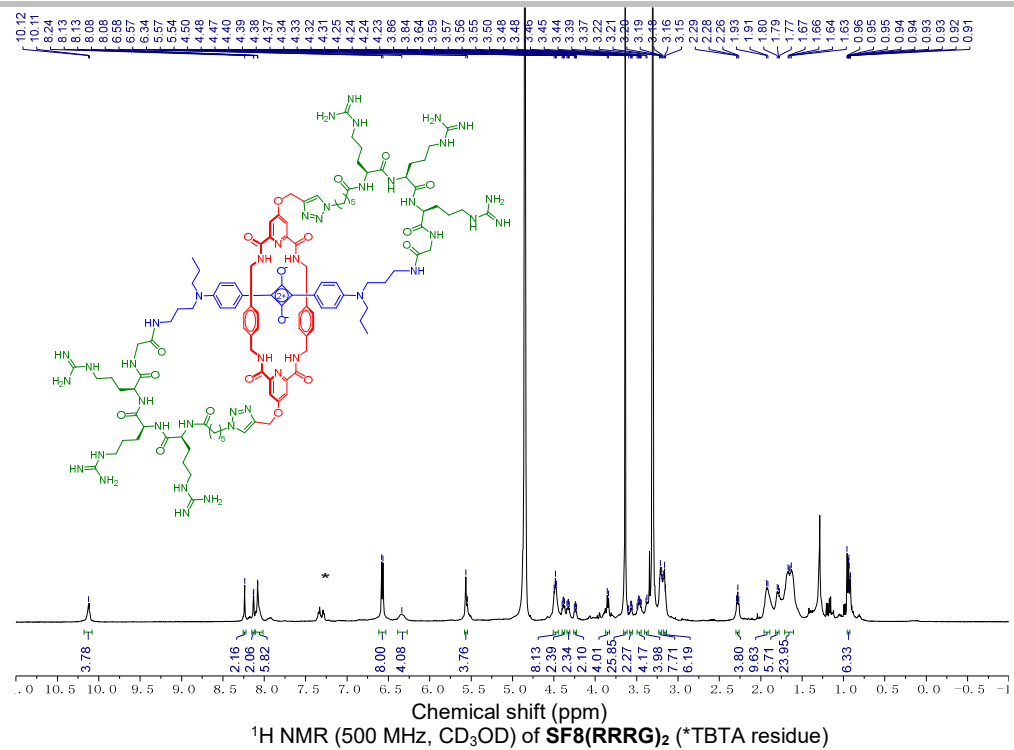
SUPPORTING INFORMATION



Meas. m/z	#	Ion Formula	m/z	err [ppm]	mSigma	# mSigma	Score	rdb	e ⁻ Conf	N-Rule
1973.9164	1	C ₁₉₄ H ₂₆₂ N ₄₂ O ₃₆ S ₆	1973.9138	-1.3	16.1	1	100.00	98.0	even	ok

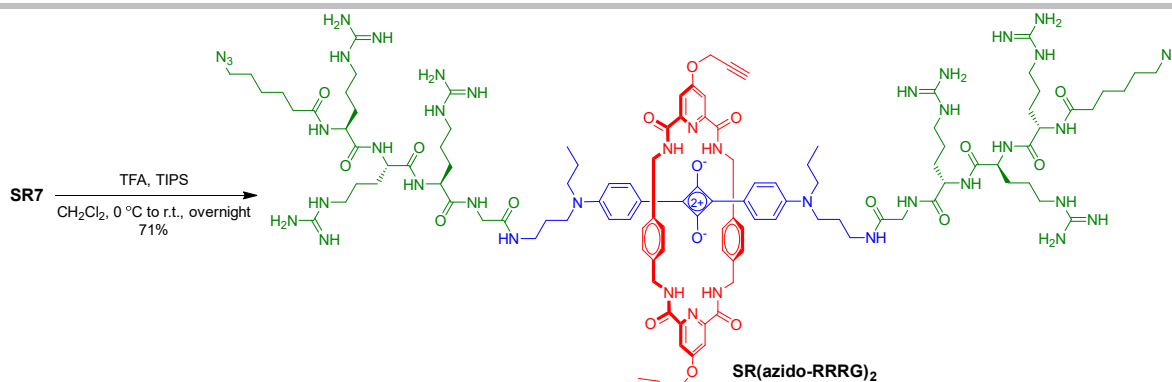
SF8(RRRG)₂. Yield 78%. ¹H NMR (500 MHz, Methanol-d₄) δ 10.18-10.08 (m, 4H), 8.24 (s, 2H), 8.13 (d, *J* = 2.5 Hz, 2H), 8.08 (d, *J* = 2.6 Hz, 6H), 6.57 (d, *J* = 8.7 Hz, 8H), 6.34 (br s, 4H), 5.57 (s, 4H), 4.48 (m, 8H), 4.38 (t, *J* = 4.3 Hz, 2H), 4.34-4.31 (m, 2H), 4.24 (dd, *J* = 8.8, 5.4 Hz, 2H), 3.85 (d, *J* = 8.2 Hz, 4H), 3.64 (s, 26H), 3.59-3.55 (m, 2H), 3.47 (q, *J* = 5.6, 4.9 Hz, 4H), 3.38 (d, *J* = 6.5 Hz, 4H), 3.20 (d, *J* = 6.6 Hz, 8H), 3.16 (d, *J* = 6.8 Hz, 6H), 2.28 (t, *J* = 7.1 Hz, 4H), 1.92 (m, 10H), 1.79 (d, *J* = 7.4 Hz, 6H), 1.71-1.60 (m, 24H), 0.94 (td, *J* = 4.8, 3.9, 2.2 Hz, 6H). HRMS (ESI-TOF) m/z: [M+2H]²⁺ Calcd for C₁₁₆H₁₆₆N₄₂O₁₈²⁺ 1217.6677; Found 1217.6705.

SUPPORTING INFORMATION

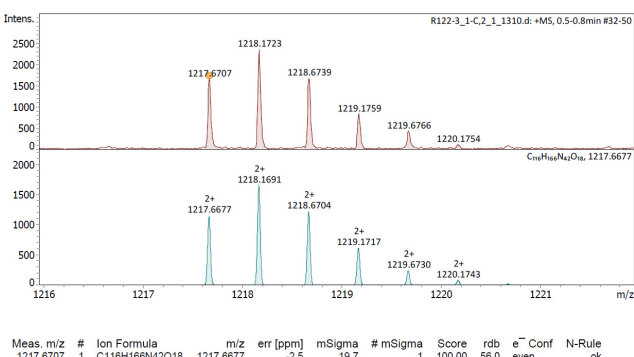
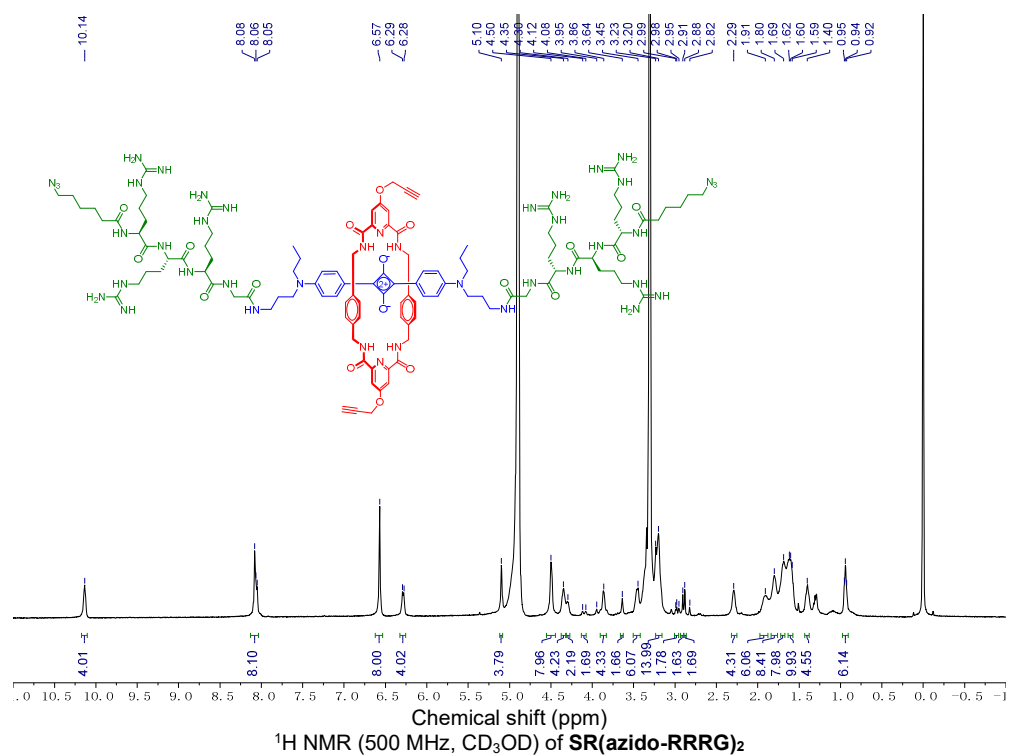


Meas. m/z	#	Ion Formula	m/z	err [ppm]	mSigma	# mSigma	Score	rdb	e- Conf	N-Rule
1217.6705	1	C116H166N42O18	1217.6677	-2.3	57.2	1	100.00	56.0	even	ok

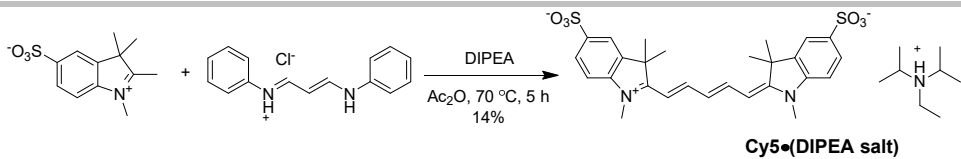
SUPPORTING INFORMATION

**Scheme S7.** Synthesis of **SR(azido-RRRG)₂**.

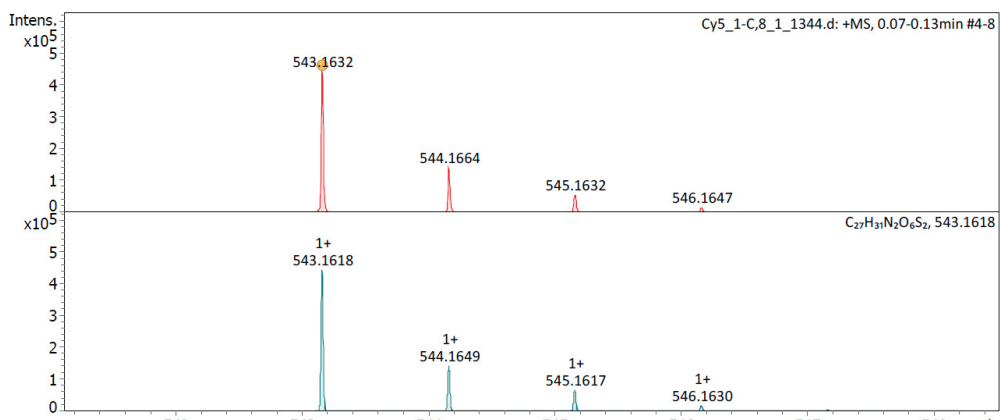
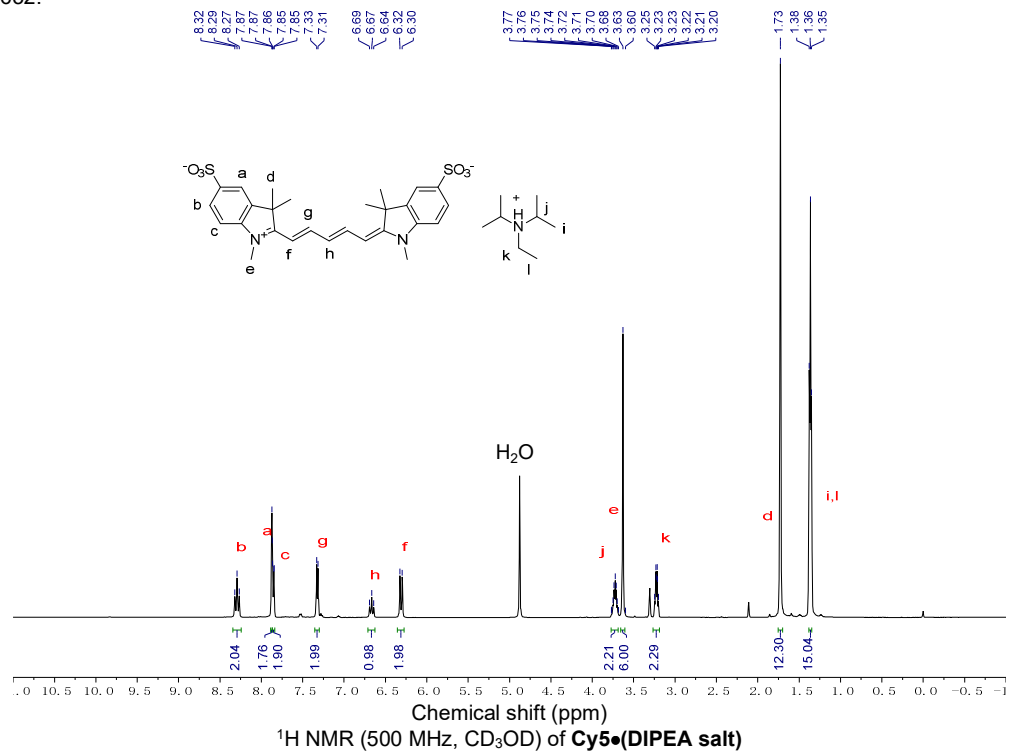
SR(azido-RRRG)₂. Yield 71%. ¹H NMR (500 MHz, Methanol-d₄) δ 10.14 (s, 4H), 8.07 (d, *J* = 7.7 Hz, 8H), 6.57 (s, 8H), 6.29 (d, *J* = 8.6 Hz, 4H), 5.10 (s, 4H), 4.50 (s, 8H), 4.35 (s, 4H), 4.30 (s, 2H), 4.10 (d, *J* = 19.6 Hz, 2H), 3.86 (m, 4H), 3.64 (s, 2H), 3.45 (s, 6H), 3.22 (d, *J* = 16.0 Hz, 14H), 2.99 (d, *J* = 6.3 Hz, 2H), 2.91 (s, 2H), 2.88 (s, 2H), 2.29 (s, 4H), 1.91 (s, 6H), 1.80 (s, 8H), 1.69 (s, 8H), 1.60 (m, 10H), 1.40 (s, 5H), 0.95 (d, *J* = 7.4 Hz, 6H). HRMS (ESI-TOF) m/z: [M+2H]²⁺ Calcd for C₁₁₆H₁₆₆N₄₂O₁₈²⁺ 1217.6677; Found 1217.6707.



SUPPORTING INFORMATION

**Scheme S8.** Synthesis of **Cy5.** (DIPEA: *N,N*-Diisopropylethylamine)

Cy5 was synthesized according to reported procedure^[6]. ¹H NMR (500 MHz, Methanol-*d*₄) δ 8.29 (t, *J* = 13.1 Hz, 2H), 7.87 (s, 2H), 7.86 (dd, *J* = 8.2, 1.9 Hz, 2H), 7.32 (d, *J* = 8.2 Hz, 2H), 6.67 (t, *J* = 12.4 Hz, 1H), 6.31 (d, *J* = 13.7 Hz, 2H), 3.73 (m, 2H), 3.63 (s, 6H), 3.22 (q, *J* = 7.4 Hz, 2H), 1.73 (s, 12H), 1.36 (t, *J* = 6.1 Hz, 15H). HRMS (ESI-TOF) *m/z*: [M+H]⁺ Calcd for C₂₇H₃₁N₂O₆S₂⁺ 543.1618; Found 543.1632.

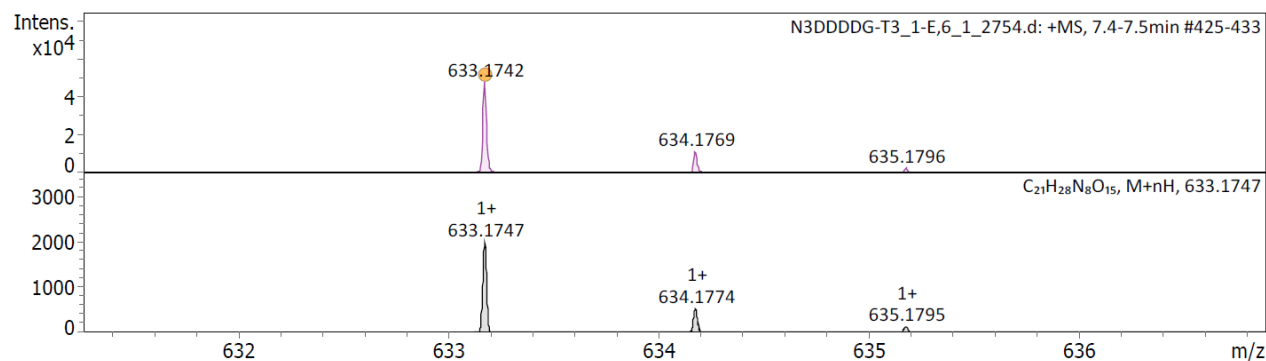
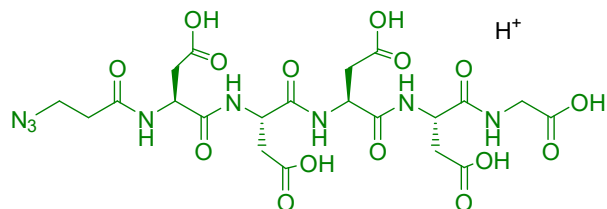


Meas. m/z	#	Ion Formula	m/z	err [ppm]	mSigma	# mSigma	Score	rdb	e ⁻ Conf	N-Rule
543.1632	1	C ₂₇ H ₃₁ N ₂ O ₆ S ₂	543.1618	-2.5	14.2	1	100.00	18.0	even	ok

HRMS-ESI of **Cy5**

SUPPORTING INFORMATION

Azido-DDDDG. Trifluoroacetic acid (TFA) (2 mL) was added dropwise to a solution of side-chain protected linear peptide **DDDDG** (Scheme S3) (19 mg) in CH_2Cl_2 (2 mL) and triisopropyl silane (TIPS) (0.2 mL) in an ice bath. The reaction was stirred overnight at room temperature. Solvent was removed and the residue was washed with Et_2O ($\times 3$) to produce light yellow powder product.. Yield quantitative. HRMS (ESI-TOF) m/z: $[\text{M}+\text{H}]^+$ Calcd for $\text{C}_{21}\text{H}_{29}\text{N}_8\text{O}_{15}^+$ 633.1747; Found 633.1742.



Meas. m/z	#	Ion Formula	m/z	err [ppm]	mSigma	# mSigma	Score	rdb	e ⁻ Conf	N-Rule
633.1742	1	$\text{C}_{21}\text{H}_{29}\text{N}_8\text{O}_{15}$	633.1747	0.8	16.0	1	100.00	12.0	even	ok

HRMS-ESI of azido-DDDDG

SUPPORTING INFORMATION

3. X-ray Crystal Structure of SF8(C6)₂

SF8(C6)₂ crystallizes as blue/green tablet-like crystals from a chloroform/MeOH/Pr₂O solution. An arbitrary sphere of data was collected on a crystal, having approximate dimensions of 0.230 × 0.214 × 0.091 mm, on a Bruker PHOTON-II diffractometer using a combination of ω - and φ -scans of 0.5°. Data were corrected for absorption and polarization effects and analyzed for space group determination [L. Krause, R. Herbst-Irmer, G. M. Sheldrick, & D. Stalke. *J. Appl. Cryst.* **2015** *48*, 3]. The structure was solved by dual-space methods and expanded routinely [G. M. Sheldrick. *Acta Cryst.*, **2015**, A71, 3]. The model was refined by full-matrix least-squares analysis of F^2 against all reflections [G. M. Sheldrick. *Acta Cryst.*, **2015**, C71, 3]. All non-hydrogen atoms were refined with anisotropic atomic displacement parameters. Unless otherwise noted, hydrogen atoms were included in calculated positions. Atomic displacement parameters for the hydrogens were tied to the equivalent isotropic displacement parameter of the atom to which they are bonded ($U_{\text{iso}}(\text{H}) = 1.5U_{\text{eq}}(\text{C})$ for methyl, $1.2U_{\text{eq}}(\text{C})$ for all others).

There are two, crystallographically independent, yet chemically identical, half molecules of the macrocycle, six molecules of chloroform of crystallization and two molecules of water in the asymmetric unit of the primitive, centrosymmetric, monoclinic space group P2₁/c. Each half macrocycle crystallizes about independent inversion centers at [0.5, 0, 0.5] and [0, 0.5, 0.5]. The prominent difference between the two molecules is that in one case, one pentyl chain exhibits some positional disorder. The central squaraine cyclobutadione ring is located between two phenylene rings of the tetralactam. Amide and water hydrogen atoms were initially located from a difference Fourier map. Water hydrogen atoms were refined with restrained O-H distances, while the amide hydrogen atoms were refined freely. The water molecules bridge independent macrocycles with hydrogen bonds to amide carbonyl oxygen atoms. One chloroform exhibits positional disorder. Examination of the bond distances and angles within the molecules reveals no unusual contacts.

The crystallographic data are available from the Cambridge Crystallographic Data Centre as deposition number CCDC-2010469. The data can be obtained free of charge via <http://www.ccdc.cam.ac.uk>.

Table 1. Crystal data and structure refinement for **SF8(C6)₂** (nd1902).

Identification code	nd1902
Empirical formula	C ₈₂ H ₉₆ Cl ₁₈ N ₁₆ O ₁₂
Formula weight	2135.84
Temperature	120(2) K
Wavelength	1.54184 Å
Crystal system	Monoclinic
Space group	P2 ₁ /c
Unit cell dimensions	 $a = 9.6610(17)$ Å $\alpha = 90^\circ$ $b = 35.249(7)$ Å $\beta = 96.371(17)^\circ$ $c = 29.042(5)$ Å $\gamma = 90^\circ$ 9829(3) Å ³
Volume	
Z	4
Density (calculated)	1.443 g.cm ⁻³
Absorption coefficient (μ)	5.135 mm ⁻¹
F(000)	4408
Crystal color, habit	red-orange, tablet
Crystal size	0.230 × 0.214 × 0.091 mm ³
θ range for data collection	1.978 to 71.497°
Index ranges	-11 ≤ h ≤ 11, -43 ≤ k ≤ 43, -35 ≤ l ≤ 35
Reflections collected	224297
Independent reflections	18976 [$R_{\text{int}} = 0.0930$]
Completeness to $\theta = 67.679^\circ$	99.7 %
Absorption correction	Numerical
Max. and min. transmission	0.9748 and 0.3947
Refinement method	Full-matrix least-squares on F^2
Data / restraints / parameters	18976 / 6 / 1217
Goodness-of-fit on F^2	1.061
Final R indices [$ I > 2\sigma(I)$]	$R_1 = 0.0715$, $wR_2 = 0.1928$
R indices (all data)	$R_1 = 0.0847$, $wR_2 = 0.2076$
Extinction coefficient	n/a
Largest diff. peak and hole	1.554 and -1.550 e. ⁻ .Å ⁻³

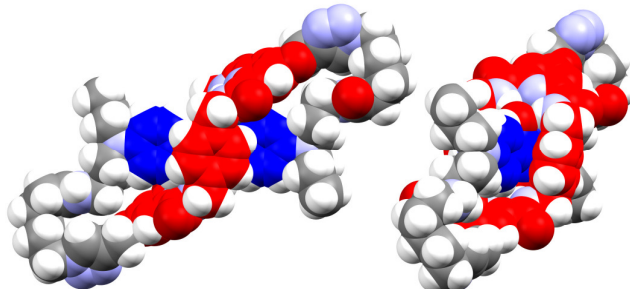


Figure S1. Spacefilling models of **SF8(C6)₂**.

SUPPORTING INFORMATION

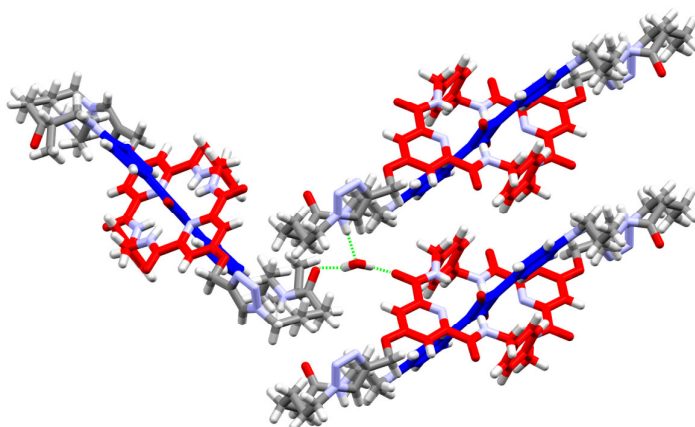


Figure S2. A crystal lattice water molecule acts as a solid-state connection point for three $\text{SF8}(\text{C}_6)_2$ molecules.

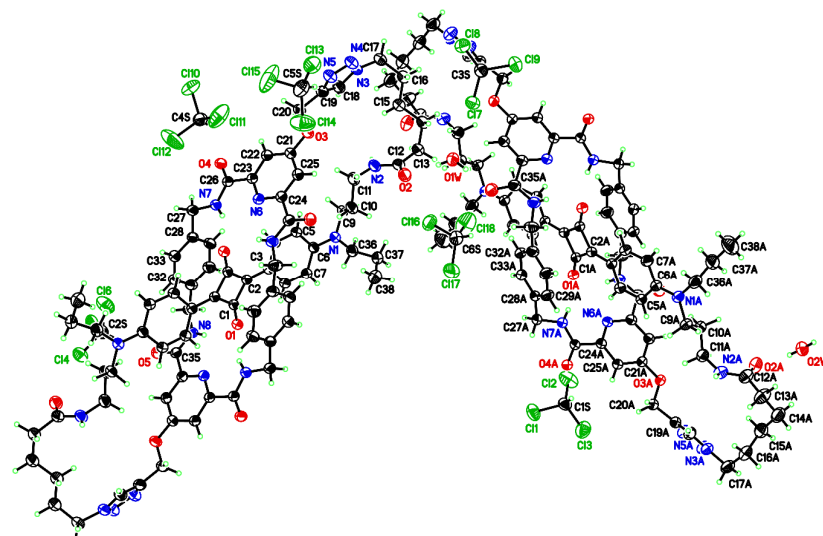


Figure S3. $\text{SF8}(\text{C}_6)_2$ as ORTEP with atom numbers and ellipsoids at 50% probability.

Table S1. Bond lengths [\AA] for $\text{SF8}(\text{C}_6)_2$ (nd1902).

atom-atom	distance	atom-atom	distance
O(1)-C(1)	1.241(4)	O(2)-C(12)	1.232(5)
O(3)-C(21)	1.353(4)	O(3)-C(20)	1.449(4)
O(4)-C(26)	1.234(4)	O(5)-C(35)	1.247(4)
N(1)-C(6)	1.359(4)	N(1)-C(36)	1.466(4)
N(1)-C(9)	1.468(4)	N(2)-C(12)	1.340(5)
N(2)-C(11)	1.450(5)	N(2)-H(2N)	0.70(4)
N(3)-N(4)	1.346(5)	N(3)-C(18)	1.347(5)
N(3)-C(17)	1.470(5)	N(4)-N(5)	1.315(4)
N(5)-C(19)	1.364(5)	N(6)-C(23)	1.335(4)
N(6)-C(24)	1.344(4)	N(7)-C(26)	1.336(4)
N(7)-C(27)	1.456(4)	N(7)-H(7N)	0.81(5)
N(8)-C(35)	1.331(4)	N(8)-C(34)	1.467(4)
N(8)-H(8N)	0.77(5)	C(1)-C(2)	1.457(4)
C(1)-C(2)#1	1.469(4)	C(2)-C(3)	1.403(4)
C(3)-C(4)	1.411(4)	C(3)-C(8)	1.412(4)
C(4)-C(5)	1.364(4)	C(4)-H(4A)	0.9500
C(5)-C(6)	1.424(4)	C(5)-H(5A)	0.9500
C(6)-C(7)	1.431(4)	C(7)-C(8)	1.371(4)

SUPPORTING INFORMATION

C(7)-H(7A)	0.9500	C(8)-H(8A)	0.9500
C(9)-C(10)	1.532(4)	C(9)-H(9A)	0.9900
C(9)-H(9B)	0.9900	C(10)-C(11)	1.531(5)
C(10)-H(10A)	0.9900	C(10)-H(10B)	0.9900
C(11)-H(11A)	0.9900	C(11)-H(11B)	0.9900
C(12)-C(13)	1.512(5)	C(13)-C(14)	1.537(5)
C(13)-H(13A)	0.9900	C(13)-H(13B)	0.9900
C(14)-C(15)	1.516(5)	C(14)-H(14A)	0.9900
C(14)-H(14B)	0.9900	C(15)-C(16)	1.533(5)
C(15)-H(15A)	0.9900	C(15)-H(15B)	0.9900
C(16)-C(17)	1.509(5)	C(16)-H(16A)	0.9900
C(16)-H(16B)	0.9900	C(17)-H(17A)	0.9900
C(17)-H(17B)	0.9900	C(18)-C(19)	1.368(5)
C(18)-H(18A)	0.9500	C(19)-C(20)	1.479(5)
C(20)-H(20A)	0.9900	C(20)-H(20B)	0.9900
C(21)-C(22)	1.392(4)	C(21)-C(25)	1.400(5)
C(22)-C(23)	1.391(4)	C(22)-H(22A)	0.9500
C(23)-C(26)	1.518(4)	C(24)-C(25)	1.376(4)
C(24)-C(35)#1	1.505(4)	C(25)-H(25A)	0.9500
C(27)-C(28)	1.517(4)	C(27)-H(27A)	0.9900
C(27)-H(27B)	0.9900	C(28)-C(33)	1.390(5)
C(28)-C(29)	1.390(5)	C(29)-C(30)	1.389(5)
C(29)-H(29A)	0.9500	C(30)-C(31)	1.390(5)
C(30)-H(30A)	0.9500	C(31)-C(32)	1.385(5)
C(31)-C(34)	1.512(4)	C(32)-C(33)	1.391(5)
C(32)-H(32A)	0.9500	C(33)-H(33A)	0.9500
C(34)-H(34A)	0.9900	C(34)-H(34B)	0.9900
C(36)-C(37)	1.521(5)	C(36)-H(36A)	0.9900
C(36)-H(36B)	0.9900	C(37)-C(38)	1.515(6)
C(37)-H(37A)	0.9900	C(37)-H(37B)	0.9900
C(38)-H(38A)	0.9800	C(38)-H(38B)	0.9800
C(38)-H(38C)	0.9800	O(1A)-C(1A)	1.235(4)
O(2A)-C(12A)	1.234(5)	O(3A)-C(21A)	1.363(4)
O(3A)-C(20A)	1.445(4)	O(4A)-C(26A)	1.239(4)
O(5A)-C(35A)	1.234(5)	N(1A)-C(6A)	1.358(4)
N(1A)-C(36A)	1.468(5)	N(1A)-C(9A)	1.472(4)
N(2A)-C(12A)	1.339(5)	N(2A)-C(11A)	1.461(5)
N(2A)-H(2NA)	0.84(4)	N(3A)-N(4A)	1.330(5)
N(3A)-C(18A)	1.351(5)	N(3A)-C(17A)	1.480(5)
N(4A)-N(5A)	1.318(4)	N(5A)-C(19A)	1.355(5)
N(6A)-C(24A)	1.335(4)	N(6A)-C(23A)	1.345(4)
N(7A)-C(26A)	1.330(4)	N(7A)-C(27A)	1.461(4)
N(7A)-H(7NA)	0.85(5)	N(8A)-C(35A)	1.328(5)
N(8A)-C(34A)	1.458(4)	N(8A)-H(8NA)	0.70(5)
C(1A)-C(2A)#2	1.458(4)	C(1A)-C(2A)	1.461(5)
C(2A)-C(3A)	1.416(4)	C(3A)-C(4A)	1.408(4)
C(3A)-C(8A)	1.410(5)	C(4A)-C(5A)	1.375(4)
C(4A)-H(4AA)	0.9500	C(5A)-C(6A)	1.419(5)
C(5A)-H(5AA)	0.9500	C(6A)-C(7A)	1.426(4)
C(7A)-C(8A)	1.370(5)	C(7A)-H(7AA)	0.9500
C(8A)-H(8AA)	0.9500	C(9A)-C(10A)	1.527(5)
C(9A)-H(9AA)	0.9900	C(9A)-H(9AB)	0.9900
C(10A)-C(11A)	1.526(5)	C(10A)-H(10C)	0.9900
C(10A)-H(10D)	0.9900	C(11A)-H(11C)	0.9900
C(11A)-H(11D)	0.9900	C(12A)-C(13A)	1.517(5)
C(13A)-C(14B)	1.47(2)	C(13A)-C(14A)	1.493(7)
C(13A)-H(13C)	0.9900	C(13A)-H(13D)	0.9900
C(13A)-H(13E)	0.9900	C(13A)-H(13F)	0.9900
C(15A)-C(14B)	1.41(2)	C(15A)-C(16B)	1.50(2)
C(15A)-C(14A)	1.532(7)	C(15A)-C(16A)	1.547(7)
C(15A)-H(15C)	0.9900	C(15A)-H(15D)	0.9900
C(15A)-H(15E)	0.9900	C(15A)-H(15F)	0.9900
C(17A)-C(16B)	1.47(2)	C(17A)-C(16A)	1.516(7)
C(17A)-H(17C)	0.9900	C(17A)-H(17D)	0.9900
C(17A)-H(17E)	0.9900	C(17A)-H(17F)	0.9900
C(14A)-H(14C)	0.9900	C(14A)-H(14D)	0.9900
C(16A)-H(16C)	0.9900	C(16A)-H(16D)	0.9900
C(14B)-H(14E)	0.9900	C(14B)-H(14F)	0.9900
C(16B)-H(16E)	0.9900	C(16B)-H(16F)	0.9900
C(18A)-C(19A)	1.366(5)	C(18A)-H(18B)	0.9500
C(19A)-C(20A)	1.488(4)	C(20A)-H(20C)	0.9900

SUPPORTING INFORMATION

C(20A)-H(20D)	0.9900	C(21A)-C(25A)	1.390(4)
C(21A)-C(22A)	1.407(4)	C(22A)-C(23A)	1.375(5)
C(22A)-H(22B)	0.9500	C(23A)-C(35A)#2	1.515(4)
C(24A)-C(25A)	1.391(4)	C(24A)-C(26A)	1.516(4)
C(25A)-H(25B)	0.9500	C(27A)-C(28A)	1.514(5)
C(27A)-H(27C)	0.9900	C(27A)-H(27D)	0.9900
C(28A)-C(29A)	1.383(6)	C(28A)-C(33A)	1.393(5)
C(29A)-C(30A)	1.390(5)	C(29A)-H(29B)	0.9500
C(30A)-C(31A)	1.399(5)	C(30A)-H(30B)	0.9500
C(31A)-C(32A)	1.380(5)	C(31A)-C(34A)	1.513(5)
C(32A)-C(33A)	1.396(5)	C(32A)-H(32B)	0.9500
C(33A)-H(33B)	0.9500	C(34A)-H(34C)	0.9900
C(34A)-H(34D)	0.9900	C(36A)-C(37A)	1.496(6)
C(36A)-H(36C)	0.9900	C(36A)-H(36D)	0.9900
C(37A)-C(38A)	1.528(7)	C(37A)-H(37C)	0.9900
C(37A)-H(37D)	0.9900	C(38A)-H(38D)	0.9800
C(38A)-H(38E)	0.9800	C(38A)-H(38F)	0.9800
C(1S)-Cl(1)	1.753(4)	C(1S)-Cl(2)	1.756(4)
C(1S)-Cl(3)	1.771(4)	C(1S)-H(1SA)	1.0000
C(2S)-Cl(6)	1.753(4)	C(2S)-Cl(4)	1.754(4)
C(2S)-Cl(5)	1.770(4)	C(2S)-H(2SA)	1.0000
C(3S)-Cl(7)	1.749(4)	C(3S)-Cl(9)	1.752(4)
C(3S)-Cl(8)	1.764(4)	C(3S)-H(3SA)	1.0000
C(4S)-Cl(2A)	1.702(12)	C(4S)-Cl(12)	1.721(4)
C(4S)-Cl(0A)	1.743(11)	C(4S)-Cl(11)	1.746(5)
C(4S)-Cl(10)	1.747(4)	C(4S)-Cl(1A)	1.816(10)
C(4S)-H(4SA)	1.0000	C(4S)-H(4SB)	1.0000
C(5S)-Cl(15)	1.713(5)	C(5S)-Cl(14)	1.759(5)
C(5S)-Cl(13)	1.766(5)	C(5S)-H(5SA)	1.0000
C(6S)-Cl(16)	1.733(5)	C(6S)-Cl(17)	1.734(5)
C(6S)-Cl(18)	1.735(5)	C(6S)-H(6SA)	1.0000
O(1W)-H(1WA)	0.865(10)	O(1W)-H(1WB)	0.866(10)
O(2W)-H(2WA)	0.862(10)	O(2W)-H(2WB)	0.863(10)

Symmetry transformations used to generate equivalent atoms:

#1 -x+1,-y,-z+1 #2 -x,-y+1,-z+1

Table S2. Bond angles [°] for SF8(C6)₂ (nd1902).

atom-atom-atom	angle	atom-atom-atom	angle
C(21)-O(3)-C(20)	116.9(3)	C(6)-N(1)-C(36)	124.1(3)
C(6)-N(1)-C(9)	119.5(3)	C(36)-N(1)-C(9)	116.3(3)
C(12)-N(2)-C(11)	121.2(3)	C(12)-N(2)-H(2N)	120(3)
C(11)-N(2)-H(2N)	119(3)	N(4)-N(3)-C(18)	111.1(3)
N(4)-N(3)-C(17)	119.5(3)	C(18)-N(3)-C(17)	129.0(3)
N(5)-N(4)-N(3)	106.9(3)	N(4)-N(5)-C(19)	109.1(3)
C(23)-N(6)-C(24)	117.0(3)	C(26)-N(7)-C(27)	121.0(3)
C(26)-N(7)-H(7N)	116(3)	C(27)-N(7)-H(7N)	123(3)
C(35)-N(8)-C(34)	121.8(3)	C(35)-N(8)-H(8N)	116(3)
C(34)-N(8)-H(8N)	121(3)	O(1)-C(1)-C(2)	133.4(3)
O(1)-C(1)-C(2)#1	135.9(3)	C(2)-C(1)-C(2)#1	90.7(3)
C(3)-C(2)-C(1)	134.1(3)	C(3)-C(2)-C(1)#1	136.6(3)
C(1)-C(2)-C(1)#1	89.3(3)	C(2)-C(3)-C(4)	120.4(3)
C(2)-C(3)-C(8)	122.2(3)	C(4)-C(3)-C(8)	117.4(3)
C(5)-C(4)-C(3)	121.7(3)	C(5)-C(4)-H(4A)	119.1
C(3)-C(4)-H(4A)	119.1	C(4)-C(5)-C(6)	121.4(3)
C(4)-C(5)-H(5A)	119.3	C(6)-C(5)-H(5A)	119.3
N(1)-C(6)-C(5)	120.5(3)	N(1)-C(6)-C(7)	122.9(3)
C(5)-C(6)-C(7)	116.7(3)	C(8)-C(7)-C(6)	121.1(3)
C(8)-C(7)-H(7A)	119.5	C(6)-C(7)-H(7A)	119.5
C(7)-C(8)-C(3)	121.6(3)	C(7)-C(8)-H(8A)	119.2
C(3)-C(8)-H(8A)	119.2	N(1)-C(9)-C(10)	113.5(3)
N(1)-C(9)-H(9A)	108.9	C(10)-C(9)-H(9A)	108.9
N(1)-C(9)-H(9B)	108.9	C(10)-C(9)-H(9B)	108.9
H(9A)-C(9)-H(9B)	107.7	C(11)-C(10)-C(9)	111.2(3)
C(11)-C(10)-H(10A)	109.4	C(9)-C(10)-H(10A)	109.4
C(11)-C(10)-H(10B)	109.4	C(9)-C(10)-H(10B)	109.4
H(10A)-C(10)-H(10B)	108.0	N(2)-C(11)-C(10)	112.8(3)
N(2)-C(11)-H(11A)	109.0	C(10)-C(11)-H(11A)	109.0

SUPPORTING INFORMATION

N(2)-C(11)-H(11B)	109.0	C(10)-C(11)-H(11B)	109.0
H(11A)-C(11)-H(11B)	107.8	O(2)-C(12)-N(2)	121.6(3)
O(2)-C(12)-C(13)	121.5(3)	N(2)-C(12)-C(13)	116.9(3)
C(12)-C(13)-C(14)	111.1(3)	C(12)-C(13)-H(13A)	109.4
C(14)-C(13)-H(13A)	109.4	C(12)-C(13)-H(13B)	109.4
C(14)-C(13)-H(13B)	109.4	H(13A)-C(13)-H(13B)	108.0
C(15)-C(14)-C(13)	112.5(3)	C(15)-C(14)-H(14A)	109.1
C(13)-C(14)-H(14A)	109.1	C(15)-C(14)-H(14B)	109.1
C(13)-C(14)-H(14B)	109.1	H(14A)-C(14)-H(14B)	107.8
C(14)-C(15)-C(16)	113.0(3)	C(14)-C(15)-H(15A)	109.0
C(16)-C(15)-H(15A)	109.0	C(14)-C(15)-H(15B)	109.0
C(16)-C(15)-H(15B)	109.0	H(15A)-C(15)-H(15B)	107.8
C(17)-C(16)-C(15)	112.0(3)	C(17)-C(16)-H(16A)	109.2
C(15)-C(16)-H(16A)	109.2	C(17)-C(16)-H(16B)	109.2
C(15)-C(16)-H(16B)	109.2	H(16A)-C(16)-H(16B)	107.9
N(3)-C(17)-C(16)	111.8(3)	N(3)-C(17)-H(17A)	109.3
C(16)-C(17)-H(17A)	109.3	N(3)-C(17)-H(17B)	109.3
C(16)-C(17)-H(17B)	109.3	H(17A)-C(17)-H(17B)	107.9
N(3)-C(18)-C(19)	104.8(3)	N(3)-C(18)-H(18A)	127.6
C(19)-C(18)-H(18A)	127.6	N(5)-C(19)-C(18)	108.1(3)
N(5)-C(19)-C(20)	122.4(3)	C(18)-C(19)-C(20)	129.5(4)
O(3)-C(20)-C(19)	106.5(3)	O(3)-C(20)-H(20A)	110.4
C(19)-C(20)-H(20A)	110.4	O(3)-C(20)-H(20B)	110.4
C(19)-C(20)-H(20B)	110.4	H(20A)-C(20)-H(20B)	108.6
O(3)-C(21)-C(22)	125.1(3)	O(3)-C(21)-C(25)	115.7(3)
C(22)-C(21)-C(25)	119.2(3)	C(23)-C(22)-C(21)	117.4(3)
C(23)-C(22)-H(22A)	121.3	C(21)-C(22)-H(22A)	121.3
N(6)-C(23)-C(22)	124.4(3)	N(6)-C(23)-C(26)	117.0(3)
C(22)-C(23)-C(26)	118.6(3)	N(6)-C(24)-C(25)	123.7(3)
N(6)-C(24)-C(35)#1	117.3(3)	C(25)-C(24)-C(35)#1	119.1(3)
C(24)-C(25)-C(21)	118.3(3)	C(24)-C(25)-H(25A)	120.8
C(21)-C(25)-H(25A)	120.8	O(4)-C(26)-N(7)	124.4(3)
O(4)-C(26)-C(23)	120.3(3)	N(7)-C(26)-C(23)	115.2(3)
N(7)-C(27)-C(28)	113.5(3)	N(7)-C(27)-H(27A)	108.9
C(28)-C(27)-H(27A)	108.9	N(7)-C(27)-H(27B)	108.9
C(28)-C(27)-H(27B)	108.9	H(27A)-C(27)-H(27B)	107.7
C(33)-C(28)-C(29)	118.8(3)	C(33)-C(28)-C(27)	120.2(3)
C(29)-C(28)-C(27)	121.0(3)	C(30)-C(29)-C(28)	120.5(3)
C(30)-C(29)-H(29A)	119.8	C(28)-C(29)-H(29A)	119.8
C(29)-C(30)-C(31)	120.9(3)	C(29)-C(30)-H(30A)	119.6
C(31)-C(30)-H(30A)	119.6	C(32)-C(31)-C(30)	118.5(3)
C(32)-C(31)-C(34)	121.1(3)	C(30)-C(31)-C(34)	120.3(3)
C(31)-C(32)-C(33)	121.0(3)	C(31)-C(32)-H(32A)	119.5
C(33)-C(32)-H(32A)	119.5	C(28)-C(33)-C(32)	120.4(3)
C(28)-C(33)-H(33A)	119.8	C(32)-C(33)-H(33A)	119.8
N(8)-C(34)-C(31)	113.4(3)	N(8)-C(34)-H(34A)	108.9
C(31)-C(34)-H(34A)	108.9	N(8)-C(34)-H(34B)	108.9
C(31)-C(34)-H(34B)	108.9	H(34A)-C(34)-H(34B)	107.7
O(5)-C(35)-N(8)	124.2(3)	O(5)-C(35)-C(24)#1	120.2(3)
N(8)-C(35)-C(24)#1	115.6(3)	N(1)-C(36)-C(37)	113.3(3)
N(1)-C(36)-H(36A)	108.9	C(37)-C(36)-H(36A)	108.9
N(1)-C(36)-H(36B)	108.9	C(37)-C(36)-H(36B)	108.9
H(36A)-C(36)-H(36B)	107.7	C(38)-C(37)-C(36)	113.1(3)
C(38)-C(37)-H(37A)	109.0	C(36)-C(37)-H(37A)	109.0
C(38)-C(37)-H(37B)	109.0	C(36)-C(37)-H(37B)	109.0
H(37A)-C(37)-H(37B)	107.8	C(37)-C(38)-H(38A)	109.5
C(37)-C(38)-H(38B)	109.5	H(38A)-C(38)-H(38B)	109.5
C(37)-C(38)-H(38C)	109.5	H(38A)-C(38)-H(38C)	109.5
H(38B)-C(38)-H(38C)	109.5	C(21A)-O(3A)-C(20A)	115.8(2)
C(6A)-N(1A)-C(36A)	121.0(3)	C(6A)-N(1A)-C(9A)	120.9(3)
C(36A)-N(1A)-C(9A)	118.1(3)	C(12A)-N(2A)-C(11A)	122.0(3)
C(12A)-N(2A)-H(2NA)	119(3)	C(11A)-N(2A)-H(2NA)	117(3)
N(4A)-N(3A)-C(18A)	111.2(3)	N(4A)-N(3A)-C(17A)	120.1(3)
C(18A)-N(3A)-C(17A)	128.8(3)	N(5A)-N(4A)-N(3A)	107.4(3)
N(4A)-N(5A)-C(19A)	108.5(3)	C(24A)-N(6A)-C(23A)	117.7(3)
C(26A)-N(7A)-C(27A)	122.8(3)	C(26A)-N(7A)-H(7NA)	121(3)
C(27A)-N(7A)-H(7NA)	116(3)	C(35A)-N(8A)-C(34A)	123.6(3)
C(35A)-N(8A)-H(8NA)	119(4)	C(34A)-N(8A)-H(8NA)	118(4)
O(1A)-C(1A)-C(2A)#2	133.0(3)	O(1A)-C(1A)-C(2A)	136.9(3)
C(2A)#2-C(1A)-C(2A)	90.1(3)	C(3A)-C(2A)-C(1A)#2	131.3(3)
C(3A)-C(2A)-C(1A)	138.8(3)	C(1A)#2-C(2A)-C(1A)	89.9(3)

SUPPORTING INFORMATION

C(4A)-C(3A)-C(8A)	117.5(3)	C(4A)-C(3A)-C(2A)	120.7(3)
C(8A)-C(3A)-C(2A)	121.7(3)	C(5A)-C(4A)-C(3A)	121.4(3)
C(5A)-C(4A)-H(4AA)	119.3	C(3A)-C(4A)-H(4AA)	119.3
C(4A)-C(5A)-C(6A)	121.3(3)	C(4A)-C(5A)-H(5AA)	119.4
C(6A)-C(5A)-H(5AA)	119.4	N(1A)-C(6A)-C(5A)	121.6(3)
N(1A)-C(6A)-C(7A)	121.2(3)	C(5A)-C(6A)-C(7A)	117.2(3)
C(8A)-C(7A)-C(6A)	120.7(3)	C(8A)-C(7A)-H(7AA)	119.6
C(6A)-C(7A)-H(7AA)	119.6	C(7A)-C(8A)-C(3A)	121.9(3)
C(7A)-C(8A)-H(8AA)	119.0	C(3A)-C(8A)-H(8AA)	119.0
N(1A)-C(9A)-C(10A)	114.4(3)	N(1A)-C(9A)-H(9AA)	108.7
C(10A)-C(9A)-H(9AA)	108.7	N(1A)-C(9A)-H(9AB)	108.7
C(10A)-C(9A)-H(9AB)	108.7	H(9AA)-C(9A)-H(9AB)	107.6
C(11A)-C(10A)-C(9A)	112.2(3)	C(11A)-C(10A)-H(10C)	109.2
C(9A)-C(10A)-H(10C)	109.2	C(11A)-C(10A)-H(10D)	109.2
C(9A)-C(10A)-H(10D)	109.2	H(10C)-C(10A)-H(10D)	107.9
N(2A)-C(11A)-C(10A)	115.3(3)	N(2A)-C(11A)-H(11C)	108.4
C(10A)-C(11A)-H(11C)	108.4	N(2A)-C(11A)-H(11D)	108.4
C(10A)-C(11A)-H(11D)	108.4	H(11C)-C(11A)-H(11D)	107.5
O(2A)-C(12A)-N(2A)	122.6(4)	O(2A)-C(12A)-C(13A)	121.4(4)
N(2A)-C(12A)-C(13A)	115.9(4)	C(14B)-C(13A)-C(12A)	110.7(10)
C(14A)-C(13A)-C(12A)	112.5(4)	C(14A)-C(13A)-H(13C)	109.1
C(12A)-C(13A)-H(13C)	109.1	C(14A)-C(13A)-H(13D)	109.1
C(12A)-C(13A)-H(13D)	109.1	H(13C)-C(13A)-H(13D)	107.8
C(14B)-C(13A)-H(13E)	109.5	C(12A)-C(13A)-H(13E)	109.5
C(14B)-C(13A)-H(13F)	109.5	C(12A)-C(13A)-H(13F)	109.5
H(13E)-C(13A)-H(13F)	108.1	C(14B)-C(15A)-C(16B)	125.8(13)
C(14A)-C(15A)-C(16A)	112.5(4)	C(14A)-C(15A)-H(15C)	109.1
C(16A)-C(15A)-H(15C)	109.1	C(14A)-C(15A)-H(15D)	109.1
C(16A)-C(15A)-H(15D)	109.1	H(15C)-C(15A)-H(15D)	107.8
C(14B)-C(15A)-H(15E)	105.9	C(16B)-C(15A)-H(15E)	105.9
C(14B)-C(15A)-H(15F)	105.9	C(16B)-C(15A)-H(15F)	105.9
H(15E)-C(15A)-H(15F)	106.2	C(16B)-C(17A)-N(3A)	110.5(9)
N(3A)-C(17A)-C(16A)	112.4(3)	N(3A)-C(17A)-H(17C)	109.1
C(16A)-C(17A)-H(17C)	109.1	N(3A)-C(17A)-H(17D)	109.1
C(16A)-C(17A)-H(17D)	109.1	H(17C)-C(17A)-H(17D)	107.8
C(16B)-C(17A)-H(17E)	109.6	N(3A)-C(17A)-H(17E)	109.6
C(16B)-C(17A)-H(17F)	109.6	N(3A)-C(17A)-H(17F)	109.6
H(17E)-C(17A)-H(17F)	108.1	C(13A)-C(14A)-C(15A)	114.6(4)
C(13A)-C(14A)-H(14C)	108.6	C(15A)-C(14A)-H(14C)	108.6
C(13A)-C(14A)-H(14D)	108.6	C(15A)-C(14A)-H(14D)	108.6
H(14C)-C(14A)-H(14D)	107.6	C(17A)-C(16A)-C(15A)	112.5(4)
C(17A)-C(16A)-H(16C)	109.1	C(15A)-C(16A)-H(16C)	109.1
C(17A)-C(16A)-H(16D)	109.1	C(15A)-C(16A)-H(16D)	109.1
H(16C)-C(16A)-H(16D)	107.8	C(15A)-C(14B)-C(13A)	124.4(17)
C(15A)-C(14B)-H(14E)	106.2	C(13A)-C(14B)-H(14E)	106.2
C(15A)-C(14B)-H(14F)	106.2	C(13A)-C(14B)-H(14F)	106.2
H(14E)-C(14B)-H(14F)	106.4	C(17A)-C(16B)-C(15A)	118.2(15)
C(17A)-C(16B)-H(16E)	107.8	C(15A)-C(16B)-H(16E)	107.8
C(17A)-C(16B)-H(16F)	107.8	C(15A)-C(16B)-H(16F)	107.8
H(16E)-C(16B)-H(16F)	107.1	N(3A)-C(18A)-C(19A)	104.3(3)
N(3A)-C(18A)-H(18B)	127.9	C(19A)-C(18A)-H(18B)	127.9
N(5A)-C(19A)-C(18A)	108.7(3)	N(5A)-C(19A)-C(20A)	122.0(3)
C(18A)-C(19A)-C(20A)	129.2(3)	O(3A)-C(20A)-C(19A)	108.3(3)
O(3A)-C(20A)-H(20C)	110.0	C(19A)-C(20A)-H(20C)	110.0
O(3A)-C(20A)-H(20D)	110.0	C(19A)-C(20A)-H(20D)	110.0
H(20C)-C(20A)-H(20D)	108.4	O(3A)-C(21A)-C(25A)	124.6(3)
O(3A)-C(21A)-C(22A)	116.1(3)	C(25A)-C(21A)-C(22A)	119.3(3)
C(23A)-C(22A)-C(21A)	117.9(3)	C(23A)-C(22A)-H(22B)	121.0
C(21A)-C(22A)-H(22B)	121.0	N(6A)-C(23A)-C(22A)	123.6(3)
N(6A)-C(23A)-C(35A)#2	115.9(3)	C(22A)-C(23A)-C(35A)#2	120.4(3)
N(6A)-C(24A)-C(25A)	123.7(3)	N(6A)-C(24A)-C(26A)	117.0(3)
C(25A)-C(24A)-C(26A)	119.2(3)	C(21A)-C(25A)-C(24A)	117.8(3)
C(21A)-C(25A)-H(25B)	121.1	C(24A)-C(25A)-H(25B)	121.1
O(4A)-C(26A)-N(7A)	125.3(3)	O(4A)-C(26A)-C(24A)	120.3(3)
N(7A)-C(26A)-C(24A)	114.4(3)	N(7A)-C(27A)-C(28A)	111.9(3)
N(7A)-C(27A)-H(27C)	109.2	C(28A)-C(27A)-H(27C)	109.2
N(7A)-C(27A)-H(27D)	109.2	C(28A)-C(27A)-H(27D)	109.2
H(27C)-C(27A)-H(27D)	107.9	C(29A)-C(28A)-C(33A)	118.5(3)
C(29A)-C(28A)-C(27A)	120.9(3)	C(33A)-C(28A)-C(27A)	120.6(3)
C(28A)-C(29A)-C(30A)	121.2(3)	C(28A)-C(29A)-H(29B)	119.4
C(30A)-C(29A)-H(29B)	119.4	C(29A)-C(30A)-C(31A)	120.5(4)

SUPPORTING INFORMATION

C(29A)-C(30A)-H(30B)	119.7	C(31A)-C(30A)-H(30B)	119.7
C(32A)-C(31A)-C(30A)	118.1(3)	C(32A)-C(31A)-C(34A)	122.3(3)
C(30A)-C(31A)-C(34A)	119.6(3)	C(31A)-C(32A)-C(33A)	121.5(3)
C(31A)-C(32A)-H(32B)	119.3	C(33A)-C(32A)-H(32B)	119.3
C(28A)-C(33A)-C(32A)	120.2(3)	C(28A)-C(33A)-H(33B)	119.9
C(32A)-C(33A)-H(33B)	119.9	N(8A)-C(34A)-C(31A)	114.3(3)
N(8A)-C(34A)-H(34C)	108.7	C(31A)-C(34A)-H(34C)	108.7
N(8A)-C(34A)-H(34D)	108.7	C(31A)-C(34A)-H(34D)	108.7
H(34C)-C(34A)-H(34D)	107.6	O(5A)-C(35A)-N(8A)	123.1(3)
O(5A)-C(35A)-C(23A)#2	121.7(3)	N(8A)-C(35A)-C(23A)#2	115.2(3)
N(1A)-C(36A)-C(37A)	113.3(4)	N(1A)-C(36A)-H(36C)	108.9
C(37A)-C(36A)-H(36C)	108.9	N(1A)-C(36A)-H(36D)	108.9
C(37A)-C(36A)-H(36D)	108.9	H(36C)-C(36A)-H(36D)	107.7
C(36A)-C(37A)-C(38A)	112.0(5)	C(36A)-C(37A)-H(37C)	109.2
C(38A)-C(37A)-H(37C)	109.2	C(36A)-C(37A)-H(37D)	109.2
C(38A)-C(37A)-H(37D)	109.2	H(37C)-C(37A)-H(37D)	107.9
C(37A)-C(38A)-H(38D)	109.5	C(37A)-C(38A)-H(38E)	109.5
H(38D)-C(38A)-H(38E)	109.5	C(37A)-C(38A)-H(38F)	109.5
H(38D)-C(38A)-H(38F)	109.5	H(38E)-C(38A)-H(38F)	109.5
Cl(1)-C(1S)-Cl(2)	110.7(2)	Cl(1)-C(1S)-Cl(3)	110.9(2)
Cl(2)-C(1S)-Cl(3)	107.9(2)	Cl(1)-C(1S)-H(1SA)	109.1
Cl(2)-C(1S)-H(1SA)	109.1	Cl(3)-C(1S)-H(1SA)	109.1
Cl(6)-C(2S)-Cl(4)	110.6(2)	Cl(6)-C(2S)-Cl(5)	110.1(2)
Cl(4)-C(2S)-Cl(5)	110.8(2)	Cl(6)-C(2S)-H(2SA)	108.4
Cl(4)-C(2S)-H(2SA)	108.4	Cl(5)-C(2S)-H(2SA)	108.4
Cl(7)-C(3S)-Cl(9)	111.4(2)	Cl(7)-C(3S)-Cl(8)	110.1(2)
Cl(9)-C(3S)-Cl(8)	110.8(2)	Cl(7)-C(3S)-H(3SA)	108.1
Cl(9)-C(3S)-H(3SA)	108.1	Cl(8)-C(3S)-H(3SA)	108.1
Cl(2A)-C(4S)-Cl(0A)	115.3(6)	Cl(12)-C(4S)-Cl(11)	110.7(3)
Cl(12)-C(4S)-Cl(10)	111.1(3)	Cl(11)-C(4S)-Cl(10)	109.2(2)
Cl(2A)-C(4S)-Cl(1A)	105.5(6)	Cl(0A)-C(4S)-Cl(1A)	102.5(5)
Cl(12)-C(4S)-H(4SA)	108.6	Cl(11)-C(4S)-H(4SA)	108.6
Cl(10)-C(4S)-H(4SA)	108.6	Cl(12)-C(4S)-H(4SB)	108.6
Cl(11)-C(4S)-H(4SB)	108.6	Cl(10)-C(4S)-H(4SB)	108.6
H(4SA)-C(4S)-H(4SB)	0.0	Cl(15)-C(5S)-Cl(14)	113.3(3)
Cl(15)-C(5S)-Cl(13)	109.6(3)	Cl(14)-C(5S)-Cl(13)	108.9(3)
Cl(15)-C(5S)-H(5SA)	108.3	Cl(14)-C(5S)-H(5SA)	108.3
Cl(13)-C(5S)-H(5SA)	108.3	Cl(16)-C(6S)-Cl(17)	111.8(3)
Cl(16)-C(6S)-Cl(18)	111.9(3)	Cl(17)-C(6S)-Cl(18)	113.2(3)
Cl(16)-C(6S)-H(6SA)	106.5	Cl(17)-C(6S)-H(6SA)	106.5
Cl(18)-C(6S)-H(6SA)	106.5	H(1WA)-O(1W)-H(1WB)	107(2)
H(2WA)-O(2W)-H(2WB)	107(2)		

Symmetry transformations used to generate equivalent atoms:

#1 -x+1,-y,-z+1 #2 -x,-y+1,-z+1

Table S3. Torsion angles [°] for SF8(C6)2 (nd1902).

atom-atom-atom-atom	angle	atom-atom-atom-atom	angle
C(18)-N(3)-N(4)-N(5)	-0.8(4)	C(17)-N(3)-N(4)-N(5)	-173.9(3)
N(3)-N(4)-N(5)-C(19)	1.2(4)	O(1)-C(1)-C(2)-C(3)	-3.6(6)
C(2)#1-C(1)-C(2)-C(3)	177.9(4)	O(1)-C(1)-C(2)-C(1)#1	178.5(4)
C(2)#1-C(1)-C(2)-C(1)#1	0.004(1)	C(1)-C(2)-C(3)-C(4)	174.2(3)
C(1)#1-C(2)-C(3)-C(4)	-8.8(6)	C(1)-C(2)-C(3)-C(8)	-8.4(5)
C(1)#1-C(2)-C(3)-C(8)	168.5(3)	C(2)-C(3)-C(4)-C(5)	176.0(3)
C(8)-C(3)-C(4)-C(5)	-1.5(5)	C(3)-C(4)-C(5)-C(6)	-2.2(5)
C(36)-N(1)-C(6)-C(5)	-175.0(3)	C(9)-N(1)-C(6)-C(5)	6.6(4)
C(36)-N(1)-C(6)-C(7)	5.5(5)	C(9)-N(1)-C(6)-C(7)	-172.9(3)
C(4)-C(5)-C(6)-N(1)	-175.5(3)	C(4)-C(5)-C(6)-C(7)	4.0(5)
N(1)-C(6)-C(7)-C(8)	177.3(3)	C(5)-C(6)-C(7)-C(8)	-2.2(5)
C(6)-C(7)-C(8)-C(3)	-1.4(5)	C(2)-C(3)-C(8)-C(7)	-174.1(3)
C(4)-C(3)-C(8)-C(7)	3.3(5)	C(6)-N(1)-C(9)-C(10)	69.8(4)
C(36)-N(1)-C(9)-C(10)	-108.8(3)	N(1)-C(9)-C(10)-C(11)	-167.7(3)
C(12)-N(2)-C(11)-C(10)	-89.3(4)	C(9)-C(10)-C(11)-N(2)	-69.2(4)
C(11)-N(2)-C(12)-O(2)	0.8(5)	C(11)-N(2)-C(12)-C(13)	-177.4(3)
O(2)-C(12)-C(13)-C(14)	-77.4(4)	N(2)-C(12)-C(13)-C(14)	100.8(4)
C(12)-C(13)-C(14)-C(15)	-66.2(4)	C(13)-C(14)-C(15)-C(16)	-178.7(3)
C(14)-C(15)-C(16)-C(17)	174.9(3)	N(4)-N(3)-C(17)-C(16)	84.2(4)
C(18)-N(3)-C(17)-C(16)	-87.4(5)	C(15)-C(16)-C(17)-N(3)	59.5(5)

SUPPORTING INFORMATION

N(4)-N(3)-C(18)-C(19)	0.1(4)	C(17)-N(3)-C(18)-C(19)	172.3(3)
N(4)-N(5)-C(19)-C(18)	-1.2(4)	N(4)-N(5)-C(19)-C(20)	177.7(3)
N(3)-C(18)-C(19)-N(5)	0.6(4)	N(3)-C(18)-C(19)-C(20)	-178.1(3)
C(21)-O(3)-C(20)-C(19)	-174.1(3)	N(5)-C(19)-C(20)-O(3)	-72.0(4)
C(18)-C(19)-C(20)-O(3)	106.6(4)	C(20)-O(3)-C(21)-C(22)	5.2(5)
C(20)-O(3)-C(21)-C(25)	-175.7(3)	O(3)-C(21)-C(22)-C(23)	177.5(3)
C(25)-C(21)-C(22)-C(23)	-1.5(5)	C(24)-N(6)-C(23)-C(22)	-1.0(5)
C(24)-N(6)-C(23)-C(26)	177.9(3)	C(21)-C(22)-C(23)-N(6)	2.0(5)
C(21)-C(22)-C(23)-C(26)	-176.9(3)	C(23)-N(6)-C(24)-C(25)	-0.4(5)
C(23)-N(6)-C(24)-C(35)#1	179.8(3)	N(6)-C(24)-C(25)-C(21)	0.8(5)
C(35)#1-C(24)-C(25)-C(21)	-179.4(3)	O(3)-C(21)-C(25)-C(24)	-178.9(3)
C(22)-C(21)-C(25)-C(24)	0.2(5)	C(27)-N(7)-C(26)-O(4)	-1.5(5)
C(27)-N(7)-C(26)-C(23)	-179.9(3)	N(6)-C(23)-C(26)-O(4)	178.3(3)
C(22)-C(23)-C(26)-O(4)	-2.7(5)	N(6)-C(23)-C(26)-N(7)	-3.2(4)
C(22)-C(23)-C(26)-N(7)	175.8(3)	C(26)-N(7)-C(27)-C(28)	138.8(3)
N(7)-C(27)-C(28)-C(33)	111.2(4)	N(7)-C(27)-C(28)-C(29)	-70.2(4)
C(33)-C(28)-C(29)-C(30)	1.0(5)	C(27)-C(28)-C(29)-C(30)	-177.7(3)
C(28)-C(29)-C(30)-C(31)	-0.1(5)	C(29)-C(30)-C(31)-C(32)	-0.9(5)
C(29)-C(30)-C(31)-C(34)	175.4(3)	C(30)-C(31)-C(32)-C(33)	1.0(5)
C(34)-C(31)-C(32)-C(33)	-175.3(3)	C(29)-C(28)-C(33)-C(32)	-0.9(5)
C(27)-C(28)-C(33)-C(32)	177.8(3)	C(31)-C(32)-C(33)-C(28)	-0.1(5)
C(35)-N(8)-C(34)-C(31)	134.2(3)	C(32)-C(31)-C(34)-N(8)	-58.2(4)
C(30)-C(31)-C(34)-N(8)	125.6(3)	C(34)-N(8)-C(35)-O(5)	-5.3(5)
C(34)-N(8)-C(35)-C(24)#1	174.9(3)	C(6)-N(1)-C(36)-C(37)	-108.3(4)
C(9)-N(1)-C(36)-C(37)	70.2(4)	N(1)-C(36)-C(37)-C(38)	65.1(4)
C(18A)-N(3A)-N(4A)-N(5A)	-0.8(4)	C(17A)-N(3A)-N(4A)-N(5A)	177.7(3)
N(3A)-N(4A)-N(5A)-C(19A)	1.3(4)	O(1A)-C(1A)-C(2A)-C(3A)	2.6(7)
C(2A)#2-C(1A)-C(2A)-C(3A)	-176.9(5)	O(1A)-C(1A)-C(2A)-C(1A)#2	179.4(5)
C(2A)#2-C(1A)-C(2A)-C(1A)#2	-0.007(1)	C(1A)#2-C(2A)-C(3A)-C(4A)	-179.6(3)
C(1A)-C(2A)-C(3A)-C(4A)	-3.8(6)	C(1A)#2-C(2A)-C(3A)-C(8A)	-4.1(6)
C(1A)-C(2A)-C(3A)-C(8A)	171.7(4)	C(8A)-C(3A)-C(4A)-C(5A)	-1.4(5)
C(2A)-C(3A)-C(4A)-C(5A)	174.3(3)	C(3A)-C(4A)-C(5A)-C(6A)	-0.5(5)
C(36A)-N(1A)-C(6A)-C(5A)	175.2(3)	C(9A)-N(1A)-C(6A)-C(5A)	-3.9(5)
C(36A)-N(1A)-C(6A)-C(7A)	-5.5(5)	C(9A)-N(1A)-C(6A)-C(7A)	175.4(3)
C(4A)-C(5A)-C(6A)-N(1A)	-178.9(3)	C(4A)-C(5A)-C(6A)-C(7A)	1.7(5)
N(1A)-C(6A)-C(7A)-C(8A)	179.5(3)	C(5A)-C(6A)-C(7A)-C(8A)	-1.2(5)
C(6A)-C(7A)-C(8A)-C(3A)	-0.7(5)	C(4A)-C(3A)-C(8A)-C(7A)	1.9(5)
C(2A)-C(3A)-C(8A)-C(7A)	-173.7(3)	C(6A)-N(1A)-C(9A)-C(10A)	79.6(4)
C(36A)-N(1A)-C(9A)-C(10A)	-99.5(4)	N(1A)-C(9A)-C(10A)-C(11A)	-167.4(3)
C(12A)-N(2A)-C(11A)-C(10A)	-93.9(4)	C(9A)-C(10A)-C(11A)-N(2A)	-68.9(4)
C(11A)-N(2A)-C(12A)-O(2A)	1.1(6)	C(11A)-N(2A)-C(12A)-C(13A)	-176.0(3)
O(2A)-C(12A)-C(13A)-C(14B)	-92.0(11)	N(2A)-C(12A)-C(13A)-C(14B)	85.3(11)
O(2A)-C(12A)-C(13A)-C(14A)	-43.0(6)	N(2A)-C(12A)-C(13A)-C(14A)	134.3(5)
N(4A)-N(3A)-C(17A)-C(16B)	72.7(10)	C(18A)-N(3A)-C(17A)-C(16B)	-109.0(10)
N(4A)-N(3A)-C(17A)-C(16A)	130.8(4)	C(18A)-N(3A)-C(17A)-C(16A)	-51.0(6)
C(12A)-C(13A)-C(14A)-C(15A)	-58.2(6)	C(16A)-C(15A)-C(14A)-C(13A)	-74.3(6)
N(3A)-C(17A)-C(16A)-C(15A)	-63.6(5)	C(14A)-C(15A)-C(16A)-C(17A)	175.8(4)
C(16B)-C(15A)-C(14B)-C(13A)	-171.9(16)	C(12A)-C(13A)-C(14B)-C(15A)	52(2)
N(3A)-C(17A)-C(16B)-C(15A)	63.7(17)	C(14B)-C(15A)-C(16B)-C(17A)	48(2)
N(4A)-N(3A)-C(18A)-C(19A)	0.0(4)	C(17A)-N(3A)-C(18A)-C(19A)	-178.4(4)
N(4A)-N(5A)-C(19A)-C(18A)	-1.3(4)	N(4A)-N(5A)-C(19A)-C(20A)	-177.7(3)
N(3A)-C(18A)-C(19A)-N(5A)	0.8(4)	N(3A)-C(18A)-C(19A)-C(20A)	176.9(3)
C(21A)-O(3A)-C(20A)-C(19A)	-178.9(3)	N(5A)-C(19A)-C(20A)-O(3A)	-70.4(4)
C(18A)-C(19A)-C(20A)-O(3A)	114.1(4)	C(20A)-O(3A)-C(21A)-C(25A)	2.5(5)
C(20A)-O(3A)-C(21A)-C(22A)	-179.0(3)	O(3A)-C(21A)-C(22A)-C(23A)	179.6(3)
C(25A)-C(21A)-C(22A)-C(23A)	-1.7(5)	C(24A)-N(6A)-C(23A)-C(22A)	1.6(5)
C(24A)-N(6A)-C(23A)-C(35A)#2	-177.2(3)	C(21A)-C(22A)-C(23A)-N(6A)	0.5(5)
C(21A)-C(22A)-C(23A)-C(35A)#2	179.3(3)	C(23A)-N(6A)-C(24A)-C(25A)	-2.5(5)
C(23A)-N(6A)-C(24A)-C(26A)	173.8(3)	O(3A)-C(21A)-C(25A)-C(24A)	179.4(3)
C(22A)-C(21A)-C(25A)-C(24A)	0.9(5)	N(6A)-C(24A)-C(25A)-C(21A)	1.3(5)
C(26A)-C(24A)-C(25A)-C(21A)	-174.9(3)	C(27A)-N(7A)-C(26A)-O(4A)	0.3(5)
C(27A)-N(7A)-C(26A)-C(24A)	-177.6(3)	N(6A)-C(24A)-C(26A)-O(4A)	176.2(3)
C(25A)-C(24A)-C(26A)-O(4A)	-7.3(5)	N(6A)-C(24A)-C(26A)-N(7A)	-5.8(4)
C(25A)-C(24A)-C(26A)-N(7A)	170.7(3)	C(26A)-N(7A)-C(27A)-C(28A)	129.6(3)
N(7A)-C(27A)-C(28A)-C(29A)	-70.1(4)	N(7A)-C(27A)-C(28A)-C(33A)	108.8(4)
C(33A)-C(28A)-C(29A)-C(30A)	-0.7(5)	C(27A)-C(28A)-C(29A)-C(30A)	178.3(3)
C(28A)-C(29A)-C(30A)-C(31A)	0.3(6)	C(29A)-C(30A)-C(31A)-C(32A)	-0.1(5)
C(29A)-C(30A)-C(31A)-C(34A)	178.5(3)	C(30A)-C(31A)-C(32A)-C(33A)	0.3(5)
C(34A)-C(31A)-C(32A)-C(33A)	-178.3(3)	C(29A)-C(28A)-C(33A)-C(32A)	0.9(5)
C(27A)-C(28A)-C(33A)-C(32A)	-178.1(3)	C(31A)-C(32A)-C(33A)-C(28A)	-0.7(5)
C(35A)-N(8A)-C(34A)-C(31A)	111.6(4)	C(32A)-C(31A)-C(34A)-N(8A)	-41.8(5)

SUPPORTING INFORMATION

C(30A)-C(31A)-C(34A)-N(8A)	139.6(4)	C(34A)-N(8A)-C(35A)-O(5A)	-7.8(6)
C(34A)-N(8A)-C(35A)-C(23A)#2	174.1(3)	C(6A)-N(1A)-C(36A)-C(37A)	-74.6(4)
C(9A)-N(1A)-C(36A)-C(37A)	104.5(4)	N(1A)-C(36A)-C(37A)-C(38A)	178.5(4)

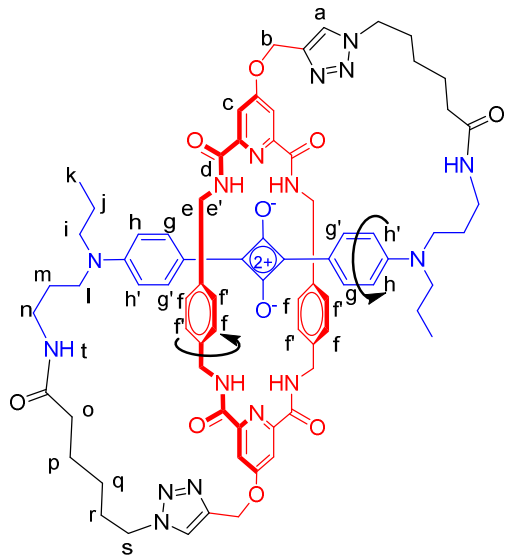
Symmetry transformations used to generate equivalent atoms:
#1 -x+1,-y,-z+1 #2 -x,-y+1,-z+1

Table S4. Hydrogen bonds for **SF8(C6)2** (nd1902) [Å and °].

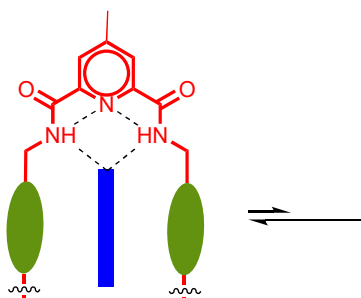
D-H...A	d(D-H)	d(H...A)	d(D...A)	<(DHA)
N(2)-H(2N)...O(2W)#2	0.70(4)	2.23(4)	2.918(5)	172(4)
N(7)-H(7N)...O(1)#1	0.81(5)	2.08(5)	2.828(4)	155(5)
N(7)-H(7N)...N(6)	0.81(5)	2.28(5)	2.694(4)	113(4)
N(8)-H(8N)...O(1)	0.77(5)	2.19(5)	2.914(4)	157(4)
N(8)-H(8N)...N(6)#1	0.77(5)	2.31(4)	2.697(4)	112(4)
N(2A)-H(2NA)...O(1W)#3	0.84(4)	1.96(4)	2.800(4)	174(4)
N(7A)-H(7NA)...O(1A)	0.85(5)	1.99(5)	2.802(4)	160(4)
N(8A)-H(8NA)...O(1A)#2	0.70(5)	2.17(5)	2.823(4)	155(5)
N(8A)-H(8NA)...N(6A)#2	0.70(5)	2.33(5)	2.670(4)	112(4)
C(1S)-H(1SA)...O(4)#4	1.00	2.45	3.232(5)	134.3
C(1S)-H(1SA)...O(4A)	1.00	2.26	3.088(5)	139.4
C(2S)-H(2SA)...O(5)	1.00	2.06	3.056(5)	172.9
C(3S)-H(3SA)...N(5A)#2	1.00	2.27	3.199(5)	153.4
C(4S)-H(4SB^a)...O(4)	1.00	2.21	3.090(5)	146.6
C(5S)-H(5SA)...N(5)	1.00	2.32	3.270(6)	159.0
O(1W)-H(1WA)...O(5A)	0.865(10)	1.858(12)	2.720(4)	175(5)
O(1W)-H(1WB)...O(2)	0.866(10)	1.887(13)	2.744(4)	170(4)
O(2W)-H(2WA)...O(5)#5	0.862(10)	2.024(16)	2.871(4)	167(5)
O(2W)-H(2WB)...O(2A)	0.863(10)	1.954(15)	2.801(4)	167(5)

Symmetry transformations used to generate equivalent atoms:
#1 -x+1,-y,-z+1 #2 -x,-y+1,-z+1 #3 -x+1,-y+1,-z+1
#4 x,-y+1/2,z-1/2 #5 x,y+1,z

SUPPORTING INFORMATION

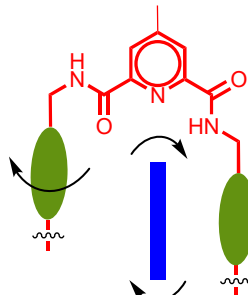
4. Variable Temperature ^1H NMR Studies of SF8(C6)₂

(a) contracted figure eight core



contracted cavity immobilizes the tetralactam phenylene and squaraine aminophenyl rings

(b) expanded figure eight core



expansion of the cavity permits spinning of the tetralactam phenylene and squaraine aminophenyl rings

Figure S4. (top) Structure of SF8(C6)₂ and atom labels. (bottom) Graphical picture of the macrocyclic breathing process that explains the internal motion within the core of an SF8 molecule. This process has been proposed before for squaraine rotaxanes.^[7] Amide bond rotation within the tetralactam core of the SF8 molecule expands the macrocycle cavity from contracted core (a) to expanded core (b) which lowers the barrier for spinning of a tetralactam phenylene ring (green) and squaraine aminophenyl ring (blue).

SUPPORTING INFORMATION

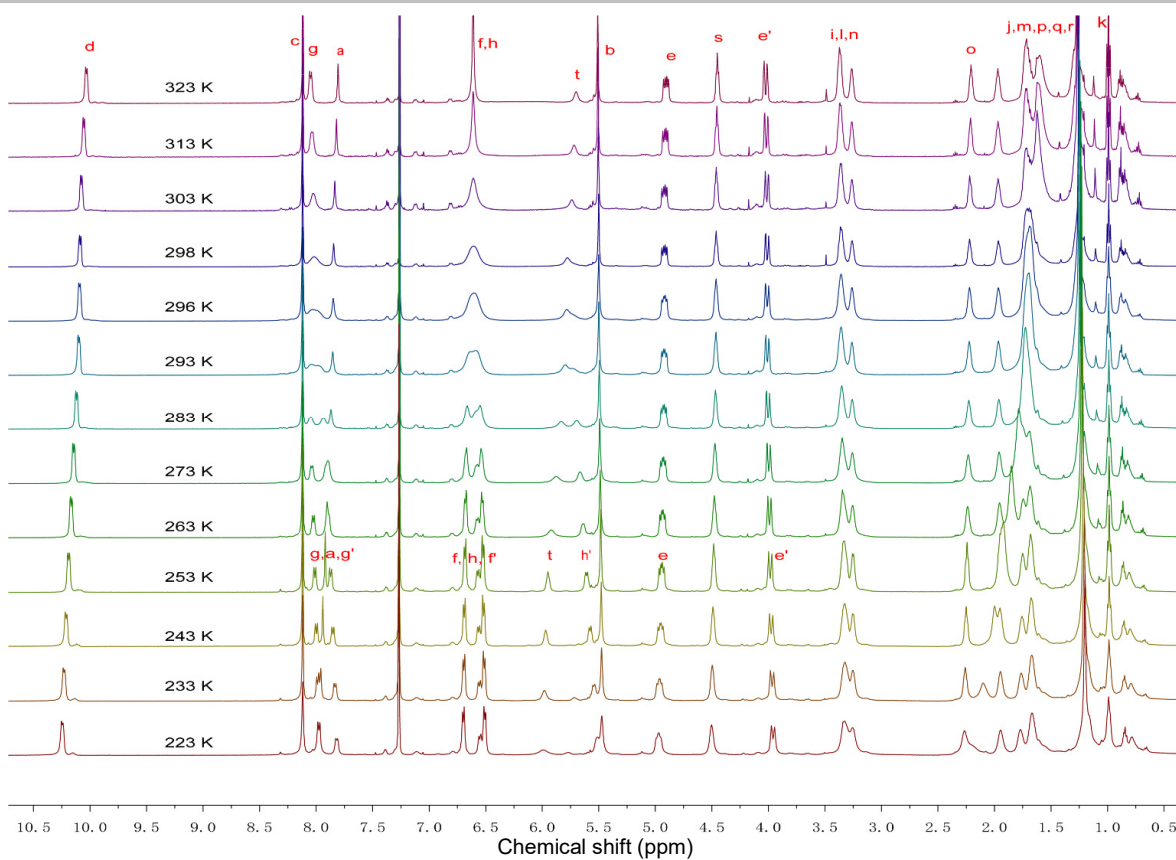
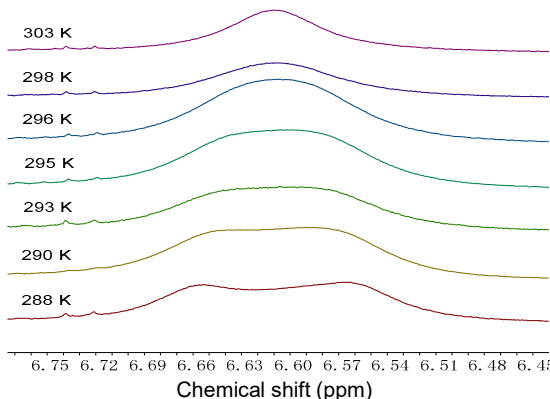
Figure S5. Variable temperature ^1H NMR (500 MHz, CDCl_3) of $\text{SF8}(\text{C6})_2$ 

Figure S6. Expanded coalescence region for proton f from Figure S5 (coalescence temperature is 295 K).

Table S4. Summary of variable temperature ^1H NMR data for compound $\text{SF8}(\text{C6})_2$.

T_c (K)	$\Delta\nu$ (Hz)	k (s^{-1})	ΔG^\ddagger (kcal/mol)
295	43	95.5	14.6

The rate of two-site exchange (k) at the coalescence temperature was determined using:

$$k = \frac{\pi}{\sqrt{2}} \Delta\nu_0$$

Where $\Delta\nu_0$ is the chemical shift frequency difference of the two protons. To determine the activation free energy (in kcal/mol), the Eyring equation was simplified as the following, where T_c is the coalescence temperature (in K):

$$\Delta G^\ddagger = 4.57 T_c [9.97 + \log_{10}(\frac{T_c}{\Delta\nu_0})]$$

SUPPORTING INFORMATION

5. Photophysical Properties and Stability Studies

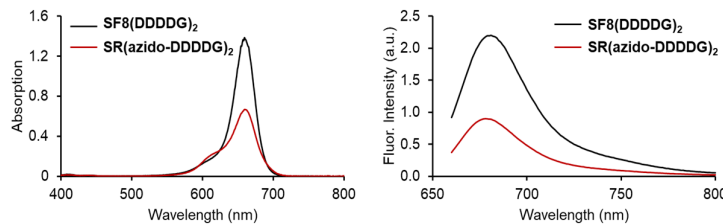
Comparison of SF8(DDDDG)₂ and SR(azido-DDDDG)₂

Figure S7. Absorption and emission spectra of **SF8(DDDDG)₂** and **SR(azido-DDDDG)₂** in water at 5 μ M, $\lambda_{\text{ex}} = 650$ nm, slit width = 2 nm. The blue-shifted shoulder in the absorption of **SR(azido-DDDDG)₂** indicates non-fluorescent H-aggregates.

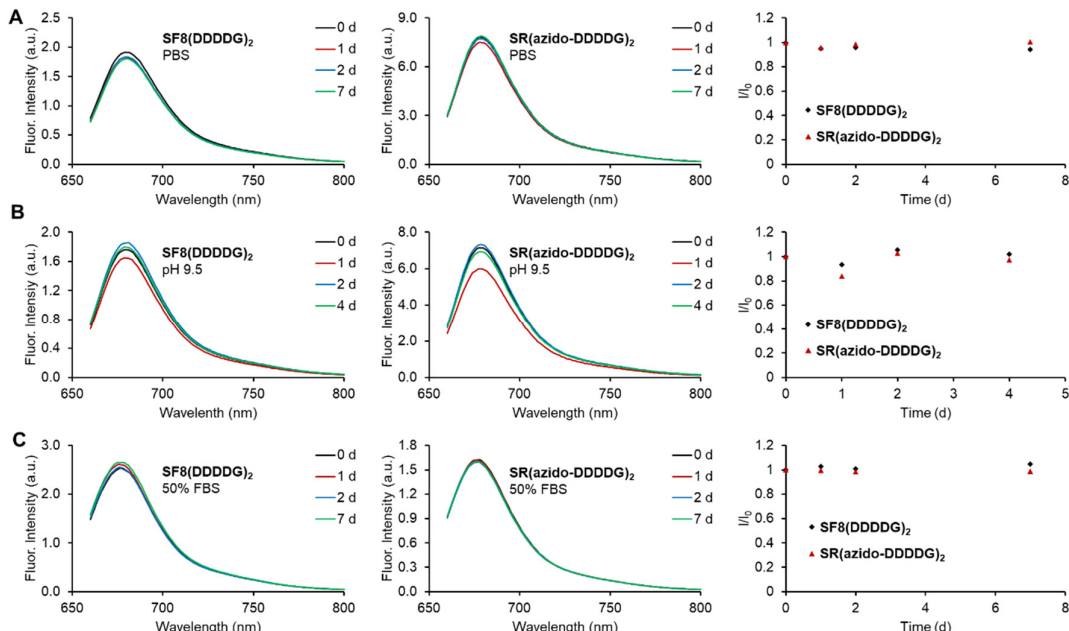


Figure S8. Chemical stability study. Change in fluorescence spectra of **SF8(DDDDG)₂** and **SR(azido-DDDDG)₂** in the dark in: (A) PBS, pH 7.4, (B) sodium bicarbonate buffer, pH 9.5, (C) 50% fetal bovine serum (FBS), at 3 μ M for a few days, r.t., $\lambda_{\text{ex}} = 650$ nm, slit width = 2 nm. The data indicates very high chemical stability.

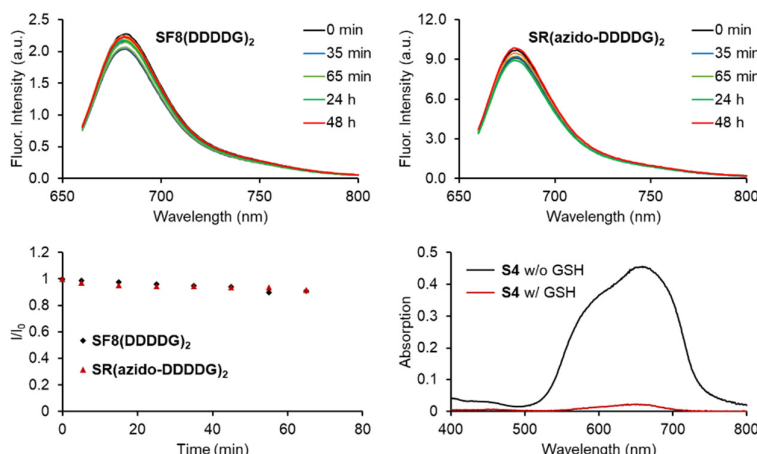


Figure S9. Chemical stability study. Fluorescence spectra of **SF8(DDDDG)₂** and **SR(azido-DDDDG)₂** (5 μ M) in the dark in potassium phosphate buffer (100 mM, pH 7.4) containing 10 mM of the reduced form of glutathione (GSH) at r.t., $\lambda_{\text{ex}} = 650$ nm, slit width = 2 nm. The bottom right panel is a control study showing that the nucleophilic thiol within GSH attacks and bleaches the free squaraine dye **S4** (Scheme S1), thus illustrating the excellent squaraine protection in **SF8(DDDDG)₂** and **SR(azido-DDDDG)₂**.

SUPPORTING INFORMATION

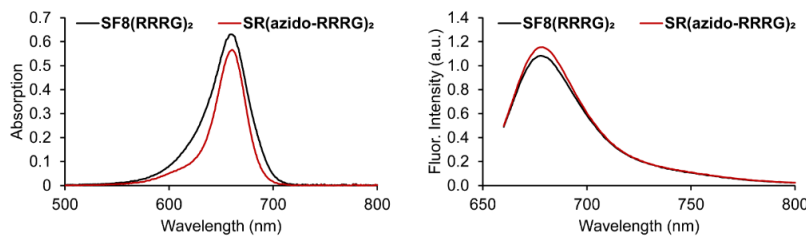
Comparison of SF8(RRRG)₂ and SR(azido-RRRG)₂

Figure S10. Absorption and emission spectra of **SF8(RRRG)₂** and **SR(azido-RRRG)₂** in water at 5 μ M, $\lambda_{\text{ex}} = 650$ nm, slit width = 2 nm. There is essentially no difference in fluorescence brightness.

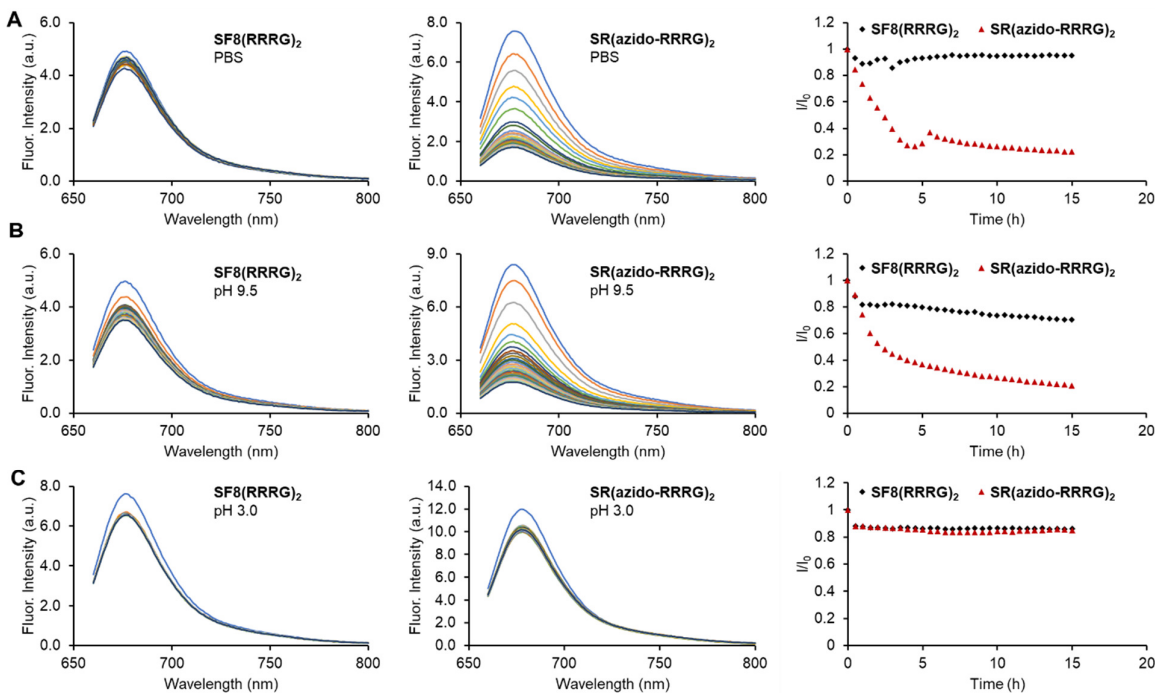


Figure S11. Chemical stability study. Change in fluorescence spectra of **SF8(RRRG)₂** and **SR(azido-RRRG)₂** in the dark in: (A) PBS, pH 7.4, (B) sodium bicarbonate buffer, pH 9.5, (C) citrate buffer, pH 3.0, at 5 μ M for 15 h, r.t., 30 min/scan, $\lambda_{\text{ex}} = 650$ nm, slit width = 2 nm. The **SF8(RRRG)₂** is chemically stable under all conditions, whereas the **SR(azido-RRRG)₂** undergoes bleaching at pH 7.4 and 9.5, but is stable at pH 3.0. This suggests that the squaraine core in **SR(azido-RRRG)₂** is attacked intramolecularly by the nucleophilic nitrogen atoms on the appended arginine side chains. Additional discussion is in the next figure caption.

SUPPORTING INFORMATION

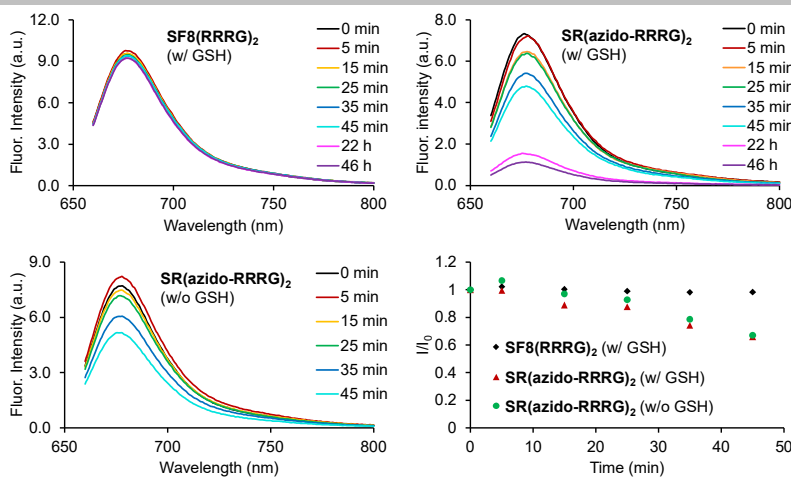
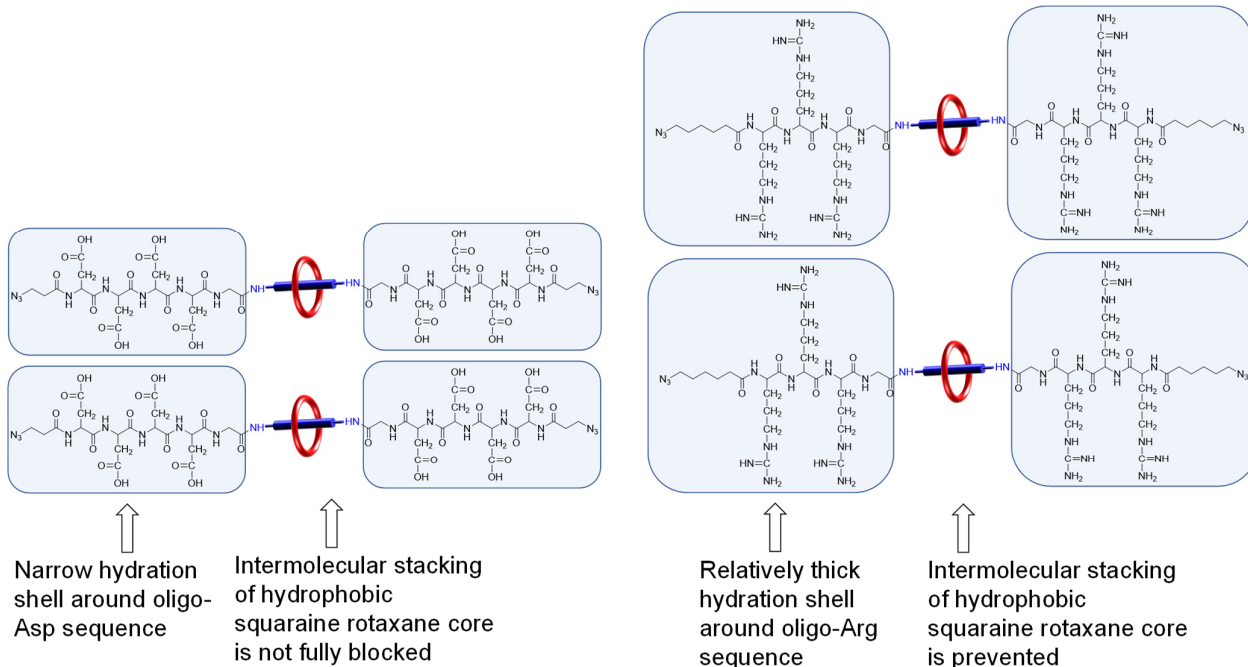


Figure S12. Fluorescence spectra of **SF8(RRRG)₂** and **SR(azido-RRRG)₂** in the dark in potassium phosphate buffer (100 mM, pH 7.4) with the reduced form of glutathione (GSH) (10 mM, r.t., $\lambda_{\text{ex}} = 650$ nm, slit width = 2 nm). After 46 hours, the fluorescence intensity for **SF8(RRRG)₂** is essentially unchanged, while the intensity for **SR(azido-RRRG)₂** is reduced to 15%. The bottom right panel shows that the added GSH did not accelerate chemical bleaching of the squaraine core in **SR(azido-RRRG)₂** consistent with the model that the squaraine core is attacked intramolecularly by the nucleophilic nitrogen atoms on the appended arginine side chains.

Comparison of **SR(azido-DDDDG)₂** and **SR(azido-RRRG)₂**

Observation 1: **SR(azido-DDDDG)₂** has a propensity to form an H-aggregate in water whereas **SR(azido-RRRG)₂** does not.

Proposed Explanation: The thicker hydration shell of the oligo-Arg sequence better prevents close contact of the hydrophobic squaraine rotaxane core that is within the triblock structure of polar-nonpolar-polar, as illustrated in Scheme S9.



Scheme S9. Illustration showing how the difference in hydration shells around each peptide sequence explains the difference in propensity for intermolecular aggregation and squaraine rotaxane absorption band broadening. The oligo-Asp sequence produces two relatively narrow hydration shells on either side of the central hydrophobic squaraine rotaxane core and is unable to fully prevent intermolecular stacking and aggregation in water. In contrast, the longer arginine side chains along an oligo-Arg sequence produce a much thicker hydration shell that more effectively blocks intermolecular aggregation of the non-polar rotaxane. The aggregation-induced squaraine rotaxane absorption broadening for **SR(azido-DDDDG)₂** agrees with previous observations with squaraine rotaxanes (*J. Am. Chem. Soc.* **2005**, *127*, 3288–3289) that the surrounding rotaxane macrocycle attenuates aggregation-induced squaraine absorption broadening but does not completely eliminate it.

SUPPORTING INFORMATION

Observation 2: Solutions of **SR(azido-DDDG)₂** are completely stable while solutions of **SR(azido-RRRG)₂** undergo chemical bleaching within 15 hours in PBS buffer.

Proposed Explanation: Squaraine bleaching is due to nucleophilic attack at its C₄O₂ core. Thus, the difference in chemical stability is attributed to extra lateral mobility of the surrounding macrocycle in the mechanically bonded rotaxane which transiently exposes the core of the encapsulated squaraine to nucleophilic attack. The following data is consistent with the picture that the squaraine core in **SR(azido-RRRG)₂** is attacked intramolecularly by a nucleophilic nitrogen atom on the appended arginine side chains.

1. The results in Figures S11 show no bleaching at pH 3.0, because the nitrogen atoms on the appended arginine side chains are fully protonated.
2. The results in Figures S12 show that addition of excess glutathione (GSH), a strong nucleophile, does not accelerate the bleaching process. Thus, intermolecular attack using GSH does not compete with intramolecular attack by nucleophilic nitrogen atoms on the appended arginine side chains.
3. The chemical stability data in Figures S13 and S14 show that **SR7** with protected arginine side chains is more stable than the **SR(azido-RRRG)₂** with unprotected arginine side chains, consistent with intramolecular attack by a nucleophilic nitrogen atom on an appended arginine side chain.
4. Mass spectra of bleached samples **SR(azido-RRRG)₂** (allowed to sit in water at room temperature in the dark for 60 h) show complete loss of the parent molecular ion and no larger molecular weight peaks. Only hydrolytic fragments are observed (see Scheme S10).
5. The mechanism in Scheme S10 shows how hydrolytic bleaching of the squaraine dye within **SR(azido-RRRG)₂** is promoted by an Arg side chain nitrogen atom, which provides intramolecular nucleophilic assistance. This mechanism is consistent with all the data.

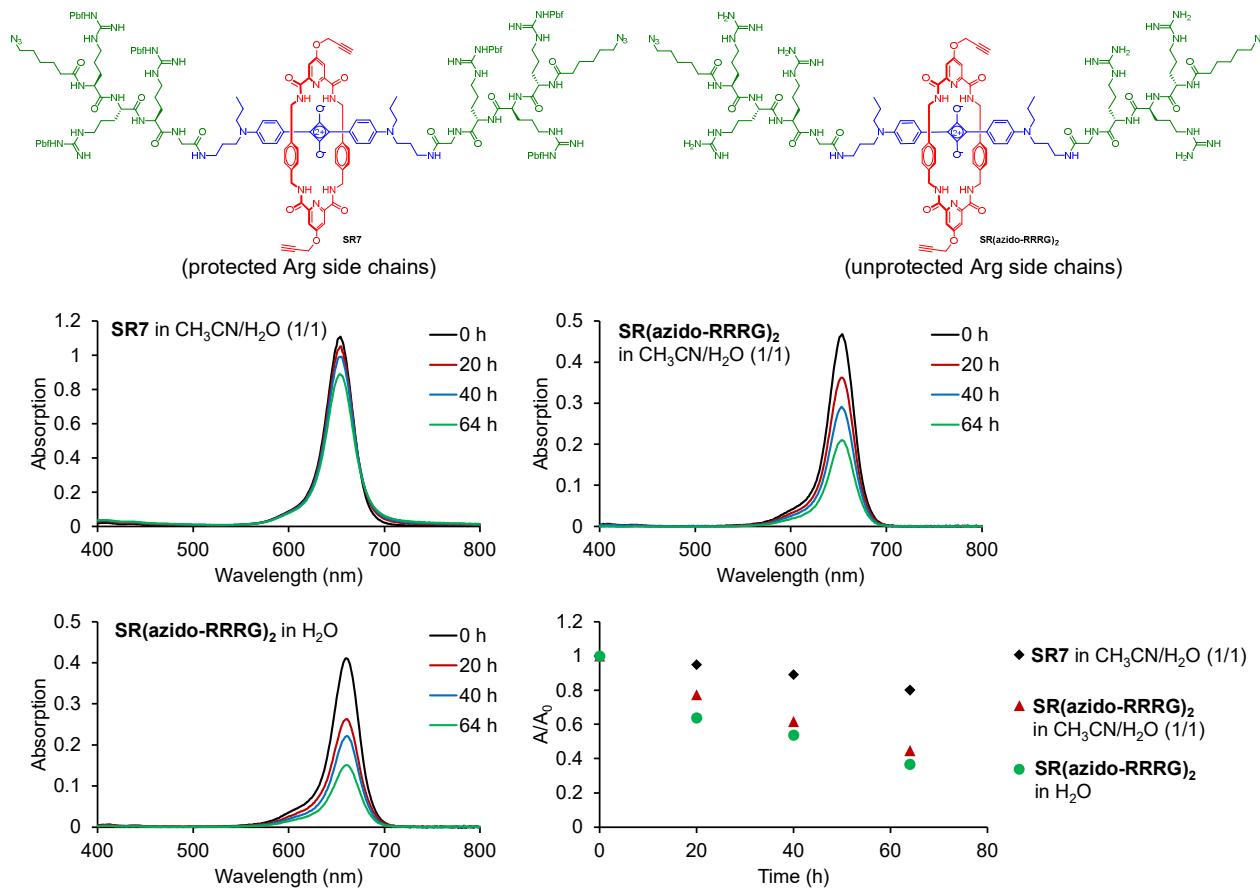


Figure S13. Chemical stability study. Change in absorption spectra of **SR7** and **SR(azido-RRRG)₂** in the dark, 5 μ M, r.t. **SR7** with protected Arg side chains is chemically more stable. This suggests that the squaraine core in **SR(azido-RRRG)₂** is attacked intramolecularly by the nucleophilic nitrogen atoms on the appended arginine side chains. See Scheme S10.

SUPPORTING INFORMATION

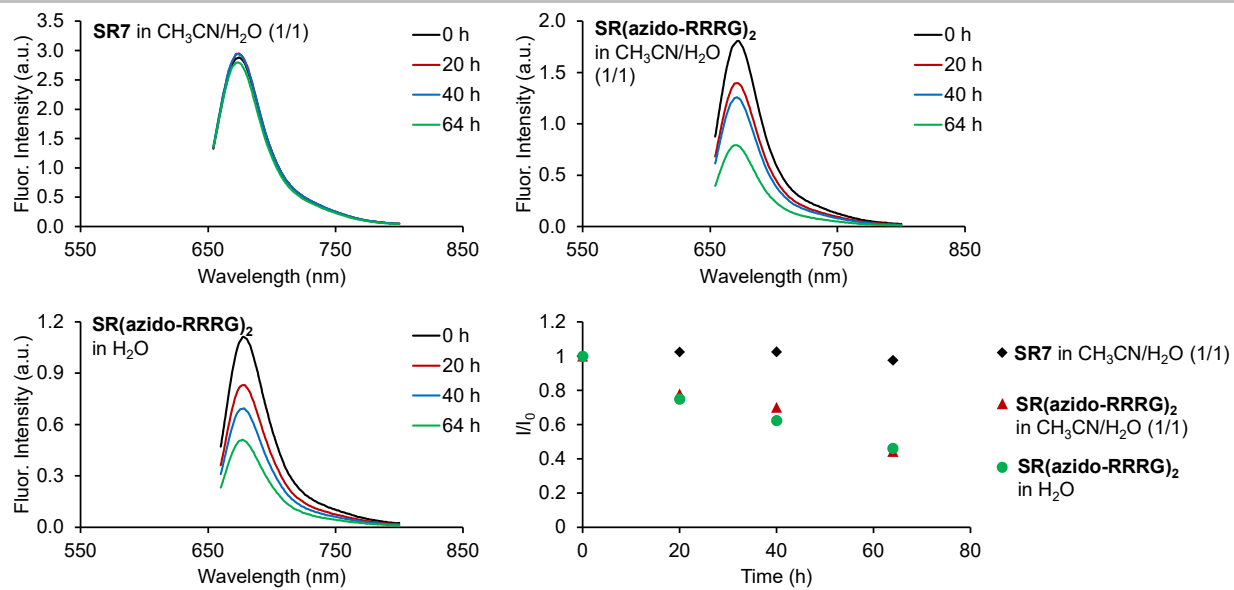
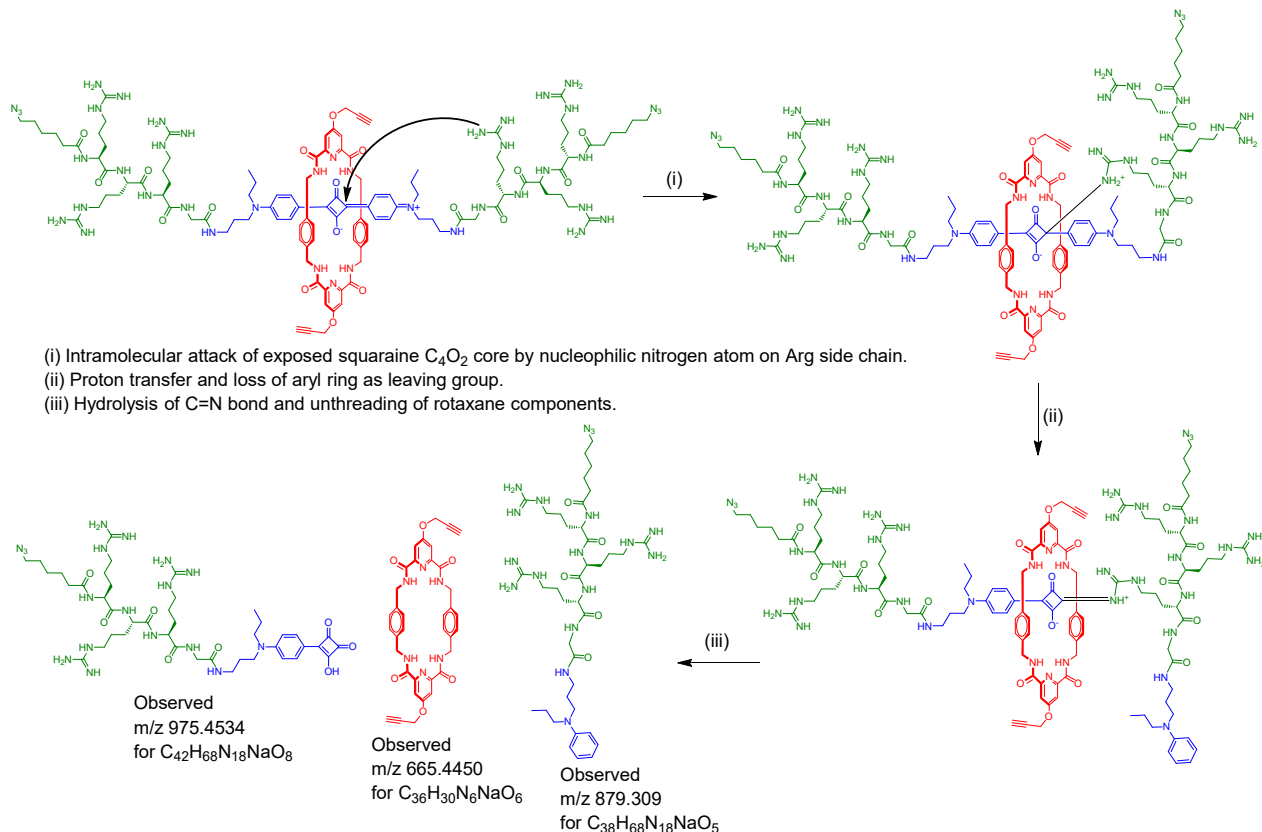


Figure S14. Chemical stability study. Change in fluorescence spectra of **SR7** and **SR(azido-RRRG)₂** in the dark, 5 μM , r.t. For samples in $\text{CH}_3\text{CN}/\text{H}_2\text{O}$ (1/1), $\lambda_{\text{ex}} = 644 \text{ nm}$, slit width = 2 nm; for samples in H_2O , $\lambda_{\text{ex}} = 650 \text{ nm}$, slit width = 2 nm. The **SR7** with protected Arg side chains is chemically more stable. This suggests that the squaraine core in **SR(azido-RRRG)₂** is attacked intramolecularly by the nucleophilic nitrogen atoms on the appended arginine side chains. See Scheme S10.

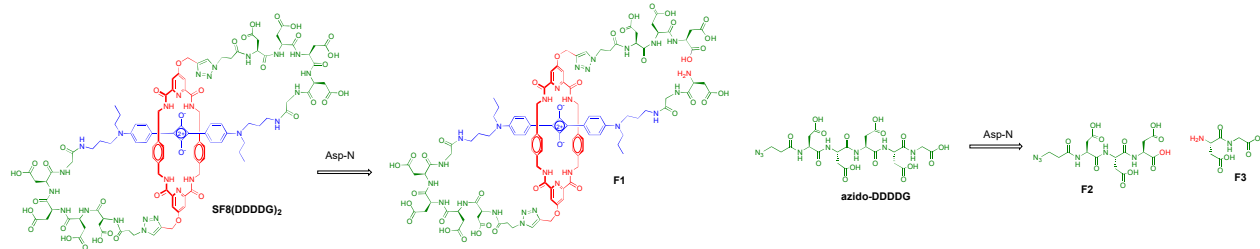


Scheme S10. Hydrolytic bleaching of squaraine dye within **SR(azido-RRRG)₂** is promoted by an Arg side chain nitrogen atom which provides intramolecular nucleophilic assistance. Mass spectral analysis of a bleached sample of **SR(azido-RRRG)₂** in water observed the three fragments produced by this hydrolytic process.

SUPPORTING INFORMATION

Proteolytic Stability (Comparison of SF8(DDDDG)₂ with azido-DDDDG)

The enzyme Asp-N endoproteinase (*Pseudomonas fragi* mutant, Enzyme Commission Number 3.4.24.33, Millipore Sigma Cat # 11420488001) hydrolyzes peptide and protein bonds on the N-terminal side of aspartic acid residues, and was used to determine if incorporation of a tetra-Asp sequence within an SF8 molecule enhanced resistance to protease degradation. Time course experiments employed LC/MS to measure the loss of **SF8(DDDDG)₂** probe or pentapeptide **azido-DDDDG** due to proteolysis by Asp-N, and also to elucidate the structures of the resulting fragments **F1 - F3**.



Separate samples of **azido-DDDDG** pentapeptide or **SF8(DDDDG)₂** probe in water (10 μ M) were incubated in the presence of Asp-N (42 nM) at 37 °C. At each time point, the reaction mixture was flash-frozen until it was analyzed by LC/MS. The LC/MS instrument consisted of a Waters Acuity UPLC H-Class system equipped with a photodiode array detector, a sample manager-FTN, and quaternary solvent manager coupled with a Bruker Impact II ultra-high resolution Qq-time-of-flight mass spectrometer using Hystar 5.0 SR1 software. The positive ion mode of the Bruker electrospray ionization source was used for the detection of **SF8(DDDDG)₂** with the following parameters: end plate offset voltage = –500 V, capillary voltage = 3000 V, and nitrogen as both a nebulizer (3 bar) and dry gas (6 L/min) at 200 °C. Mass spectra were accumulated over the mass range 400 - 4500 Da. The negative ion mode of the Bruker electrospray ionization source was used for the detection of **azido-DDDDG** with the following parameters: end plate offset voltage = –500 V, capillary voltage = 1800 V, and nitrogen as both a nebulizer (3 bar) and dry gas (7 L/min) at 200 °C. Mass spectra were accumulated over the mass range 150 - 3000 Da. LC separations were performed on a Waters UPLC Acuity HSS T3 column (1.7 μ m, 2.1 mm i.d. \times 150 mm) at 40 °C. LC gradient for analysis of **SF8(DDDDG)₂** probe was a 20-min gradient of a 3 min isocratic at 75% A/25% B, a 7 min linear gradient to 60% A/40% B, a 5.9 min linear gradient to 0% A/100% B, a 0.1-min linear gradient to 75% A/25% B, and then a 4 min isocratic at 75% A/25% B (A = 0.1% formic acid in water, B = 0.1% formic acid in acetonitrile) with a flow rate of 0.3 mL/min. LC gradient for analysis of **azido-DDDDG** was a 14-min gradient of a 2 min isocratic at 100% A/0% B, a 8 min linear gradient to 80% A/20% B, a 0.1-min linear gradient to 100% A/0% B, and then a 4 min isocratic at 100% A/0% B with a flow rate of 0.3 mL/min.

time (h)	Relative Amount (%)	
	SF8(DDDDG) ₂	azido-DDDDG
0	100	100
1	92	83
2	87	51

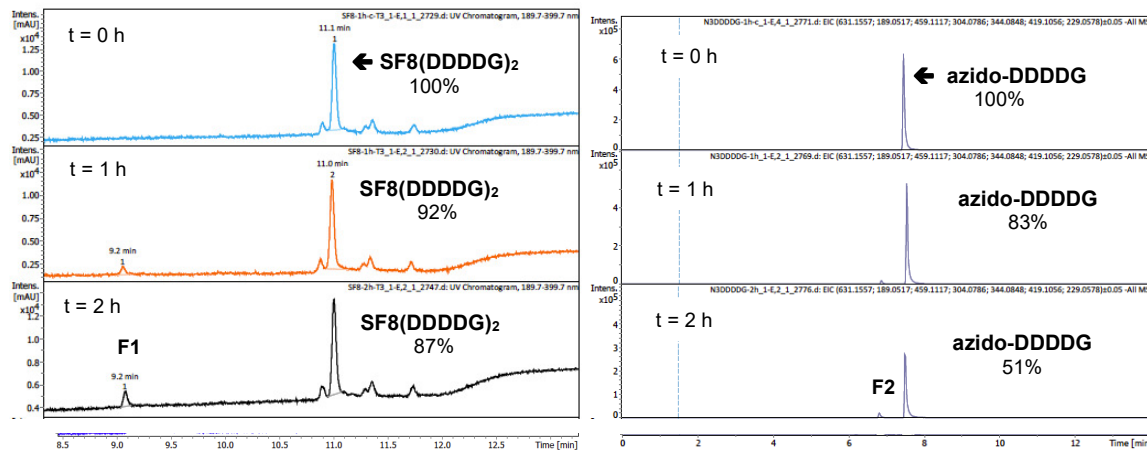


Figure S15. LC chromatograms for 10 μ M solutions of **SF8(DDDDG)₂** (left) or **azido-DDDDG** (right) over the time course of incubation with Asp-N in water at 37 °C. The traces indicate minor loss of **SF8(DDDDG)₂** probe and appearance of fragment **F1**, and much greater loss of **azido-DDDDG** pentapeptide and appearance of fragment **F2**. Fragment **F3** and other small, polar fragments eluted in the column void volume peak and do not appear in the trace.

SUPPORTING INFORMATION

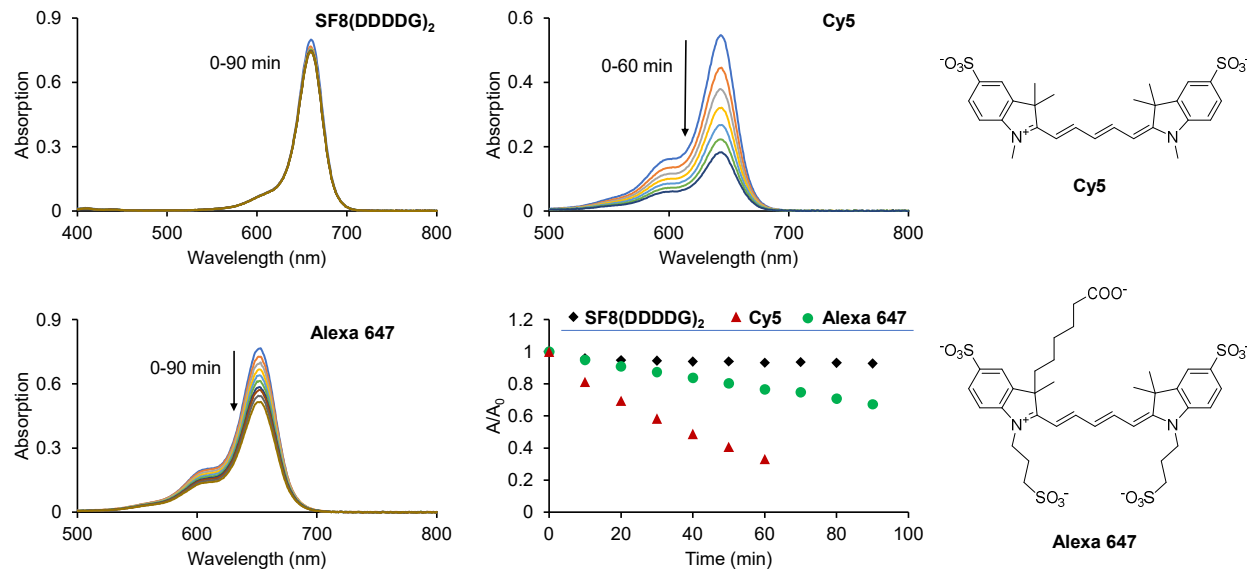
Photostabilities (Comparison of SF8(DDDDG)₂ with Cy5, Alexa 647)

Figure S16. Photostability study. Change in absorption spectra of **SF8(DDDDG)₂**, **Cy5** and **Alexa 647** irradiated at a distance of 3 cm with a Xenon lamp (150 W, > 495 nm filter) for 60 mins or 90 mins, 3 μ M in PBS, pH 7.4. Absorption spectra were collected every 10 mins.

SUPPORTING INFORMATION

6. Liposomes Studies

Liposome Leakage Studies

A lipid film of 1-palmitoyl-2-oleoyl-sn-glycero-3-phosphocholine (100% POPC) or a film that included 5% of 1-palmitoyl-2-oleoyl-sn-glycero-3-phospho-L-serine (95:5, POPC:POPS) was formed from a chloroform solution under reduced pressure and dried under high vacuum overnight. Standard thin film hydration methods were conducted using HEPES buffer (10 mM HEPES, 145 mM NaCl, pH 7.4) containing carboxyfluorescein (CF, 50 mM), followed by a brief vortex dispersion and five freeze/thaw cycles. Lipid suspensions were extruded 21 times through a 0.2 µm polycarbonate filter (Whatman) to produce a suspension of large unilamellar vesicles. Unencapsulated CF was removed by use of a PD-10 desalting column (GE Healthcare) using HEPES buffer as an eluent. Dynamic light scattering was used to determine the hydrodynamic diameters of CF-free POPC and POPC:POPS liposomes in HEPES buffer (10 mM, 150 mM NaCl, pH 7.4). At high concentrations within liposomes, CF is self-quenched resulting in low fluorescence (ex: 480 nm, em: 515 nm). An increase in CF fluorescence is indicative of release from liposomes into bulk solution. Addition of 1% (w/v) Triton X-100 lysed the vesicles, allowing for normalization of the release to 100% leakage. The percentage of CF release F (%) was calculated using the equation $F (\%) = 100 (F_t - F_0)/(F_{total} - F_0)$, where F_t is the intensity at the measured time point, F_0 is the intensity at $t = 0$, and F_{total} is the intensity after treatment with Triton X-100.

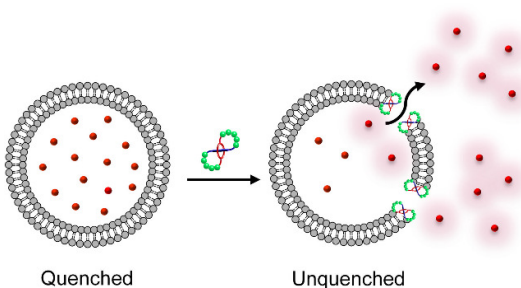


Figure S17. Schematic representation of SF8-induced leakage of carboxyfluorescein (CF) from liposomes.

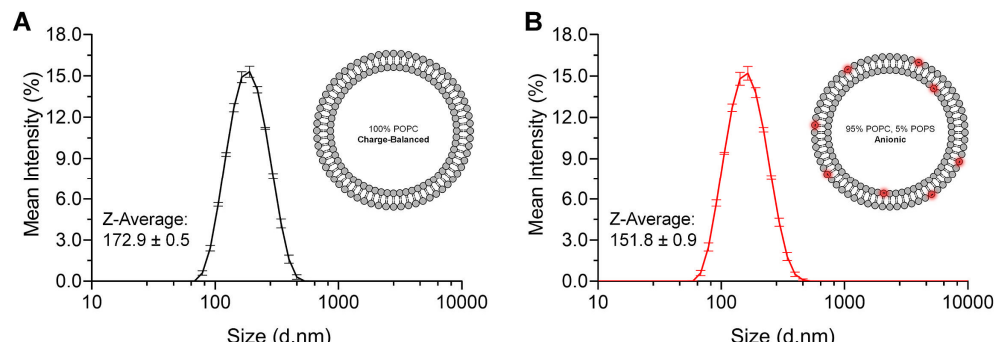


Figure S18. Dynamic light scattering measurements of: (A) empty charge-balanced (100% POPC), or (B) empty anionic (95% POPC, 5% POPS) liposomes in 20 mM HEPES buffer with 150 mM NaCl, pH 7.4.

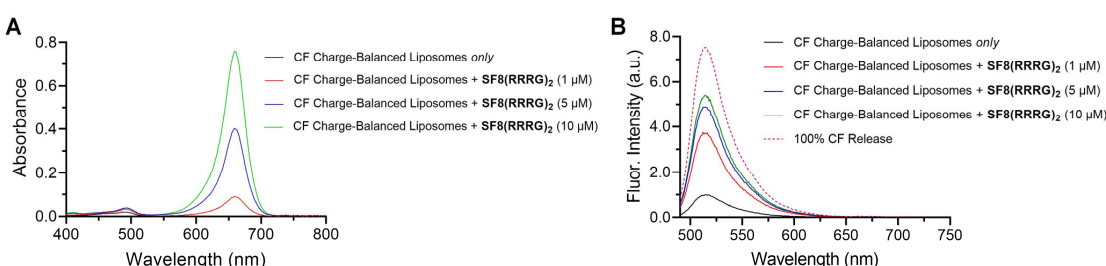


Figure S19. (A) Absorbance and (B) fluorescence spectra (ex: 480 nm) of CF containing **charge-balanced liposomes** (100% POPC) in the presence of 1-10 µM **SF8(RRRG)₂** in 20 mM HEPES buffer with 150 mM NaCl, pH 7.4. Spectra taken 60 mins after addition of **SF8(RRRG)₂**.

SUPPORTING INFORMATION

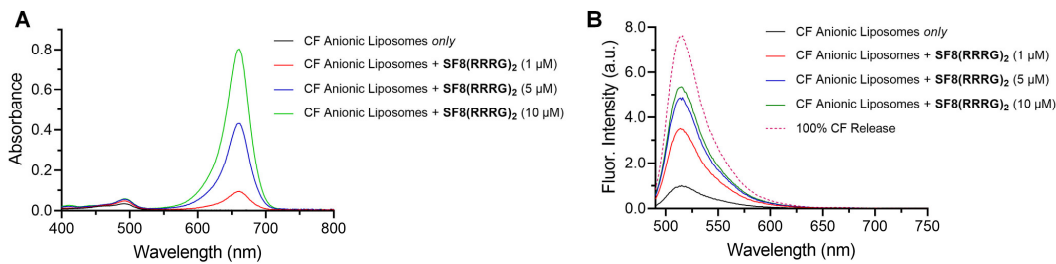


Figure S20. (A) Absorbance and (B) fluorescence spectra (ex: 480 nm) of CF containing **anionic liposomes** (95% POPC, 5% POPS) in the presence of 1–10 μM **SF8(RRRG)₂** in 20 mM HEPES buffer with 150 mM NaCl, pH 7.4. Spectra taken 60 mins after addition of **SF8(RRRG)₂**.

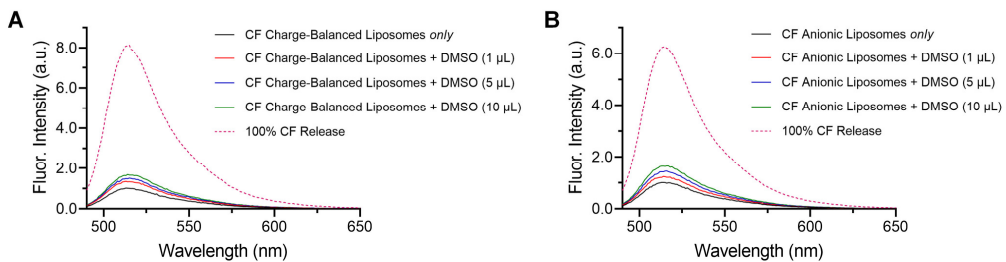


Figure S21. Fluorescence emission spectra (ex: 480 nm) of CF containing (A) charge-balanced (100% POPC) or (B) anionic (95% POPC, 5% POPS) liposomes in the absence or presence of DMSO in 20 mM HEPES buffer with 150 mM NaCl, pH 7.4. Spectra taken 60 mins after addition of DMSO.

Octanol Partitioning Studies

Stock solutions of polar lipids were prepared at 10 mM in 1-octanol. Sodium laurate was warmed to 50 °C prior to experiments to improve solubilization. Probe stock solutions were 1 mM in DMSO. In each experiment, 10 μM **SF8(RRRG)₂** and 200 μM polar lipid were combined and vortexed for 30 seconds in a biphasic mixture composed of octanol/TES buffer (5 mM, 145 mM NaCl, pH 7.4) in a volume ratio of 1:1 (1 mL total volume). Samples were then centrifuged at 1000 g for 2 minutes to rapidly separate phases. After obtaining photographs in ambient light, the phases were transferred to a 96-well plate, and the absorbance at 655 nm was measured. All measurements were performed in triplicate. Log *P* was calculated using the formula log *P* = log(A_{octanol}/A_{buffer}).

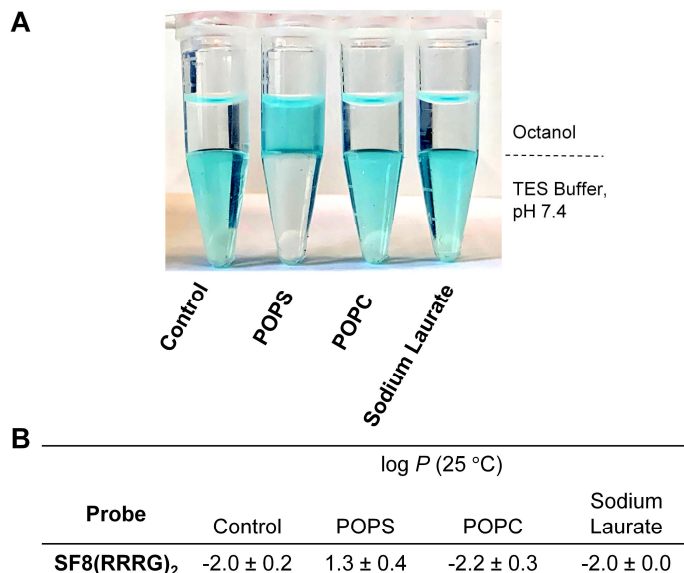


Figure S22. Effect of the polar lipids, 1-palmitoyl-2-oleoyl-sn-glycero-3-phospho-L-serine (POPS), 1-palmitoyl-2-oleoyl-sn-glycero-3-phosphocholine (POPC) or sodium laurate, on the octanol–water partitioning of **SF8(RRRG)₂** at 25 °C. (A) Color photographs of **SF8(RRRG)₂** (10 μM) partitioned between octanol and TES buffer (5 mM TES, 145 mM NaCl, pH 7.4) containing 200 μM of polar lipid. (B) Calculated log *P* values for the probe in each solution.

SUPPORTING INFORMATION

7. Cell and Bone Studies

Cell Culture

All cells were cultured and maintained in a humidified incubator at 37 °C under 5% CO₂. The F12-K cell medium was purchased from ATCC. Fetal bovine serum was purchased from Atlanta Biologicals, and all other supplies were purchased from Sigma Aldrich. The A549 (ATCC CCL-185) human non-small cell lung adenocarcinoma cells and the CHO-K1 (ATCC CCL-61) Chinese hamster ovary cells were grown in F-12K medium supplemented with 10% fetal bovine serum and 1% penicillin/streptomycin.

Cell Viability

The CHO-K1 cells were seeded into 96-microwell plates and grown to 70% confluence. The medium was then removed and replaced with probe in F12-K medium for 24 h at 37 °C and 5% CO₂ in a humidified incubator. After 24 h, the probe was removed and replaced with F-12K medium containing [3-(4,5-dimethylthiazol-2-yl)-2,5-diphenyltetrazolium bromide] (MTT, 1.1 mM). The samples were incubated at 37 °C and 5% CO₂ for 2 h and an SDS-HCl detergent solution was then added. The samples were incubated overnight, and the absorbance of each well was measured at 570 nm, where the readings were normalized relative to untreated cells.

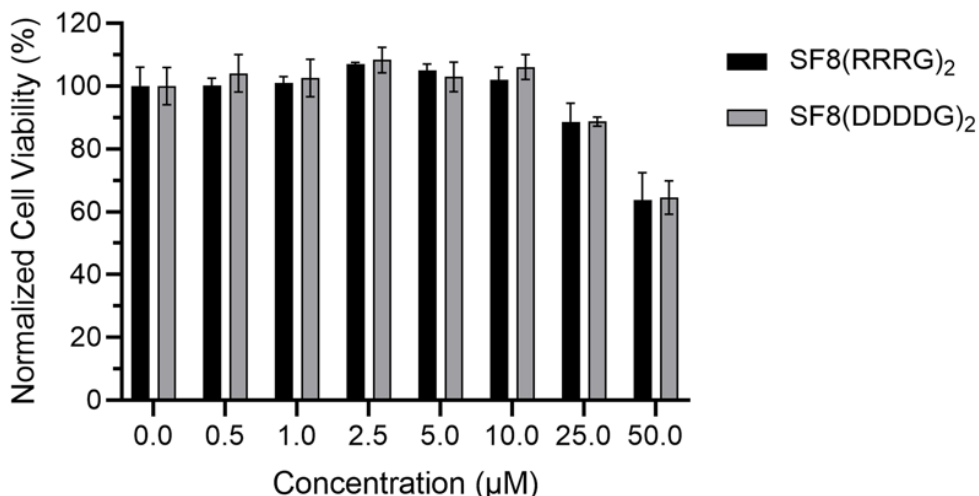


Figure S23. Cell viability of CHO-K1 cells treated with various concentrations of **SF8(RRRG)₂** and **SF8(DDDG)₂** for 24 hours followed by MTT assay.

Cell Microscopy: SF8 Probe Uptake Studies

The A549 and CHO-K1 cells were seeded into 8-well chambered slides and were grown to 70% confluence. Cells were incubated with either **SF8(RRRG)₂** or **SF8(DDDG)₂** at 5 μM in media for 30 min or 4 h at 37 °C. Cells were washed two times with 1xPBS and incubated with 3 μM Hoechst 33342 for 10 min at room temperature. Cells were washed two additional times and imaged on a Zeiss Axiovert 100 TV epifluorescence microscope equipped with a UV filter (ex: 387/11, em: 447/60), FITC filter (ex: 485/20, em: 524/24), TxRed filter (ex: 562/40, em: 624/40), and Cy5.5 filter (ex: 655/40, em: 716/40). Image processing for each micrograph was then conducted using ImageJ2 software with a 10-pixel rolling ball radius background subtraction. The JaCoP co-localization test plugin on ImageJ2 software was employed to measure the Pearson's Correlation Coefficient (PCC).

Cell Microscopy: Probe Colocalization Studies

Three sets of colocalization studies were performed: (a) Living A549 cells were coincubated with a mixture of **SF8(RRRG)₂** (5 μM) and Dextran-Fluorescein (1 mg/mL, Thermo Fisher Scientific) in media for 1 or 2 h at 37 °C. (b) Living A549 cells were incubated with **SF8(RRRG)₂** (5 μM) for 4 h and co-stained with Lysotracker Red DND-99 (100 nM, Thermo Fisher Scientific) for 15 min at 37 °C. (c) Living CHO cells were incubated with **SF8(RRRG)₂** (5 μM) for 4 h and co-stained with 2 mg/mL Dextran-Fluorescein for 15 min. In each case, after coincubation the living cells were washed two times with 1xPBS and incubated with 3 μM Hoechst 33342 for 10 min at room temperature, washed two additional times and imaged as described above.

Summary of Results in Figure S24

The live cell micrographs in Figure S24A showed negligible cell uptake of **SF8(DDDG)₂** after 4 h, but significantly more uptake of **SF8(RRRG)₂** which does not accumulate in the nucleus, or the reticulated organelles such as the Golgi or endoplasmic reticulum. The live cell colocalization experiments in Figure S24B-D show that there is partial overlap of the motile, punctate deep-red **SF8(RRRG)₂** fluorescence with green punctate fluorescence of Dextran-Fluorescein (known marker of endocytosis) or Lysotracker Red (known marker for lysosomes). The PCC values in the range 0.2-0.4 are close to values seen in closely related literature colocalization experiments using an oligo-arginine peptide and fluorescent endosome/lysosome markers.^[8] [9]

The live cell microscopy data indicates that **SF8(RRRG)₂** primarily enters cells by endocytosis (probably macropinocytosis) and accumulates in a mixture endosomes and lysosomes, which is consistent with the cell permeation behavior exhibited by many fluorescent probes that have oligo-arginine sequences.^[10]

SUPPORTING INFORMATION

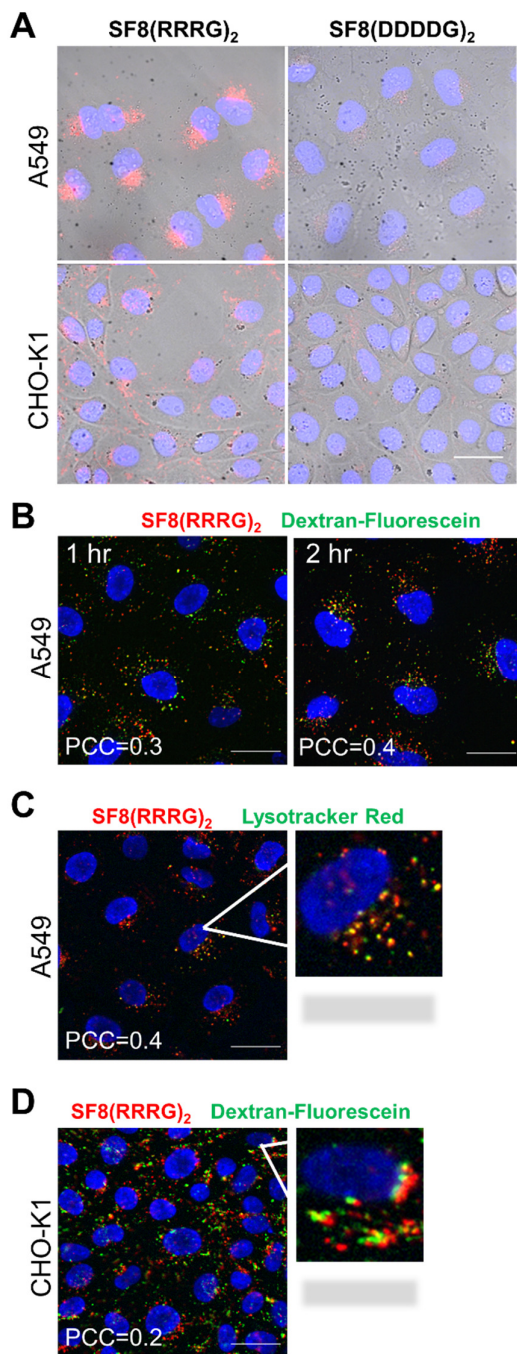


Figure S24. Targeting eukaryotic cells with peptidyl SF8 probes. (A) Representative epifluorescence micrographs with bright field showing probe uptake by A549 and CHO-K1 cells after a 4 h incubation with 5 μ M of either SF8(RRRG)₂ or SF8(DDDG)₂. Each micrograph was acquired under identical conditions and presented with the same fluorescence intensity scale. (B, D) Representative epifluorescence micrographs showing colocalization of SF8(RRRG)₂ with Dextran-Fluorescein (known marker for endosomes) in A549 or CHO-K1 cells. (C) Colocalization of SF8(RRRG)₂ with Lysotracker Red (known marker for lysosomes) in A549 cells. Red fluorescence shows SF8 probes; blue fluorescence shows Hoechst 33342 nuclear stain.; green fluorescence shows Dextran-Fluorescein or Lysotracker Red; yellow fluorescence shows colocalization. Length scale bar = 30 μ m. PCC is Pearson's Correlation Coefficient.

SUPPORTING INFORMATION

Powdered Bone Binding

Tibia and femur bones were excised from euthanized mice, flash frozen with liquid nitrogen, and ground into bone powder. The bone powder (50 mg) was placed into a microcentrifuge tube and incubated with either **SF8(RADG)₂** (4 μ M) or **SF8(DDDG)₂** (4 μ M). The microcentrifuge tubes were shaken for 60 min at room temperature and were then centrifuged (2,000 g, 5 min). Photographic images were then taken under ambient light, and the fluorescence spectrum (ex: 660 nm, slit width: 2 nm) of the supernatant was collected.

Bone Histological Staining

Mouse tibia bones were excised, fixed, and processed using a Leica TP 1020 Tissue Processor. The bone tissue was then embedded into paraffin, sectioned into 4 μ m slices, and placed onto a glass slide. The slides were incubated with either deionized water or 0.25 M ethylenediaminetetraacetic acid (EDTA) for 16 hr. The slides were then briefly washed two times with deionized water. Next, the slices were stained with either **SF8(RADG)₂** (5 μ M) or **SF8(DDDG)₂** (5 μ M) for 30 min in the dark and were then washed three times with deionized water for 5 min each. ProLongTM Gold Antifade Mountant (Thermo Fisher Scientific) was added to the slides followed by a coverslip, and the slide was allowed to dry for at least 1 h. Brightfield and fluorescence images of the slices were acquired using a Zeiss Axiovert 100 TV epifluorescence microscope equipped with a Cy5.5 filter (ex: 655/40, em: 716/40).

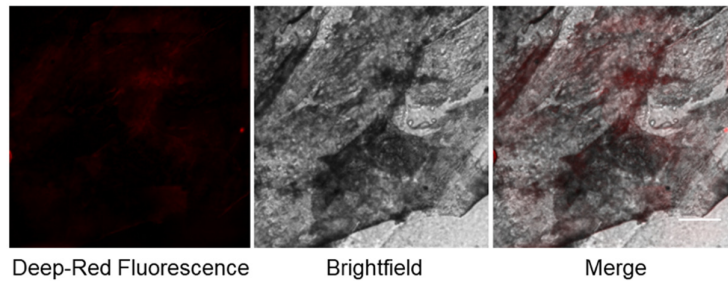


Figure S25. In-vitro bone histological staining with **SF8(RADG)₂**. Histological slices of tibia extracted from healthy mice were incubated for 30 min with **SF8(RADG)₂**. Fluorescence micrographs were acquired using Cy5.5 filter. Scale bar = 0.15 mm.

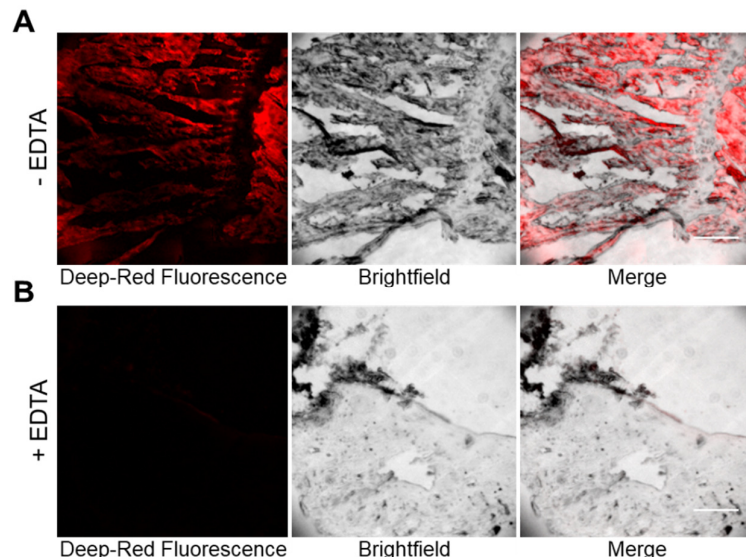


Figure S26. In-vitro bone histological staining with **SF8(DDDG)₂** in the presence of ethylenediaminetetraacetic acid (EDTA). Histological slices of tibia extracted from healthy mice were incubated for 16 h with either (A) deionized water or (B) 0.25 M EDTA. The slices were then incubated with **SF8(DDDG)₂** (5 μ M) for 30 min. Fluorescence micrographs were acquired using Cy5.5 filter. Scale bar = 0.15 mm.

SUPPORTING INFORMATION

8. Mouse Imaging Studies

Animal experiments were conducted under a protocol approved by the Notre Dame Institutional Animal Care and Use Committee (protocol number 19-09-5516, Bradley Smith: principal investigator). Female SKH1 hairless mice ($N = 3$, 36-42 days old) were anesthetized with 2-3% isoflurane with an oxygen flow rate of 2 L min^{-1} and imaged using an in-vivo imaging station (AMI Spectral Imaging) (ex: 640 nm, em: 710 nm, exposure: 3 sec, percent power: 50%, F-stop: 2, binning: small). The mice then received a retro-orbital injection of **SF8(DDDDG)₂** in saline with 2% DMSO (200 μM , 50 μL , 10 nmol/mouse) and were imaged at 0, 1.5, and 3 h. At 3 h, the mice were anesthetized and sacrificed via cervical dislocation, and blood was collected from the heart. All the major organs were removed and imaged, including the liver, heart, lungs, spleen, kidneys, skin, and muscle. The skin was then fully removed from the mouse, and the mouse skeleton was imaged. Image processing of full-body mouse images was conducted using ImageJ2 software with a 1000-pixel rolling ball radius background subtraction. The maximum fluorescence was set to 4000 and the images were pseudocolored “fire.” Biodistribution analysis was performed by importing fluorescence images of excised organs into ImageJ2 and applying a 1000-pixel rolling ball radius background subtraction. The amount of probe in each organ was obtained by adjusting the color threshold to create a region of interest (ROI) around each organ. The mean pixel intensity (MPI) of each selected ROI was measured and graphed to show organ fluorescence relative to the muscle. The above protocol was repeated again where mice ($N = 2$) received a retro-orbital injection of **SF8(DDDDG)₂** (200 μM , 50 μL , 10 nmol/mouse), and the experiment was carried out to 48 h.

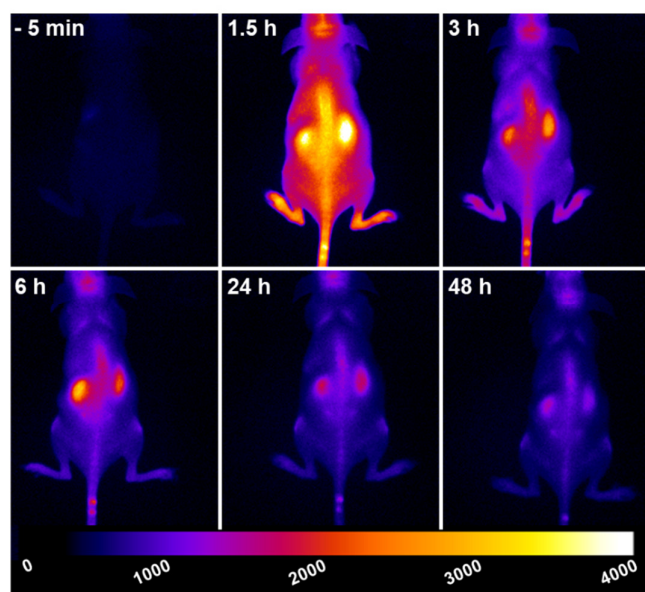


Figure S27. Representative deep-red fluorescent images of a live mouse injected with **SF8(DDDDG)₂**. Mice received intravenous injection of **SF8(DDDDG)₂** (10 nmol) and were imaged at -5 min, 1.5, 3, 6, 24, and 48 h post-injection (ex: 640 nm, em: 710 nm, exposure: 3 s, percent power: 50%, F-stop: 2, binning: small), ($N = 3$). Like all live animal fluorescence images, the signal is heavily surface-weighted and emphasizes probe perfusion through the blood vessels, organs and skeletal regions that are near the surface of the living animal. The mice exhibited no behavioral change after intravenous injection dosing with **SF8(DDDDG)₂**.

SUPPORTING INFORMATION

References

- [1] M. H. Ghasemi, E. Kowsari, *Res. Chem. Intermed.* **2017**, *43*, 1957–1968.
- [2] C.-V. T. Vo, M. U. Luescher, J. W. Bode, *Nat. Chem.* **2014**, *6*, 310–314.
- [3] F. Wang, J. Zhang, X. Ding, S. Dong, M. Liu, B. Zheng, S. Li, L. Wu, Y. Yu, H. W. Gibson, F. Huang, *Angew. Chem. Int. Ed.* **2010**, *49*, 1090–1094.
- [4] Y.-C. Su, Y.-L. Lo, C.-C. Hwang, L.-F. Wang, M. H. Wu, E.-C. Wang, Y.-M. Wang, T.-P. Wang, *Org. Biomol. Chem.* **2014**, *12*, 6624–6633.
- [5] S. K. Shaw, W. Liu, C. F. A. Gómez Durán, C. L. Schreiber, M. de L. Betancourt Mendiola, C. Zhai, F. M. Roland, S. J. Padanilam, B. D. Smith, *Chem. Eur. J.* **2018**, *24*, 13821–13829.
- [6] M. A. Spitsyn, V. E. Kuznetsova, V. E. Shershov, M. A. Emelyanova, T. O. Guseinov, S. A. Lapa, T. V Nasedkina, A. S. Zasedatelev, A. V Chudinov, *Dye. Pigment.* **2017**, *147*, 199–210.
- [7] I. Murgu, J. M. Baumes, J. Eberhard, J. J. Gassensmith, E. Arunkumar, B. D. Smith, *J. Org. Chem.* **2011**, *76*, 688–691.
- [8] C. Cordier, F. Boutimah, M. Bourdeloux, F. Dupuy, E. Met, P. Alberti, F. Loll, G. Chassaing, F. Burlina, T. E. Saison-Behmoaras, *PLoS One* **2014**, *9*, e104999.
- [9] S. Al-Taei, N. A. Penning, J. C. Simpson, S. Futaki, T. Takeuchi, I. Nakase, A. T. Jones, *Bioconjug. Chem.* **2006**, *17*, 90–100.
- [10] T. Takeuchi, S. Futaki, *Chem. Pharm. Bull.* **2016**, *64*, 1431–1437.

Author Contributions

CZ designed, synthesized and characterized the structure and properties of all compounds and grew the crystals. CLS designed and conducted the cell microscopy, histology studies, and mouse imaging experiments, and analyzed the results. SPC conducted liposomes studies and cell studies. AGO determined the X-ray crystal structure. BDS conceived the project and supervised the research. All co-authors helped with manuscript preparation.